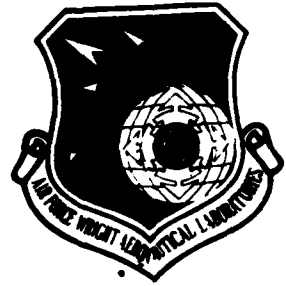MICROCOPY RESOLUTION TEST CHART

NATIONAL BUREAU OF STANDARDS 1963 A

AFWAL-TR-80-2056

LEVEL

AD A093122

MULTI-PLANE HIGH SPEED BALANCING TECHNIQUES AND THE USE OF A HIGH SPECIFIC STIFFNESS TI-BORSIC MATERIAL FOR VIBRATION CONTROL

G. Hamburg
W. Pentek

Teledyne CAE
1330 Laskey Road
Toledo, Ohio 43612

July 1980

TECHNICAL REPORT AFWAL-TR-80-2056

Final Technical Report for Period 9 February 1979 — 31 January 1980

Approved for public release, distribution unlimited.

80 12 22 125

This technical report has been reviewed and is approved for publication.

JAMES F. WALTON, Captain, USAF
Project Engineer

ISAK J. GERSHON
Tech Area Manager, Mechanical Design

FOR THE COMMANDER

DAVID H. QUICK, Lt Col, USAF
Actg Chief, Turbine Engine Division

REPORT DOCUMENTATION PAGE		READ INSTRUCTIONS BEFORE COMPLETING FORM
1. REPORT NUMBER AFWAL-TR-80-2056	2. GOVT ACCESSION NO. AD-A093 122	3. RECIPIENT'S CATALOG NUMBER
4. TITLE (and Subtitle) MULTI-PLANE HIGH SPEED BALANCING TECHNIQUES AND THE USE OF A HIGH SPECIFIC STIFFNESS TI-BORSIC MATERIAL FOR VIBRATION CONTROL.		5. TYPE OF REPORT & PERIOD COVERED Final Technical 9 Feb 79 - 31 Jan 80
		6. PERFORMING ORG. REPORT NUMBER TCAE-1701
7. AUTHOR(s) G. Hamburg and W. Pentek		8. CONTRACT OR GRANT NUMBER(s) F33615-79-C-2018 NEW
9. PERFORMING ORGANIZATION NAME AND ADDRESS Teledyne CAE 1330 Laskey Road Toledo, Ohio 43612		10. PROGRAM ELEMENT, PROJECT, TASK AREA & WORK UNIT NUMBERS Project 306612
11. CONTROLLING OFFICE NAME AND ADDRESS AIR FORCE WRIGHT AERONAUTICS LABORATORIES AIR FORCE SYSTEMS COMMAND WRIGHT-PATTERSON AFB, OHIO 45433		12. REPORT DATE February 1980
		13. NUMBER OF PAGES 114 115
14. MONITORING AGENCY NAME & ADDRESS(if different from Controlling Office)		15. SECURITY CLASS. (of this report) Unclassified
		15a. DECLASSIFICATION/DOWNGRADING SCHEDULE

16. DISTRIBUTION STATEMENT (of this Report)

Approved for public release; distribution unlimited.

17. DISTRIBUTION STATEMENT (of the abstract entered in Block 20, if different from Report)

DEC 22 1980

18. SUPPLEMENTARY NOTES

Project Engineer, Captain James F. Walton II
AFAPL/TBP/52081

19. KEY WORDS (Continue on reverse side if necessary and identify by block number)

Balancing, Multi Plane High Speed, Flexible, Rotor, Ti-Borsic, Composite Shaft, Super Critical, Response, Damping
studies

20. ABSTRACT (Continue on reverse side if necessary and identify by block number)

This report documents the results of a multi-plane high-speed balancing demonstration of a flexible rotor and a preliminary design analysis for a high specific stiffness composite material shaft. Both the balancing demonstration and the composite shaft design had as their objective the management of small turbofan engine low pressure (LP) shaft bending critical speeds. The prototype flexible rotor was successfully balanced through —> over

DD 1 JAN 73 1473 EDITION OF 1 NOV 65 IS OBSOLETE

ABSTRACT (continued)

3

~~three~~ critical speeds reaching a maximum of 28,000 rpm,
which was 74% of the maximum intended rotor speed of
38,000 rpm. Balancing for operation above the ~~fourth~~ 4
critical speed, which was predicted to occur at 33,000 rpm,
was prevented due to a sub-synchronous rotor instability.
Causes of the instability ~~have been~~ attributed to the con-
figuration of the squeeze film bearing damper and the
engine rotor support structure as opposed to any limitation
of the balancing techniques employed.

The preliminary composite shaft design was completed
assuming that a Ti-Borsic metal matrix composite with 60%
fiber volume and 40% metal matrix would be used. This
"stiff" shaft was designed as a direct substitute for the
multi-plane high speed balancing demonstrator rotor. Analy-
tical studies ~~performed~~ indicate that the composite rotor
will have a 24% third critical speed margin when operating
at 38,000 rpm.

FOREWORD

This document is the final Technical Report on the High Speed Multi-Plane Balancing Rig Demonstration Evaluation and the Composite Material Shaft Design and Analysis for Contract F33615-79-C-2018 Revision P00001 Project 306612. The contract was sponsored by the Aero-Propulsion Laboratory, Air Force Wright Aeronautical Laboratories, Air Force Systems Command, United States Air Force, Wright-Patterson AFB, Ohio, 45433, under the direction of Captain James F. Walton II, Project Engineer. Mr. Glenn Hamburg, Department Head, Rotating Systems Analysis Department, Teledyne CAE, had overall technical responsibility for the program. Mr. Thomas Walter, Project Engineer, Mechanical Technology Incorporated, was responsible for his company's analytical efforts, the balancing rig design and fabrication, and the balancing demonstration. Mechanical Technology Incorporated was a subcontractor to Teledyne CAE in this program.

Accession For

NTIS GRA&I	
DTIC TAB	☑
Unannounced	☐
Justification	☐

By

Distribution/

Availability Codes

| Dist | Avail and/or Special |

A

iii

TABLE OF CONTENTS

TABLE OF CONTENTS

LIST OF ILLUSTRATIONS

LIST OF ILLUSTRATIONS

LIST OF ILLUSTRATIONS

LIST OF ILLUSTRATIONS

LIST OF ILLUSTRATIONS

LIST OF TABLES

LIST OF TABLES

SUMMARY

The purpose of the Multi-Plane, High Speed Balancing Program was to demonstrate the balancing of a flexible, prototype, solid (steel) low speed (LP) shaft of a cruise missile rotor through four critical speeds, thereby reducing unbalance related vibration.

A rotordynamics analysis of the LP rotor was conducted to predict the undamped critical speeds and associated mode shapes. The location of the anti-nodes established the location of the balancing planes required to traverse the four predicted critical speeds.

A test rig was designed and fabricated using engine hardware and adaptive support hardware. The rig included both an air turbine motor to drive the shaft through the required speed range, and a vacuum chamber to permit high rotor speeds with relatively low drive power requirements. Displacement sensors were used to monitor shaft displacement in four planes.

Temporary balance weight additions were achieved by using washers placed under bolts on the nose cone, lead tape for the balance lands on the shaft, and safety wire on the turbine stages.

The rotor was successfully balanced through three critical speeds and reached a maximum speed of 28,000 RPM, which is 74% of the maximum rotor speed of 38,000 RPM. Balancing at the fourth critical speed, which was predicted to occur at 33,000 RPM, was prevented by rotor instability. Causes of the instability have been attributed to the existing configuration of the damper and engine support structure.

SECTION I

INTRODUCTION

1.   INTRODUCTION

Advanced, Air Force turbine engine requirements are dictating higher speeds, lighter weight, fewer parts and the need for increased life. As a result it is becoming more likely that turbine engine rotor design techniques that appear practical are: (1) to design for operating above one or more bending critical speeds and to employ multi-plane high speed balancing, or (2) to design for operation below the bending critical speeds through the use of high specific stiffness composite materials. Both alternatives are addressed in this report as a means of meeting future engine requirements, with specific application to the small cruise missile sized turbofan engines.

When designing supercritical shafting for turbine engines, the unbalance must be kept to a minimum to achieve safe and smooth operation throughout the engine speed range. Because the unbalance is distributed along the length of the rotor, it is unlikely that a single plane balancing method would neutralize the unbalance forces and couples sufficiently to allow supercritical operation. The recently developed techniques of multi-plane, high speed balancing provide a better balancing capability and appear to provide the best approach for allowing supercritical shaft operation. A successful demonstration of the multi-plane, high speed balancing technique would give the designer the ability to design supercritical rotors with the added benefits of reducing hardware, simplifying engine configuration, and reducing the engine life cycle cost.

An alternate approach to the problem of supercritical speed operation is to avoid running through the bending modes by using a high specific stiffness composite shaft design which is capable of moving the lowest bending mode above the maximum operating speed of the rotor. To accomplish this, the design and analysis of a metal matrix composite low pressure (LP) shaft should be completed. The design criteria should include both sufficient third critical speed margin above the maximum speed (38,000 rpm) and the following structural criteria: (1) sufficient torsional shear strength to transmit fan driving torque, (2) adequate flexural strength to accommodate both fan and turbine rotor gyroscopic bending moments under all anticipated maneuver conditions, (3) adequate tensile strength to sustain axial pressure and aerodynamic gas forces coupled between the fan and turbine sections.

The design criteria must be met in the thermal environment imposed by the engine under the most severe operating condition. These design criteria must also be considered in designing the method of attaching the composite section to the turbine and fan rotors.

1

To verify the design and analysis, an LP rotor which includes a composite metal matrix shaft should be tested in a rig.

2. BACKGROUND

Past government studies have shown the potential of the multi-plane high speed balancing techniques to reduce rotor unbalance levels, and thus vibrations, to a point that will allow supercritical shaft operation. However, this technology has not yet been demonstrated with a rotor operating above the fourth critical speed in an actual engine environment. While there has been limited use of this technology in the turbine engine industry, primarily for single plane trim balancing of subcritical rotors, it has not been used to its full potential.

Since current trends in turbine engine design are towards lighter weight and higher rotational speeds, it is evident that supercritical shafting will be required in advanced turbine engines. As a test-bed for the use of supercritical shafting, the non-man-rated, limited life cruise missile engines are ideal. The design methodology that is necessary for the application of these advanced techniques may be developed and demonstrated with an engine of the cruise missile variety because of its size and environment.

Since the engine low pressure spool is small, the power requirements necessary for high-speed balancing can be minimized through the use of a vacuum chamber. Additionally, since the cruise missile engine life is limited to 50 hours with a maximum of 5 to 7 hours running time between refurbishments, the degradation of system balance due to erosion and other time-dependent factors is minimized. Thus, to achieve the goals of increased performance and life at reduced cost, the application of the multi-plane high speed balancing concepts in turbine engines must be investigated and exploited.

Previous investigations of the relationship between critical speed and the ratio of elastic modulus to density (specific stiffness) of the shaft material indicate that for a simply-supported (two bearing) shaft, the system critical speed varies closely with this ratio. This relationship was established from analyses of geometrically identical hollow shafts comprised of various composite materials (40/60 Ti-Borsic, 50/50 Ti-Borsic, 60/40 Ti-Borsic, 50/50 Al-Borsic, 60/40 Al-Borsic), and steel and beryllium. These investigations indicated that a composite shaft could be designed to provide a third critical speed above the maximum engine operating range.

Alternative composite shaft design concepts, based on the selective reinforcement (SERIF) of metal shafts, have also been investigated for both internal and external reinforcement of sleeves with composites in which the fibers had a longitudinal and also a cross-ply orientation. SERIF configurations have lower stiffness characteristics than do the all-composite

2

designs for a given shaft geometry due to the inherent lower fiber volume percent, which effectively reduces the elastic modulus to density ratio.

3. SCOPE

The Multi-Plane, High Speed Balancing Program was approximately a twelve month effort and approached the problem of supercritical speed operation in two ways. The first was to demonstrate the feasibility of using the multi-plane, high speed balancing techniques to balance a supercritical low pressure (LP) shaft of a limited life turbofan engine. The second was to design a shaft which would have the lowest bending mode above its maximum operating speed through the use of a high specific stiffness material. The fabrication of this shaft was made feasible by the use of recently developed advanced manufacturing techniques..

a. Task Definition

The balancing task was to provide a small gas turbine rotor, balance it using multi-plane balancing techniques, and demonstrate it in a simulated engine assembly and operation. The original program schedule is shown in Figure 1.

The composite shaft design task was to design a shaft with high specific stiffness so that its lowest bending mode was above its maximum operating speed.

The balancing and composite shaft design tasks were to be conducted through seven tasks described in the following paragraphs.

(1) Task I - Shaft Design

Teledyne CAE, teamed with their subcontractor, Mechanical Technology Incorporated (MTI), was to analyze and establish a multi-rotor shaft system for an existing turbofan engine applicable to a limited-life, cruise missile mission, for an unmanned vehicle (Figure 2). The configuration was to be such that a simply supported supercritical operation occurred below the maximum shaft speed. Design features to be provided with this configuration included: (1) simplified solid low pressure (LP) spool of the two-spool system, and (2) removal of two intershaft bearings which currently maintain the third critical speed (first bending) above the LP spool operating regime (Figures 3 and 4).

A balancing procedure was to be established to identify balance planes and speeds to provide acceptable vibration response throughout the operational speed range of the LP shaft.

3

WEEKS ARO

LEAD	ITEM	2	4	6	8	10	12	14	16	18	20	22	24	26	28	30	32	34	36
	1.0 SHAFT DESIGN																		
TCAE/MTI	1.1 SOLID CONFIGURATION																		
TCAE	1.1.1 CRITICAL SPEED ANALYSIS																		
TCAE/MTI	1.1.2 DESIGN LAYOUT																		
TCAE/MTI	1.2 SELECTION OF BALANCING PLANES AND SPEEDS																		
MTI	1.3 UNBALANCED SENSITIVITY																		
	1.4 ROTOR INSTABILITY STUDIES																		
	2.0 RIG DESIGN																		
TCAE/MTI	2.1 REVIEW EXISTING ENGINE HARDWARE																		
MTI	2.2 LAYOUT ADAPTIVE HARDWARE																		
TCAE/MTI	INTERIM BRIEFING																		
	3.0 FABRICATION AND PROCUREMENT																		
	3.1 SHAFT																		
TCAE	3.1.1 DETAIL, CHECK AND RELEASE DRW.																		
TCAE	3.1.2 FABRICATE																		
TCAE	3.1.3 ASSEMBLE SHAFT, SHIP TO MTI																		
	3.2 RIG ADAPTIVE HARDWARE																		
MTI	3.2.1 DETAIL, CHECK AND RELEASE DRW																		
MTI	3.2.2 FABRICATE																		
MTI	3.2.3 BALANCING COLLAR DETAIL FAB.																		
MTI	3.3 ASSEMBLE RIG																		
MTI	4.0 BALANCING DEMO																		
TCAE/MTI	5.0 EVALUATION																		
	FINAL REPORT																		

39832

Figure 1. High Speed Balancing Program Schedule.

4
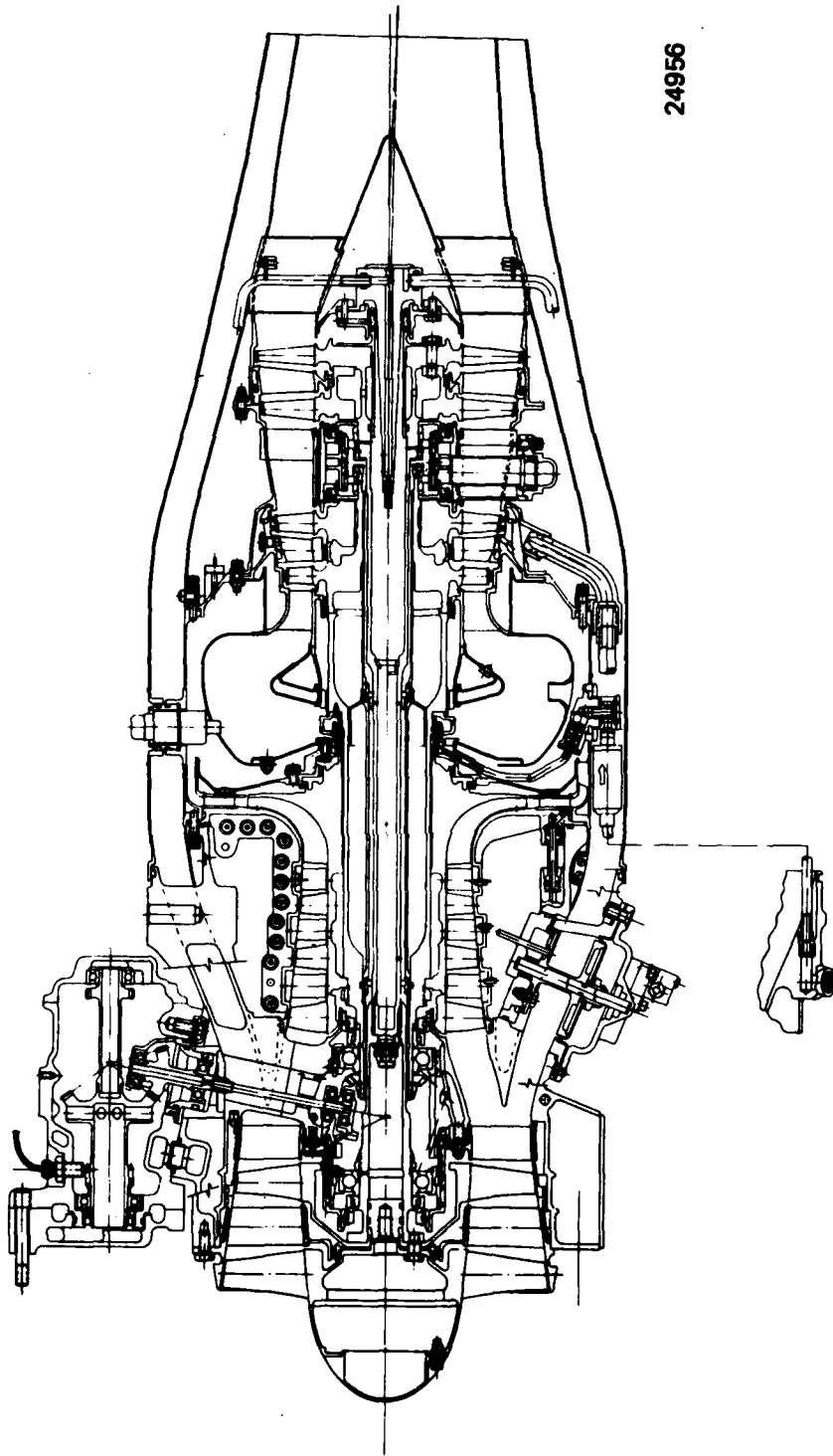
24956

Figure 2. Teledyne CAE Model 471-11DX Turbofan Engine; Cruise Missile Program DFRT Configuration.

5

NEW OIL TUBE REPLACES EXISTING
TUBE AND INTERSHAFT BEARINGS

NEW FAN SHAFT CONFIGURATION
INCORPORATED FORWARD OF THIS
WELD JOINT
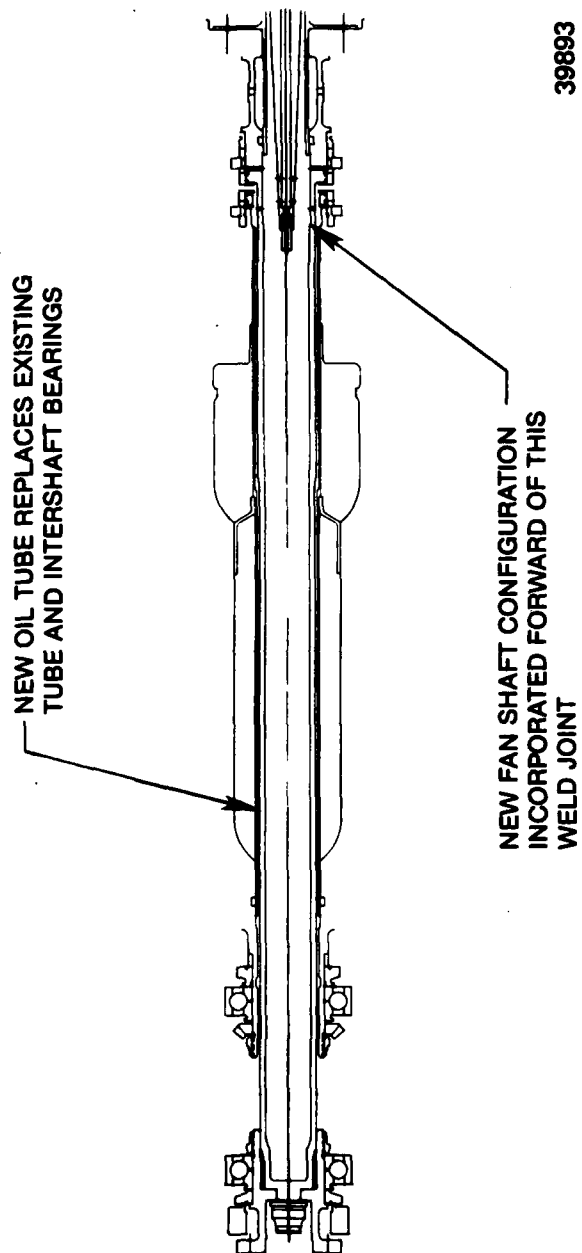
39893

Figure 3. Model 471-11DX Fan and HP Shaft Configuration Modifi-
cations; Intershaft Bearings are Eliminated.

6
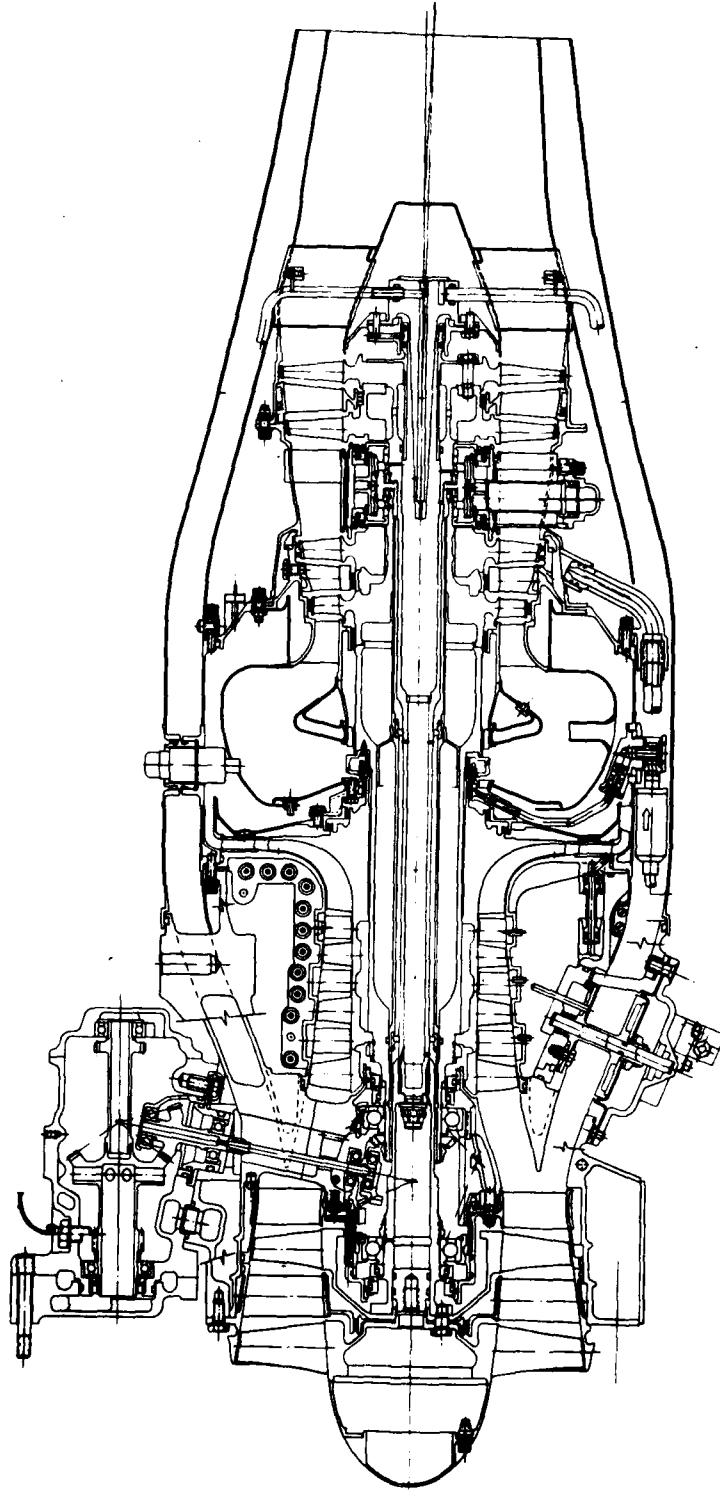
18951

Figure 4. Model 471-11DX Supercritical LP Shaft Configuration. Modification Eliminates Intershaft Bearings and Simplifies the Shaft Configuration.

The balancing criteria necessary to identify a successful balance of the LP shaft were to be established. These criteria were to be based on the results of analytical studies and existing vibration characteristics of the candidate turbofan engine. Sensitivity analyses for varying degrees of rotor unbalance, were to be independently conducted by Teledyne CAE and MTI, using state-of-the-art, rotor unbalance, response analytical techniques. Potential rotor instabilities resulting from the supercritical operating design of the shaft system were to be evaluated by MTI and the results incorporated into the final shaft configuration.

(2) Task II - Balancing Rig Design

Teledyne CAE and MTI were to jointly determine the amount of existing engine hardware which could be used in the construction of the high speed balancing demonstration rig. The final configuration of this rig, including support systems such as bearing services, vibration and displacement sensors, and the drive system, was to be designed by MTI. Teledyne CAE and MTI were to present a briefing detailing the shaft and balancing rig designs to obtain Air Force approval prior to proceeding with Task III (Fabrication and Procurement). Teledyne CAE and MTI were to present an interim briefing of the activities and results of the first two design tasks for Air Force evaluation.

(3) Task III - Fabrication

Final shaft drawings were to be prepared by Teledyne CAE. Teledyne CAE was to fabricate, assemble and ship the shaft assembly to MTI for the rig demonstration.

MTI was to prepare the final drawings for the fabrication of all rig adaptive hardware. The demonstration rig was to be assembled by MTI upon the receipt of all shaft and adaptive hardware.

(4) Task IV - Multi-Plane High Speed Balancing Rig
      Demonstration

Mechanical Technology Inccorporated was to balance the assembled rotor in the demonstration rig. The balanced rotor vibratory response characteristics were to be evaluated against the design criteria as established in Task I. Following successful balance of the rotor and its demonstrated operation on the balancing rig, the rotor was to be disassembled, then reassembled and the balance checked to verify repeatability. MTI was to document the rotor dynamics characteristics including critical speeds, mode shapes and unbalance sensitivity for the configuration tested.

(5) Task V - Balancing Demonstration Evaluation

At the conclusion of the program, Teledyne CAE was to evaluate the results and present them in the form of a final report. Specific attention was to be given to the following program criteria: (1) feasibility of using multi-plane, multi-speed balancing techniques to operate rotors above bending critical speeds, and (2) evaluation of using multi-plane, multi-speed balancing techniques for simplified, flexible, cost effective rotors.

(b) Technical Approach

The LP rotor assembly of a limited life turbofan engine was to be modified to ensure that the simply supported rotor's third and fourth critical speeds occurred in the operating speed range. To accomplish this modification, analyses were to be performed to determine the shaft critical speeds, shaft sensitivity to imbalance, and rotor system stability. The modified rotor system (with fan and turbine stages included) was to be procured and assembled in a balancing rig and balanced. After balancing, the necessary rotor disassembly to remove the rotor from the balancing rig was to be accomplished. The disassembly procedures were to be representative of those required to prepare the rotor assembly for engine installation. Once disassembly was accomplished, the LP rotor was to be reassembled in a manner representative of engine assembly procedures in the balancing rig and then rerun. This test was designed to verify that the rotor system balance could be maintained after removal from the balancing rig and engine installation and that the rotor would meet the established vibration criteria.

The balancing rig was to be designed to use as much existing engine hardware as possible so that the LP shaft support characteristics (stiffness and damping) would be accurately simulated. The balancing rig was intended to serve not only to balance the LP shaft assembly but to also demonstrate the feasibility of operating a complete rotor assembly above the fourth critical speed.

SECTION II

ACCOMPLISHMENTS

1. **INTRODUCTION**

   This section summarizes the accomplishments of the Multi-Plane, High Speed Balancing Program.

2. **SHAFT DESIGN**

   The rotor dynamics analyses, including undamped critical speeds, unbalance response sensitivity and instability studies were conducted to establish the solid LP shaft design, and to assure that the third and fourth modes (critical speeds) would be in the operating speed range of the LP shaft. The mode shapes which resulted from the undamped critical speed analysis were used to define the locations of the balancing planes.

3. **RIG DESIGN**

   The balancing rig was designed to accommodate the demonstration LP rotor with available engine hardware and adaptive hardware to duplicate the structural stiffness and damping provided by the engine structure. Bearing lubrication and damper oil supply services were provided. Proximity probe brackets were designed to sense shaft displacement in four planes. An air turbine with a spline drive was incorporated into the test rig design as the prime mover. The test rig was housed in a vacuum chamber which lowered the drive air turbine power requirements.

4. **FABRICATION AND PROCUREMENT**

   a. **Shaft**

   The solid LP shaft was a newly fabricated item to which an existing second stage turbine rotor was electron beam welded. The fan shaft was a newly fabricated item. The two fans and two turbine rotors were available from existing engine parts inventory as were the front and rear bearings, the front bearing support and the rear bearing support spring ring.

   b. **Rig**

   The required adaptive hardware was fabricated after reviewing the available engine hardware. The bearing support pedestals were designed to simulate the stiffness of the engine static structure.

11

5. BALANCING DEMONSTRATION

The solid steel LP rotor was successfully balanced through three critical speeds and reached a maximum speed of 28,000 rpm, which is 74% of the maximum required shaft speed. Balancing at the fourth critical speed was prevented by sub-harmonic rotor instability. Causes of the instability have been attributed to the existing configuration of the oil squeeze film damper and the engine support structure.

6. TI-BORSIC SHAFT ANALYSIS AND DESIGN

The Ti-Borsic Shaft Analysis and Design included structural and rotordynamics analysis (undamped critical speed analysis and unbalance response analysis) of a metal matrix LP shaft for the same limited life engine. The shaft geometry and percent fiber volume mixture of titanium-borsic was finalized by iterative critical speed and structural analyses predicated on front and rear bearing support spring rates of 150,000 and 300,000 pounds per. inch, respectively, and a goal of 25 percent margin of the third critical speed above maximum LP rotor speed 38,000 RPM. The 24 percent margin obtained in the final design represented a compromise between available manufacturing technology and critical speed requirements.

A thermal heat balance analysis was also completed for the LP shaft from which it was determined that the shaft temperature would not exceed 550°F due to HP shaft thermal radiation. All material physical characteristics and properties used in the analyses were based on the maximum predicted temperature of 550°F.

SECTION III

DISCUSSION

1. INTRODUCTION

The purpose of the Multi-Plane High Speed Balancing Program was to demonstrate the feasibility of controlling vibrations in a supercritical low pressure (LP) shaft of a limited life turbofan engine by high speed balancing at each of the critical speeds. The program consisted of five separate tasks: (1) analysis and design of a supercritical rotor; (2) design of a test rig to balance the supercritical rotor; (3) fabrication and procurement of the shaft and balancing rig; (4) balancing demonstration; (5) evaluation of the balancing demonstration.

The purpose of the Ti-Borsic shaft program was to control resonant vibrations by avoiding running through the bending critical speeds. This approach uses a high specific stiffness composite, Ti-Borsic shaft which is capable of placing the bending modes beyond the maximum operating speed.

2. SHAFT DESIGN

The constraints of using as much of the existing engine hardware as practical for the Multi-Plane High Speed Balancing Program immediately imposed the use of the engine front and rear bearing supports with experimentally determined stiffnesses of 6,000 and 51,000 lb/in, respectively. The front bearing support also included an oil squeeze film damper.

a. Critical Speed Analysis

The solid LP shaft was designed on the basis of the close agreement of the results of independent critical speed analyses by Teledyne CAE (prime contractor) and Mechanical Technology Incorporated (sub-contractor). Both analyses utilized the actual hardware stiffness values of the front and rear bearing supports of 6,000 and 51,000 lb/in, respectively. Teledyne CAE's analysis is a matrix solution for multiple shaft systems. The analysis considers both bending and shear effects, flexible bearings and gyroscopic effects from attached disks.

The actual rotor is transformed into an idealized equivalent system consisting of a series of disks connected by sections of elastic but massless shaft. The mass of the disks and their spacing are chosen so as to approximate the distribution of mass in the actual rotor (See Figure 5). The bending flexibility of the connecting sections of the shaft corresponds to the actual flexibility of the rotor. The matrix solution used in this program is essentially an iterative method. At a selected frequency it is used to compute progressively the deflection, slope, moment and shear from one station to the next

13

LEGEND:

⊙ ... ① 17 SHAFT NO. 1, STATION 1-17

▢ ... 1 42 SHAFT NO. 2, STATION 1-42

△ ... ⚠ 7 SHAFT NO. 3, STATION 1-7

▢ 8 FRONT BEARING SUPPORT SPRING RATE 6,000 LB/IN

▨ 33 REAR BEARING SUPPORT SPRING RATE 51,000 LB/IN   39905

Figure 5.   471-11DX Solid LP Shaft Undamped Critical Speed Model.

14

in a manner similar to the Holzer method. Mechanical Technology Incorporated used a lumped mass geometric model and the mathematical model is included in Appendix A.

b.   Selection of Balancing Planes

The results of the two independent undamped critical speed analyses by Teledyne CAE and MTI compared favorably for the first five modes, with critical speed variances for modes one through five being 2, 6, 3, 8 and 4 percent respectively (See Table 1). The corresponding mode shapes (Figures 6 through 10) were in good agreement, and the location of the anti-nodes (maximum relative deflections) were used to define the location of the balancing planes on the shaft. These planes were located at 5, 10 and 16 inches from the front flange of the fan shaft (Figure 11).

c.   Unbalance Response Sensitivity

Teledyne CAE and Mechanical Technology Incorporated independently conducted the unbalance response sensitivity analyses using calculated values of viscous damping coefficients for the front bearing support. MTI used a viscous damping coefficient of 6.7 lb-sec/in, and Teledyne CAE used a value of 3.78 lb-sec/in. The results of the MTI unbalance response analysis are summarized in tabular form in Appendix B. The results of the Teledyne CAE unbalance response analysis are summarized in Figures 12 through 17 and Table 2. Both analyses indicate that the rotor is extremely sensitive to unbalance.

d.   Rotor Instability Analysis

Mechanical Technology Incorporated conducted the rotor instability analysis using a low value of 0.1 lb-sec/in. viscous damping coefficient at the front bearing support and also 6.7 lb-sec/in. to show the effects of minimum damping compared to existing calculated values of damping on the stability of the rotor. The results of the instability analysis indicated that all mode shapes were stable, although the level of stability, measured by the log decrement, was very low, particularly for the third mode (see Figures 18 and 19).

e.   Design Layout

The final design layout of the LP shaft was completed as well as the detail drawings prior to the interim review meeting with AFWAL.

TABLE 1

SUMMARY: UNDAMPED CRITICAL SPEEDS, 471-11DX SOLID
LP SHAFT TELEDYNE CAE AND MTI MODELS MATERIAL
PROPERTIES AT 200°F

	K_FRONT (LB/IN)	K_REAR (LB/IN)	MODE 1 (RPM)	MODE 2 (RPM)	MODE 3 (RPM)	MODE 4 (RPM)	MODE 5 (RPM)
TCAE	5,000	51,000	5,158	7,997	13,969	30,244	66,890
MTI	6,000	51,000	5,274	7,523	13,578	32,612	69,896
% DIFF			2	6	3	8	4

MATERIAL PROPERTIES ADJUSTED FOR ENGINE
TEMPERATURE ENVIRONMENT (200-900°F)

	K_FRONT (LB/IN)	K_REAR (LB/IN)	MODE 1 (RPM)	MODE 2 (RPM)	MODE 3 (RPM)	MODE 4 (RPM)	MODE 5 (RPM)
TCAE	6,000	51,000	5,146	7,420	13,626	30,233	58,305

16
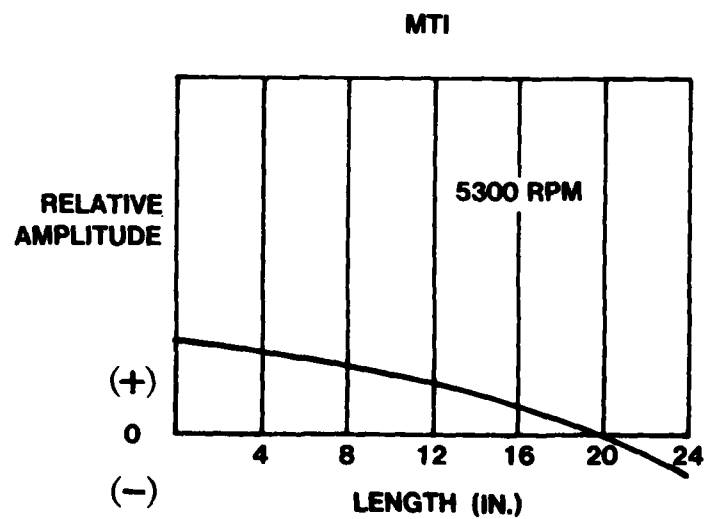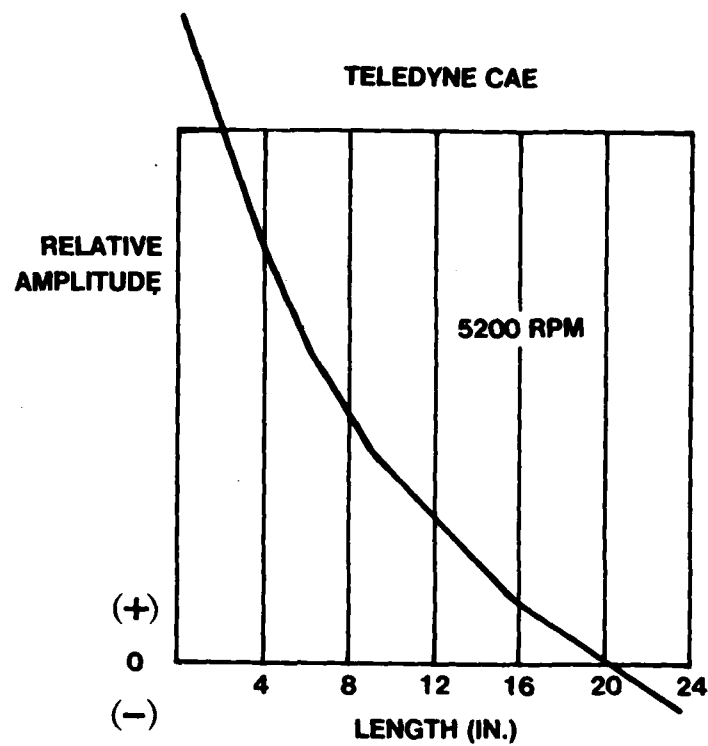
Figure 6.   471-11DX Solid Steel LP Shaft Undamped Critical
Speed Mode Shapes - Mode 1.

TELEDYNE CAE

8000 RPM

MTI

7500 RPM
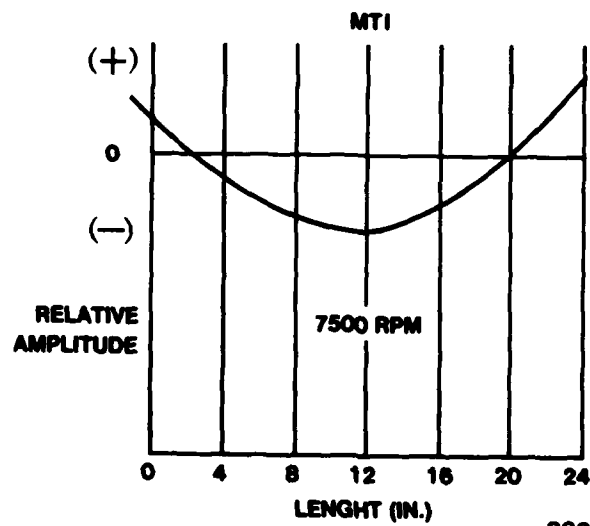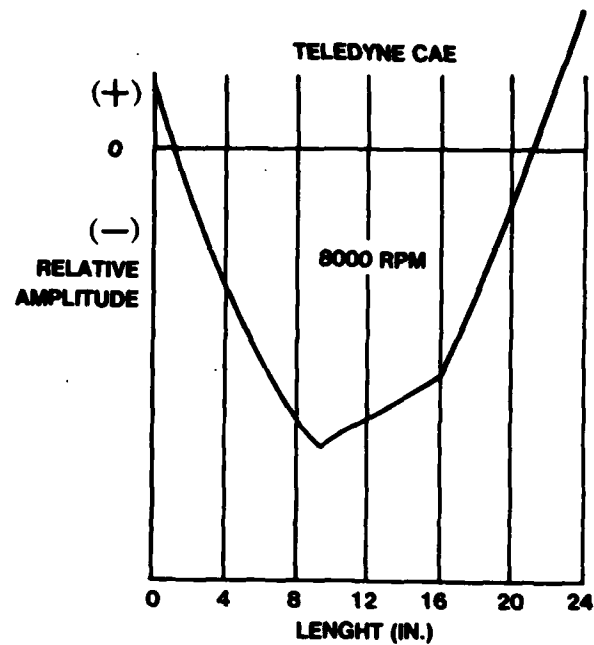
33214

Figure 7. 471-11DX Solid Steel LP Shaft Undamped Critical
Speed Mode Shapes - Mode 2.

18

TELEDYNE CAE

MTI
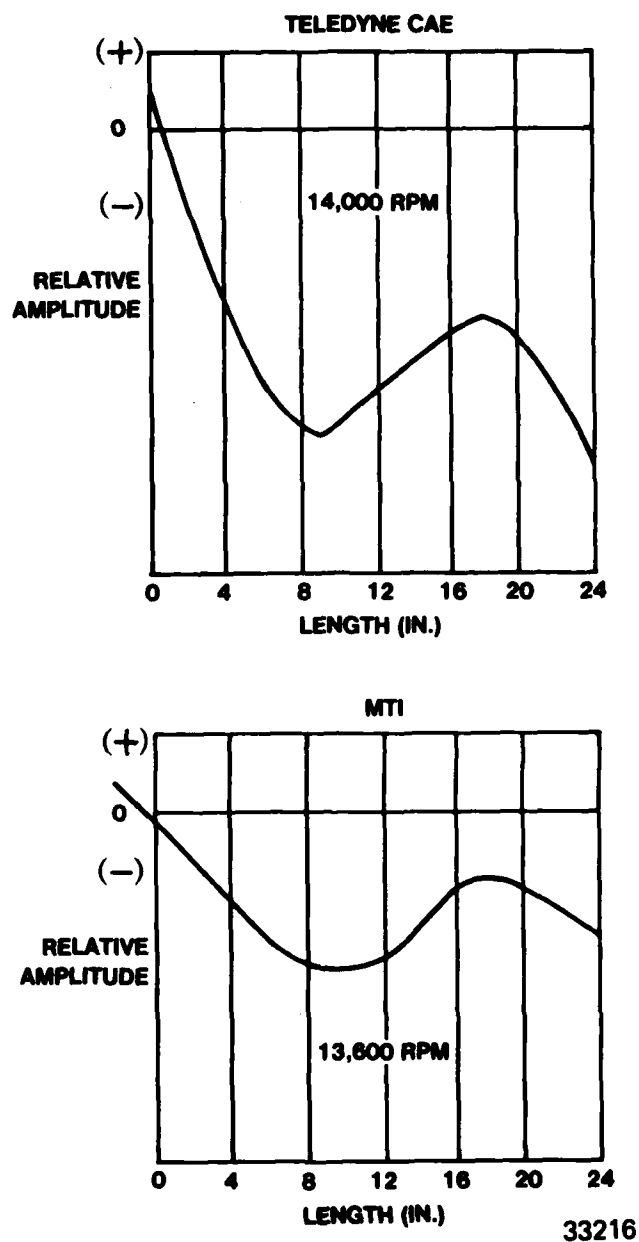
Figure 8.   471-11DX Solid Steel LP Shaft Undamped Critical
            Speed Mode Shapes - Mode 3.

19

TELEDYNE CAE

30,200 RPM

RELATIVE AMPLITUDE

(+)

0

(−)

0 4 8 12 16 20 24
LENGTH (IN.)

MTI

RELATIVE AMPLITUDE

32,600 RPM

(+)

0

(−)

0 4 8 12 16 20 24
LENGTH (IN.)
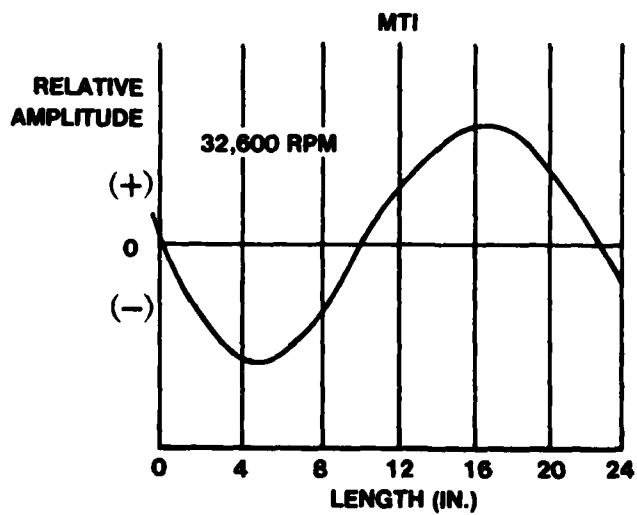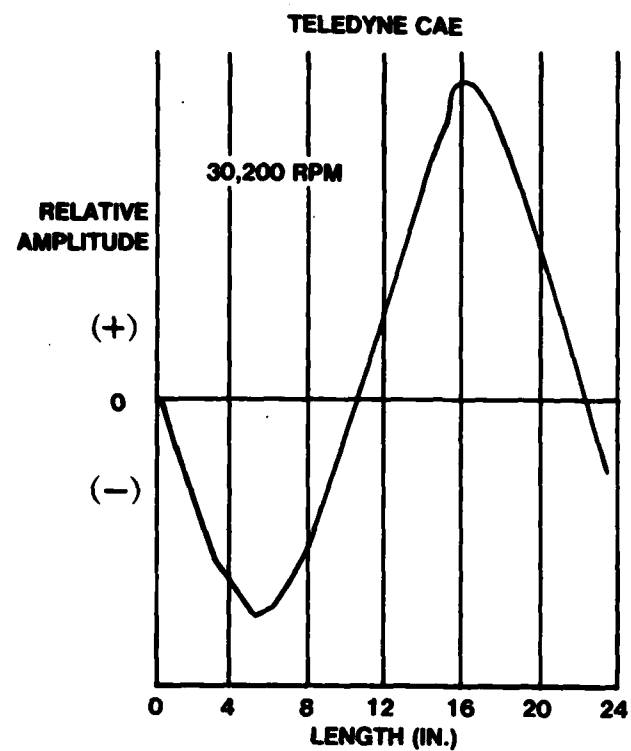
33215

Figure 9.   471-11DX Solid Steel LP Shaft Undamped Critical
Speed Mode Shapes - Mode 4.

20
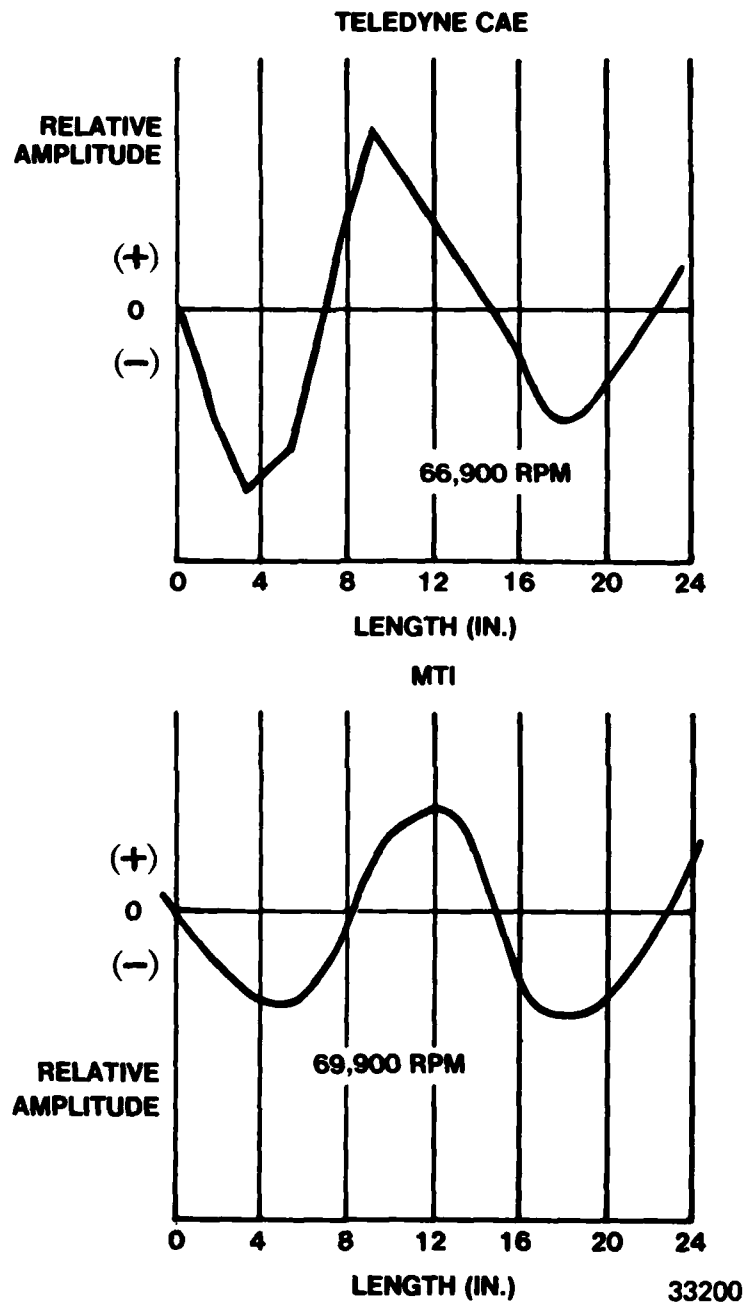
Figure 10. 471-11DX Solid Steel LP Shaft Undamped Critical
Speed Mode Shapes - Mode 5.

21
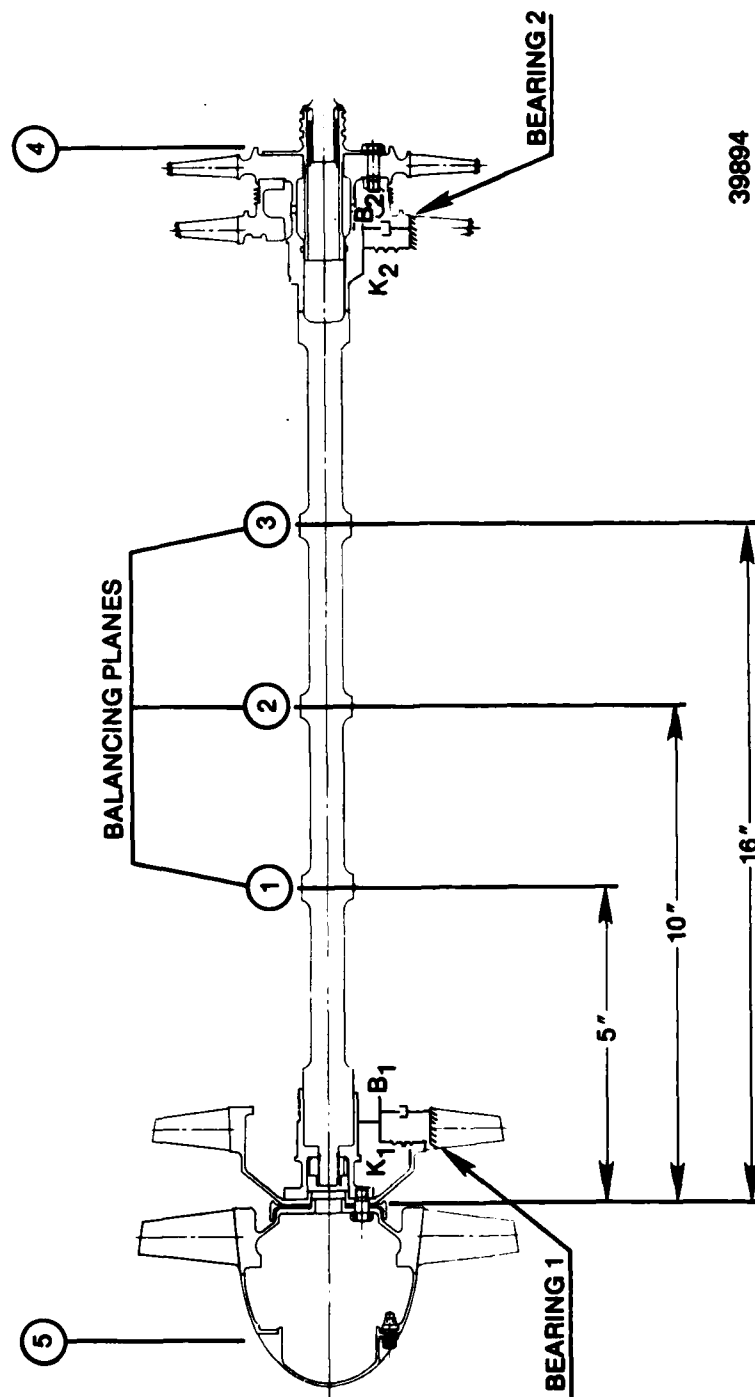
Figure 11. Designation of Balancing Planes and Bearing Model.

39894

22

TABLE 2

SUMMARY: BEARING REACTION FORCE 471-11DX
SOLID STEEL LP SHAFT AT APPROXIMATE CRITICAL
SPEEDS DUE TO UNBALANCE AT THREE SEPARATE
BALANCING PLANES

UNBAL. STATION	SPEED (RPM)	BEARING REACTION FORCE (POUNDS)	
		FRONT	REAR
1gm. 23	5,110	0.15	0.36
	7,330	9.5	14.7
	13,900	2.5	53.5
	31,792	10.8	94.1
	57,352	19.1	101.0
1 gm. 18	5,110	0.5	0.15
	7,330	13.0	21.0
	13,900	3.5	80.3
	31,792	2.3	5.6
	57,352	27.2	164.0
1 gm. 13	5,110	1.1	0.1
	7,330	7.6	12.7
	13,900	3.0	77.1
	31,792	9.0	72.2
	57,352	18.4	128.6

$$B_1 = 3.781 \frac{LB\text{-}SEC}{IN}, \ g = .02$$

$$K_{FRONT} = 6000 \ LB/IN, \ K_{REAR} = 51,000 \ LB/IN$$

ST. 13 @ 5 In.
ST. 18 @ 10 In.
ST. 23 @ 16 In.

PEAK DEFLECTIONS (INCH)

RPM x 10^3
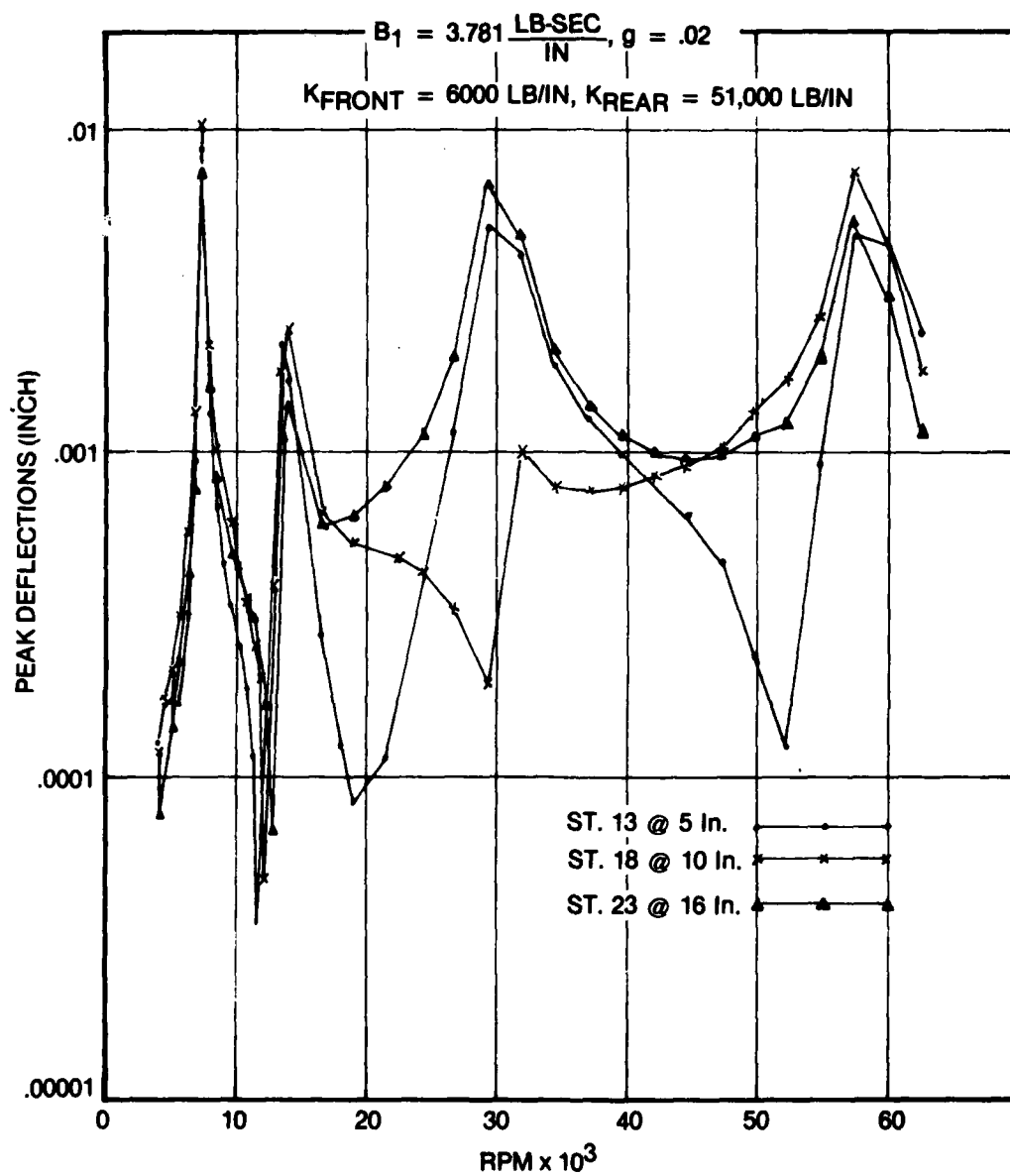
39847

Figure 12.   471-11DX LP Shaft Unbalance Response One Gram at
             Station 13 (Five Inches From Front).

24
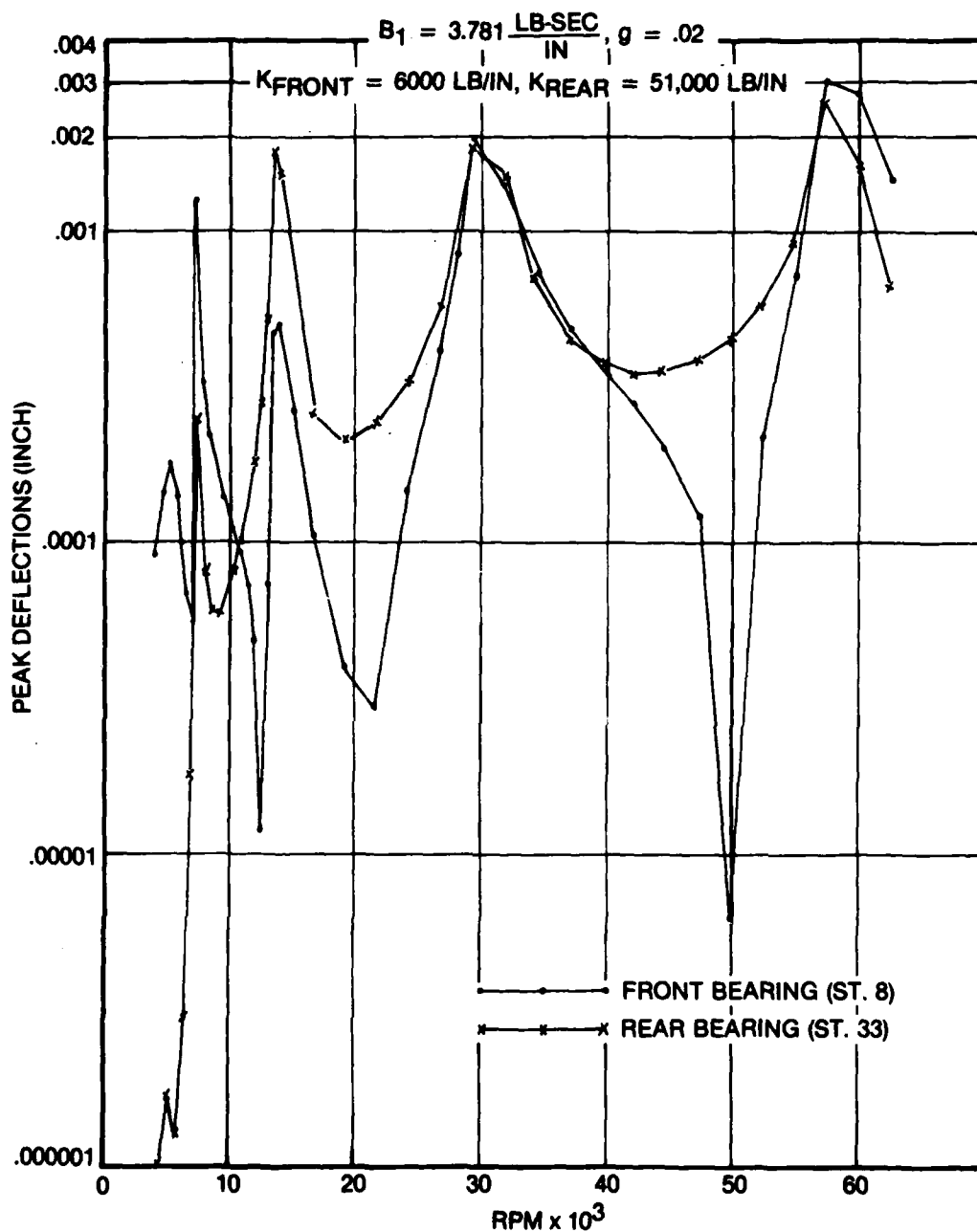
Figure 13.   471-11DX LP Shaft Unbalance Response One Gram
            Unbalance at Station 13 (Five Inches From
            Front).

25

$$B_1 = 3.781 \frac{LB\text{-}SEC}{IN}, g = .02$$

$K_{FRONT} = 6000$ Lb/In., $K_{REAR} = 51,000$ Lb/In.

PEAK DEFLECTIONS (INCHES)

RPM x 10³

ST. @ 5 In. ————•———
ST. @ 10 In. ×——×——×
ST. @ 16 In. △——△——△
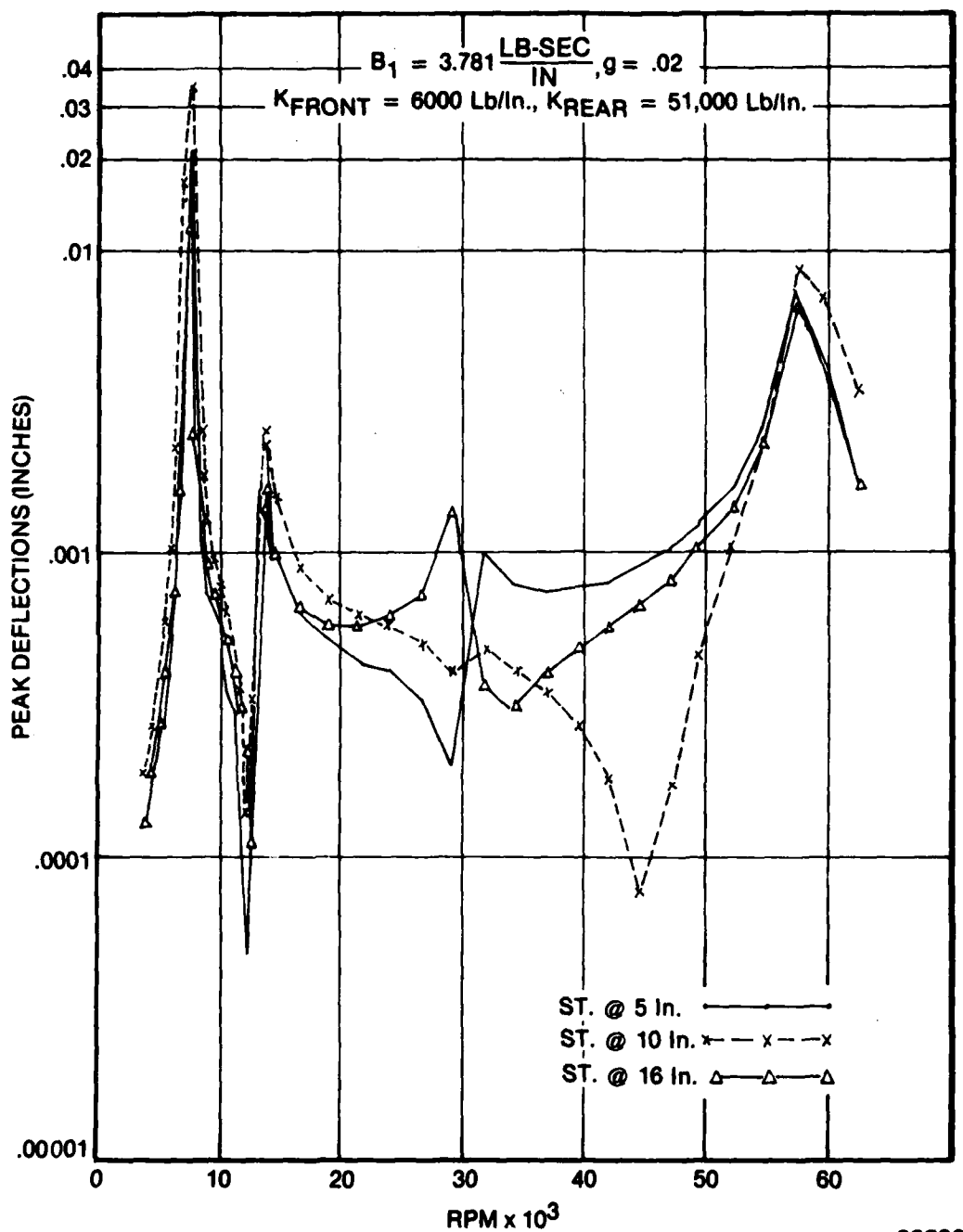
39860

Figure 14.   471-11DX Unbalance Response One Gram Unbalance at
             Station 18 (Ten Inches From Front).

26
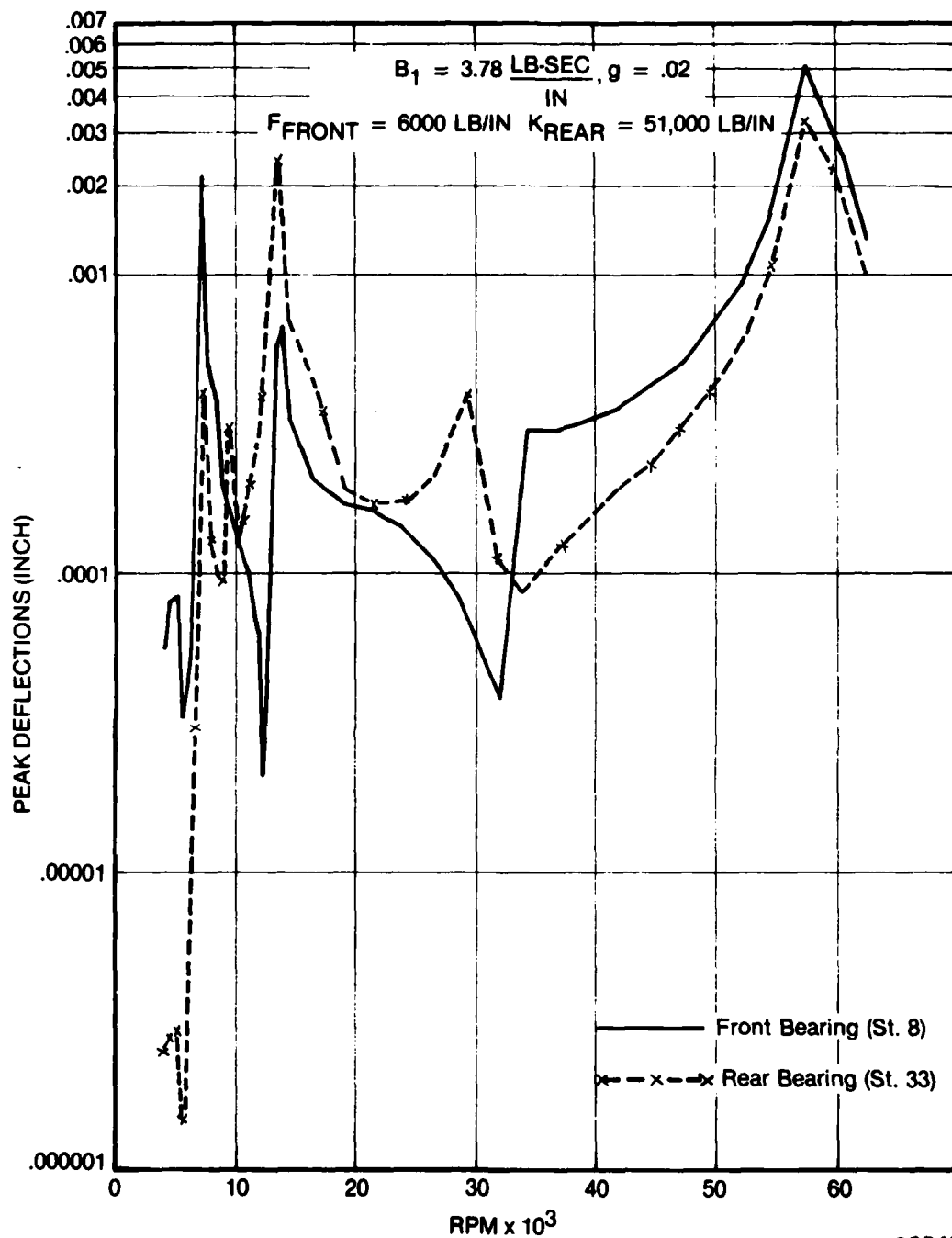
Figure 15. 471-11DX LP Shaft Unbalance Response One Gram
Unbalance at Station 18 (Ten Inches From Front).
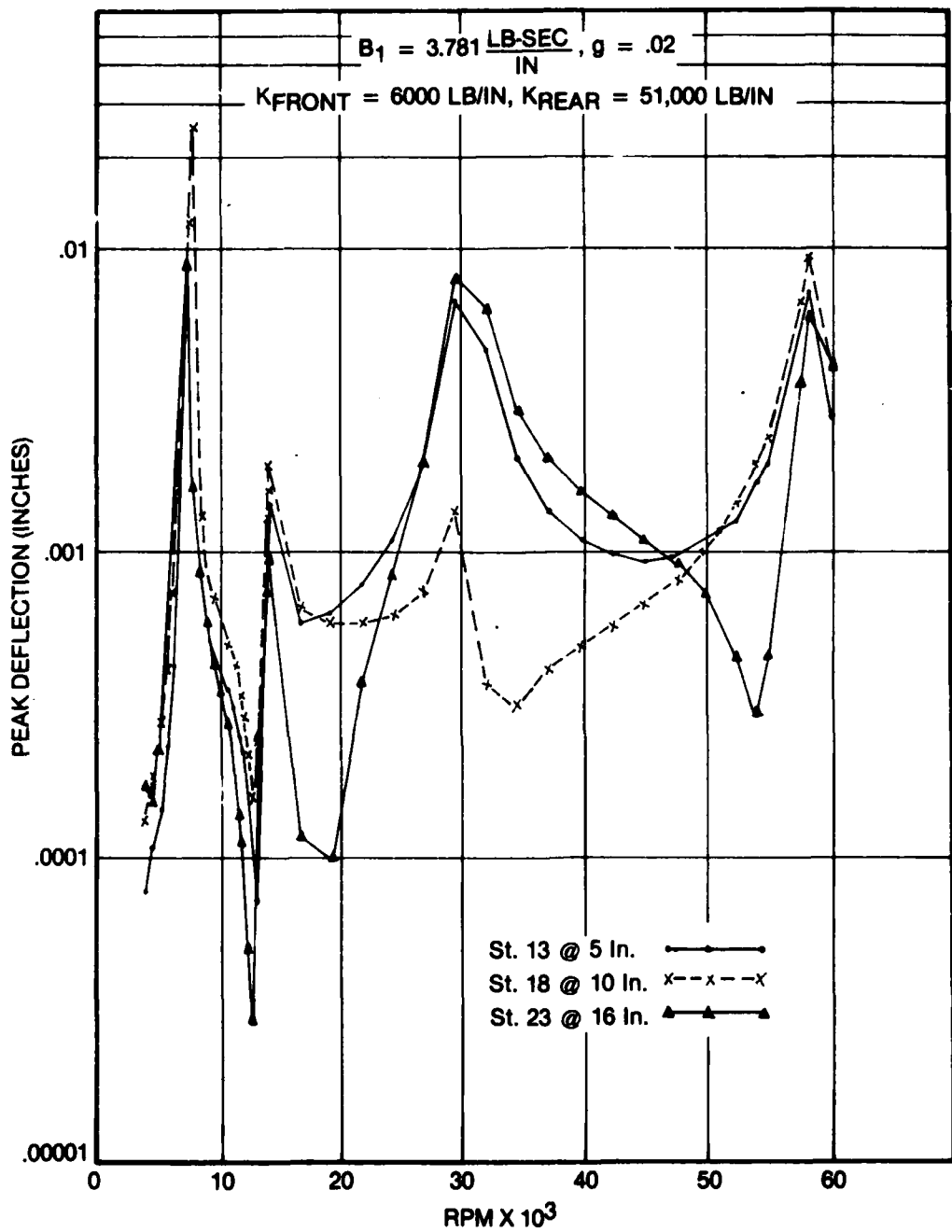
Figure 16. 471-11DX LP Shaft Unbalance Response One Gram
Unbalance at Station 23 (Sixteen Inches From
Front).

28
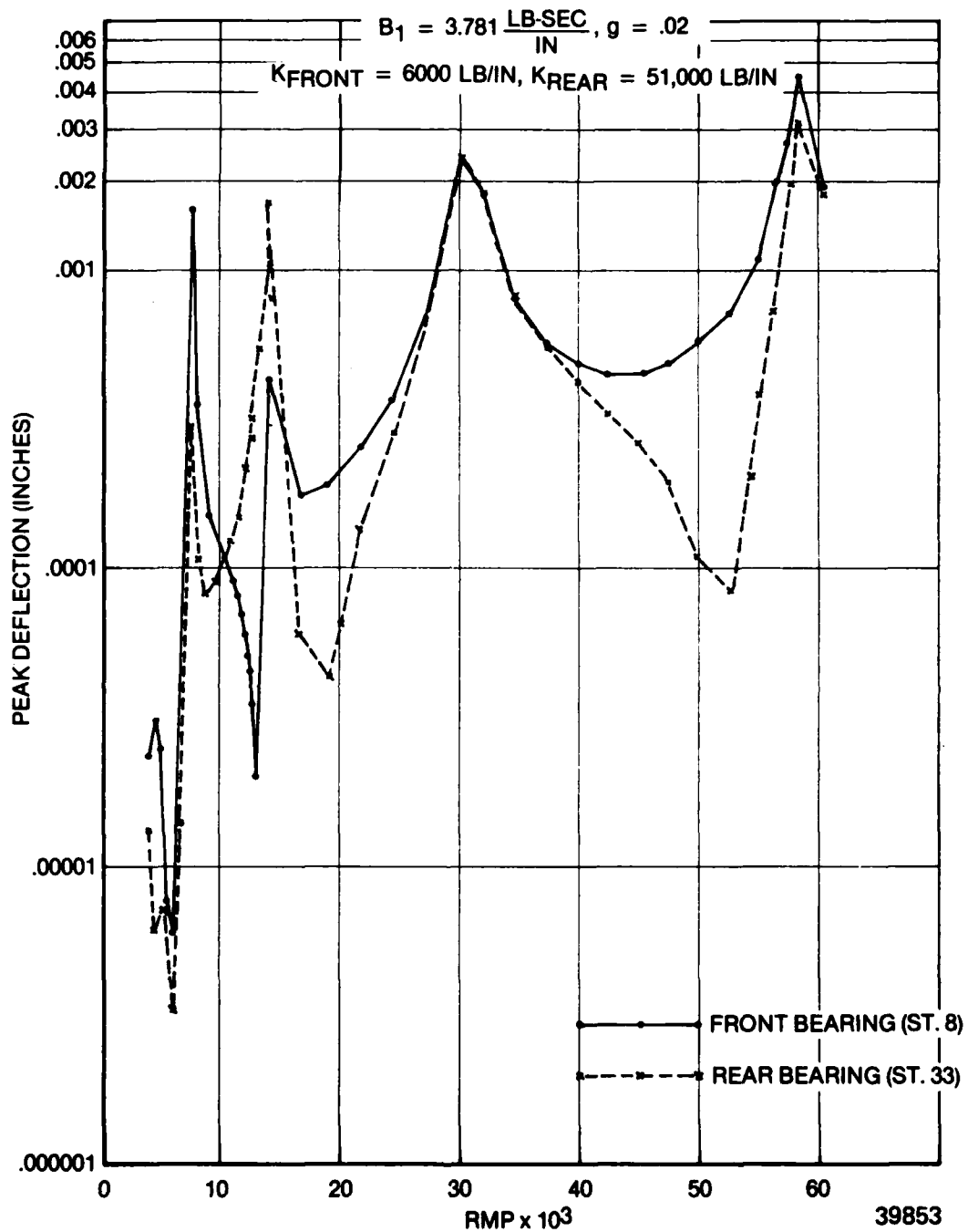
Figure 17. 471-11DX LP Shaft Unbalance Response One Gram
Unbalance at Station 23 (Sixteen Inches From
Front).

29
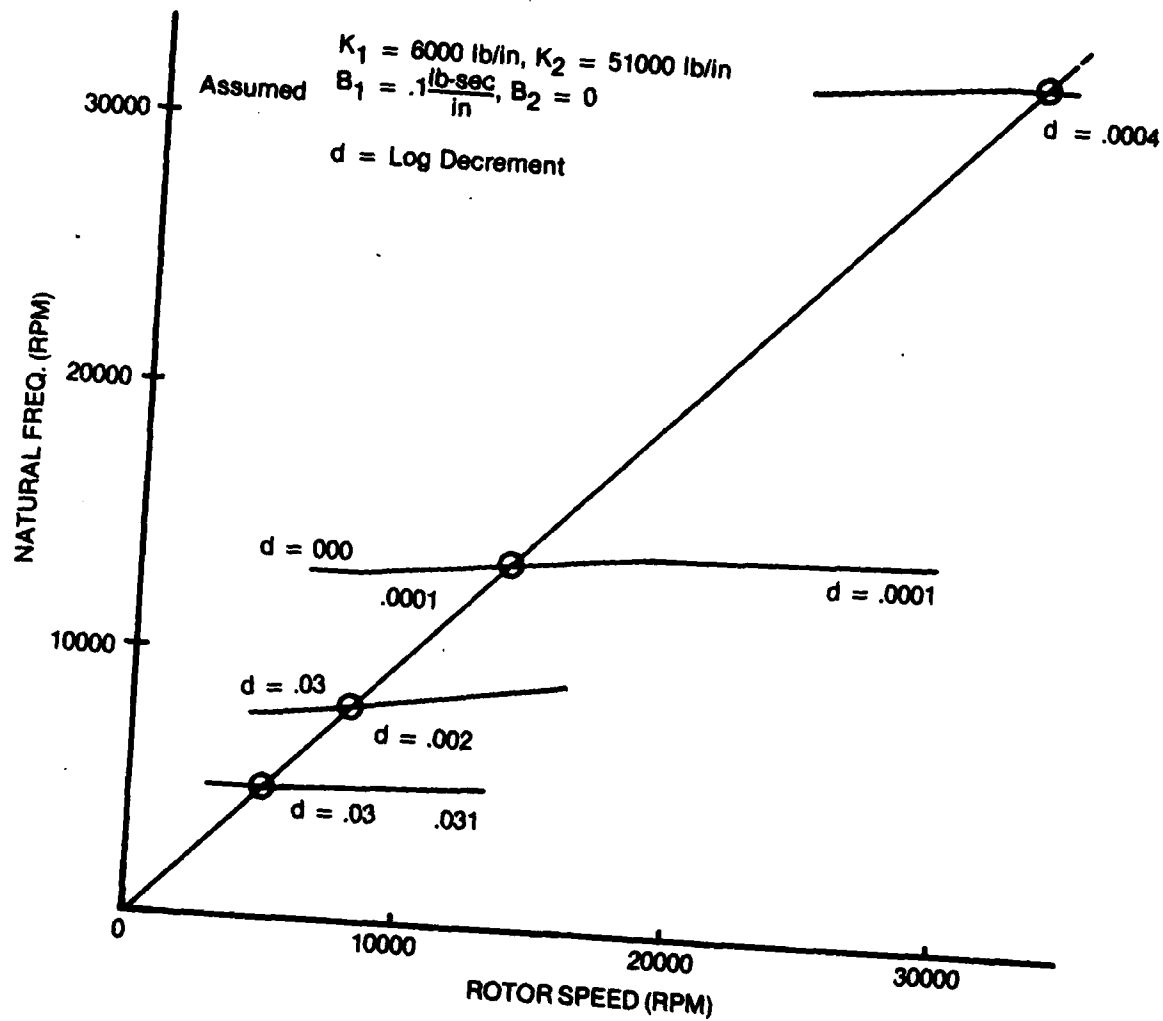
Figure 18. Damped Natural Frequencies of Modes With Low
Assumed Damping Values.

39861

K₁ = 6000 LB/IN, K₂ = 51000 LB/IN
B₁ = 6.7 LB-SEC/IN, B₂ = 0.0
d = LOG DECREMENT
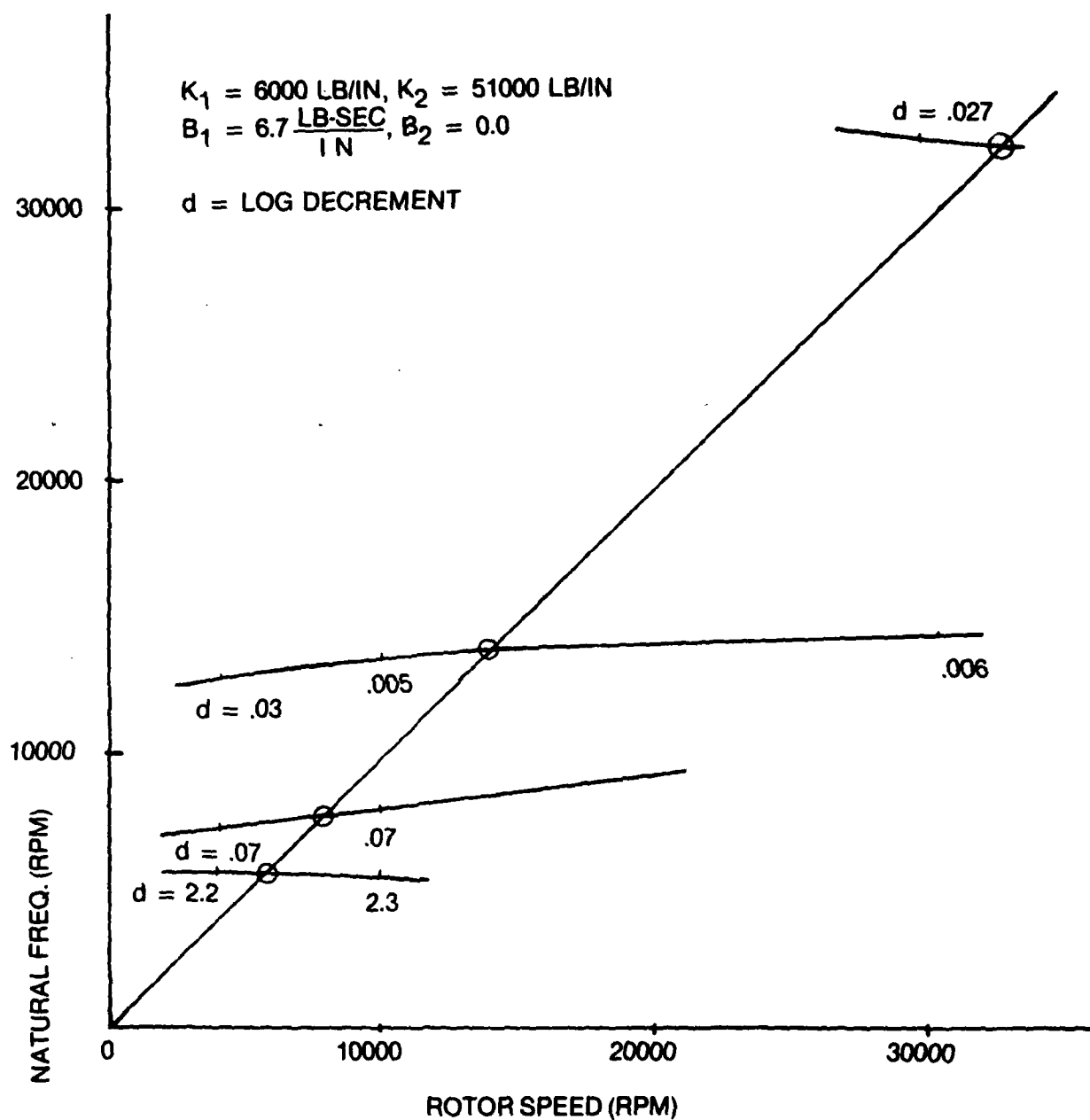
Figure 19. Damped Natural Frequencies of Modes With MTI Calcu-
lated Damping Values.

31

3. RIG DESIGN

The balancing demonstration rig was designed to accommodate the solid LP shaft and as much of the engine hardware as applicable (Figure 20). The bearing support pedestals (Figures 21 through 23) were designed to accurately duplicate actual engine hardware stiffnesses. The rig was designed to be enclosed in a vacuum chamber (Figure 25) to reduce the power requirements on the available drive air turbine.

a. Existing Hardware Review

A review of the available engine hardware which comprise the non rotating parts associated with the LP rotor showed that the following parts were required as new design items: front and rear bearing support pedestals, oil lubrication system, oil supply for front squeeze film damper, proximity probe bracket for sensing shaft motion in four planes, spline drive coupling from air turbine drive to the LP rotor, and a vacuum chamber to house the balancing rig and reduce the power requirements for the drive air turbine.

b. Adaptive Hardware Layout

The final design of the adaptive hardware and vacuum chamber was completed prior to the interim review meeting with AFWAL.

4. FABRICATION AND PROCUREMENT

a. Shaft

The solid LP shaft was a newly fabricated item to which a second stage turbine disk was electron beam welded after being cut off of an existng LP shaft. The fan shaft was also a newly fabricated item.

b. Rig Adaptive Hardware

All of the balancing rig adaptive hardware was newly fabricated for this program as was the vacuum chamber.

5. BALANCING DEMONSTRATION

a. Test Plan

(1) Background

The purpose of the balancing test was to demonstrate the applicability of multi-plane multi-speed balancing techniques in reducing unbalance related vibration in a prototype solid LP shaft cruise missile rotor. Analyses have shown that the rotor will traverse four critical speeds within its 38,000 RPM operating speed range.

32

Figure 20. Solid LP Shaft With Adaptive Hardware.
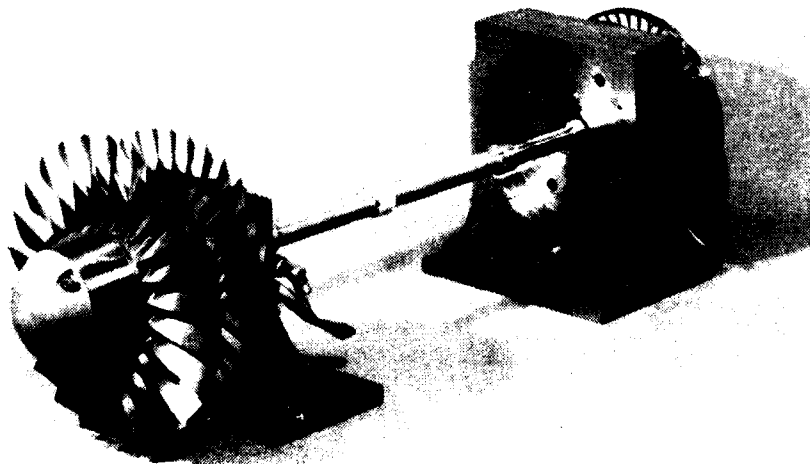
Figure 21. Solid LP Rotor Assembled in Bearing Pedestals -
Fan End View.
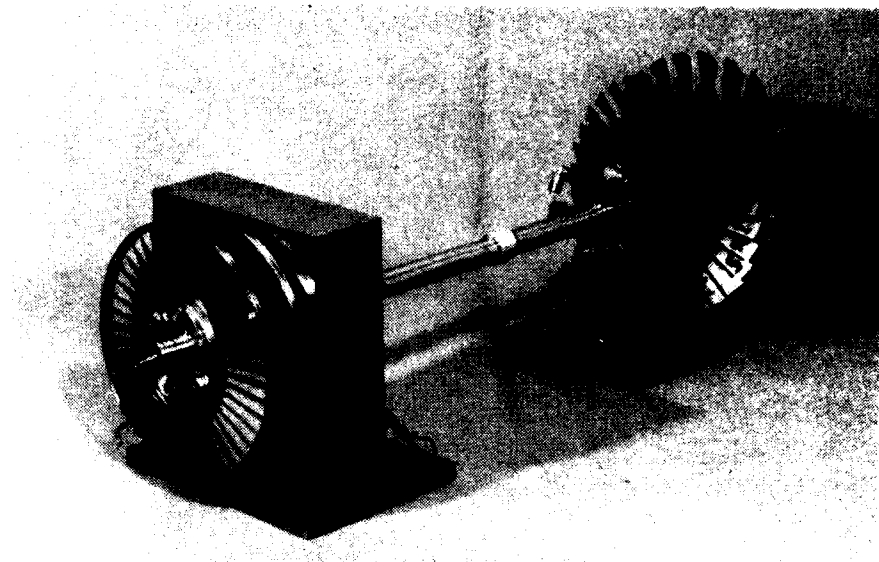
18213   39876

Figure 22.   Solid LP Shaft Assembled in Bearing Pedestals -
             Turbine End View.
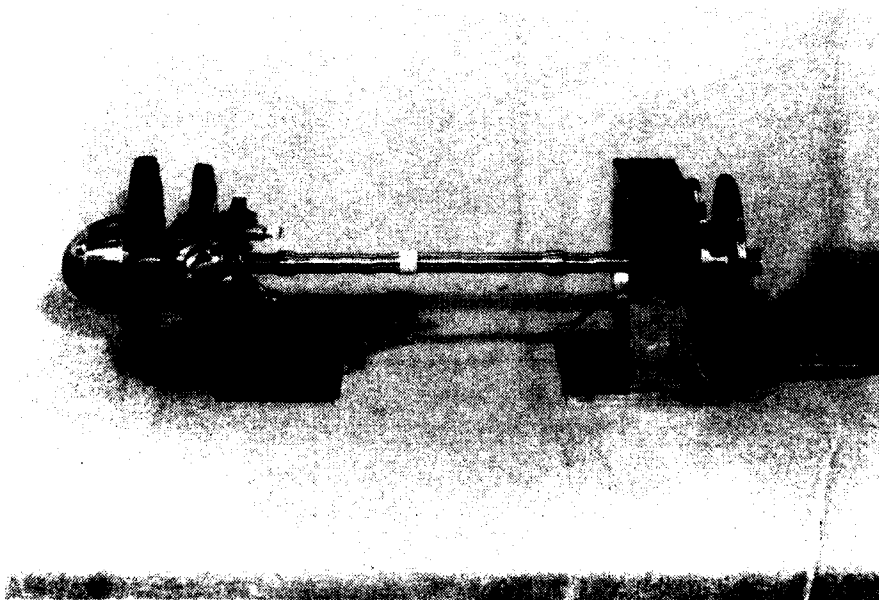
18215   39877

Figure 23.   Solid LP Rotor Assembled in Bearing Pedestals
             (Side View).

18024   39878
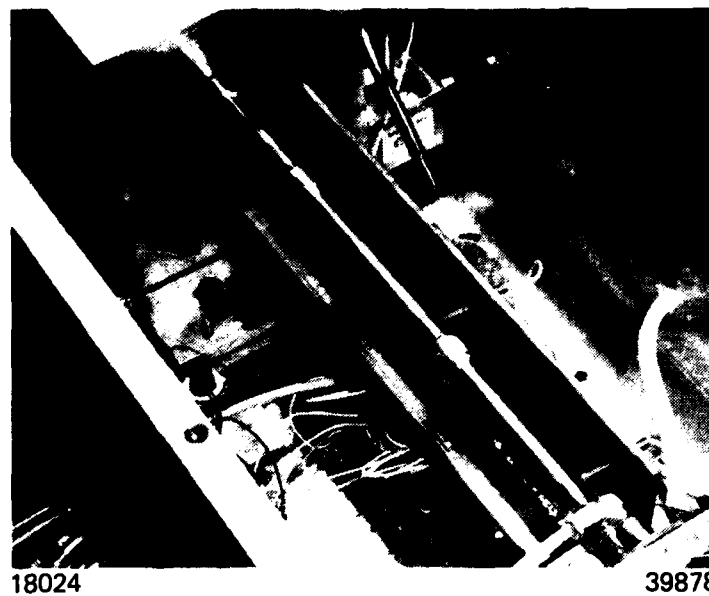
Figure 24.   Solid LP Rotor Assembly in Balancing Rig and
             Vacuum Chamber.

18022   39879
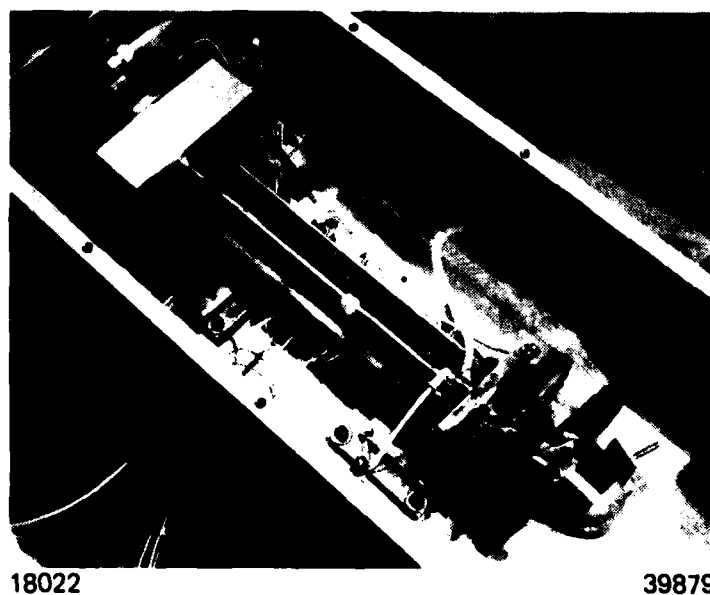
Figure 25.   Solid LP Rotor Assembled in Balancing Rig and
             Vacuum Chamber.

(2) Test Plan

(a) General Procedure

For flexible shaft balancing, data are usually taken at speeds just below the shaft's critical speeds. If the shaft is to be balanced through more than one critical, it is often impossible to safely traverse (because of excessive rotor vibration) the lower critical speed to take balancing data at higher critical speeds. It is then necessary to perform an "intermediate" balance to correct shaft response to the lower critical speed. Subsequent balances can then correct response at higher critical speeds as well as at the lower critical speed.

(b) Predicted Critical Speeds and Balancing Locations

Rotordynamics analyses resulted in predicted rotor critical speeds at approximately 5,000, 8,000, 14,000 and 30,000 RPM. Based on calculated mode shapes, three balancing planes were located along the shaft. Depending on the actual amount of rotor unbalance, the balancing planes at the center and forward end of the shaft should be most effective in reducing vibration for the first three critical speeds. At the fourth critical speed, the center balancing plane should be almost nodal, and the end balancing planes would be more effective in reducing unbalance.

(c) Balancing Criteria

The objective of the high speed balancing effort was to maintain acceptable unbalance related bearing loads at maximum rotor speed as well as limit maximum shaft deflection (and stress) through each critical rotor speed.

Final balancing criteria was to be established during balancing tests based on actual rotor behavior and response. The criteria used were: bearing loads at operating speed: 50 lb (front), 100 lb (rear), maximum shaft deflection through critical speeds: 0.04 inch (peak-to-peak)

(d) Trial Weights

Analytical studies indicated that the rotor was very sensitive to mass changes, especially at the shaft balance planes. Calculations showed that although the mode shapes would remain relatively unchanged, the added mass of balancing collars at the three shaft balancing planes could significantly alter the rotor's critical speeds. The added mass from the balancing collars would also lower the fifth critical speed to a speed just above the maximum rotor RPM. The final impact of the balancing collars was that, while in place on the shaft, they would prevent rotor disassembly. This disassembly/ reassembly check simulates the disassembly required to install the shaft in the engine case. Use of balance collars for the

36

balancing tests was eliminated, therefore, in favor of presssure sensitive lead tape for initial trial weights. This tape would be effective in providing the amount of trial weight mass required without adding a large amount of mass to the overall rotor. Because of the small increase in shaft diameter at the balance planes, the tape would also allow rotor components to be disassembled and reassembled without interference.

(e) Check Run

After high speed balancing had been successfully completed (and with the trial weights in place), it was planned to disassembly the modified LP shaft. This action would simulate the disassembly required to install the shaft in the engine case. The shaft would then be reassembled and installed in the demonstration rig. A check run of the reassembled shaft and comparison to pre-disassembly vibration levels would indicate the change, if any, in unbalance that could be anticipated when a balanced shaft is installed in an engine case. This evaluation might also suggest modifications in assembly tolerances and reveal the effect of shifted components on shaft unbalance.

Only one disassembly/reassembly check run was planned at this time. Final decisions regarding this effort were to be made based on the observed changes in vibration, as well as schedule and funding restraints.

(f) Grinding of Final Correction Weight

Following disassembly/reassembly checks, the final correction weights were to be ground on the rotor. Pre and post-balance shaft responses of the first and second rotor assemblies were to be compared.

(g) Rotor Operation With All Engine Bearings

At the conclusion of all balancing and check runs, the balance rig rear ball bearing was to be removed from the rotor and replaced with the engine roller bearing. Operation of the rotor in the low thrust condition (vacuum chamber) of the balancing rig without positive preload on the remaining engine ball bearing might cause bearing skidding, instability, overheating and possible reduced life and/or damage to the bearing and rotor system. The balancing test rig was designed to accommodate the engine roller bearing. MTI planned to perform this final test of the rotor within the schedule and funding constraints established.

(h)   Impact of Actual Test Data on Test Plan

A prime consideration concerning details of the high speed balancing test plan is an on-the-spot analysis of actual test data. Actual critical speeds and rotor response may differ from calculated values, thereby necessitating modification of the plan for subsequent balancing runs. This test plan was intended to serve only as a guide to the tests to be conducted. The actual test sequence depended on evaluation of the test data acquired in process.

b.   Low Speed Balancing

Prior to the multi-plane high speed balancing demonstration the assembled solid LP rotor was low speed check balanced, and a permanent correction weight of .94 inch grams was ground on the turbine end of the rotor. The correction on the fan end was not installed; however, its magnitude and angle were recorded so that, if required during high speed balancing, a correction weight could be added.

c.   Rig Checkout

The balancing rig with the LP rotor system was checked out at low speed for alignment, bearing lubrication, air turbine drive control, and proximity probe response.

d.   Multi-Plane High Speed Balancing

This section describes the actual balancing of the LP turbine rotor. Details of balancing methodology, monitoring instrumentation and balance weight addition are discussed.

(1)   Instrumentation

Primary vibration measurements were from Bently Nevada displacement probes placed at the nose cone, adjacent to the first and second balance lands, and at the second turbine stage.

Signals from the instrumentation were input to oscilloscopes for visual display, to an X-Y plotter and tape recorder for record purposes, and to an MTI Command^{tm} Balancing System for calculation of balance weights.

Additional instrumentation included:

o   Thermocouples for each bearing.

o   Air temperature thermocouple sensing probe environment.

38

o   RPM/Zero phase indication from a fiber optic
     system.

o   Vacuum gauge.

(2)   Trial and Balance Weight Addition

        Three different weight-addition methods were
required. At the nose cone precisely weighed washers were
placed under the bolts. On the shaft balance lands, lead tape,
cut into strips and stacked as required, was used. Fiberglass
packing tape was then wrapped to secure the weight. At the
turbine stage, safety wire was twisted around the appropriate
blade. Permanent balance corrections on the shaft were made by
hand-grinding on the appropriate balance land.

(3)   Results by Configuration

        Because engine hardware modifications were
required to progress to higher rotor speeds, the results of the
balancing tests are presented by rotor configuration. Appendix
C includes sketches of the various configurations and a brief
summary for each.

(a)   Initial Configuration

        Initial tests were conducted with the shaft
and supports in the as-received condition. The damper assembly
was installed and damper oil was supplied to the damper. Lube
oil was supplied to both bearings in the form of oil mist.

        Figure 26 shows the vibration response of
the rotor in the as-received condition for shaft center vertical
probe. Maximum speed attained was 7,500 RPM. Using the center
balancing land, speed was gradually increased with repeated
balancing steps until the rotor became unstable at a speed
running of 11,500 RPM. Figure 27 represents the maximum speed
run for this configuration. The dips in Figures 26 and 27 are
phenomena of the non-contacting proximity sensors and run out of
the shaft. Figures 28 and 29 show the rapid growth of the
subsynchronous vibration (9,000 CPM) that prevented reaching
higher speeds. Attempts to investigate the instability were
hampered by poor rotor repeatability. It was decided to
disassemble and carefully examine the rotor for the source of
the non-repeatability. Disassembly revealed no sign of oil in
the damper surface between "O" rings. It was discovered that a
bleed hole designed to permit entrapped air to be forced out of
damper and allow oil to enter, had not been drilled in the part
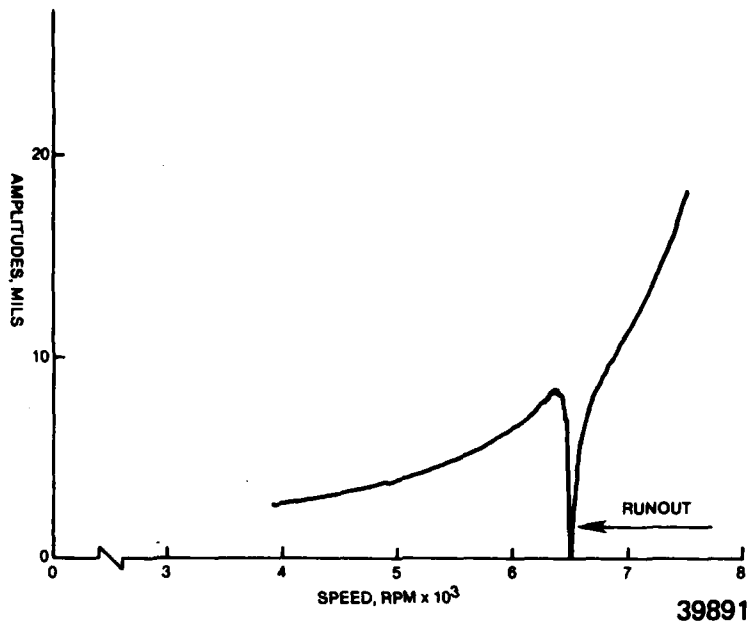sent to MTI. This modification was made at MTI and the rotor
was reassembled.

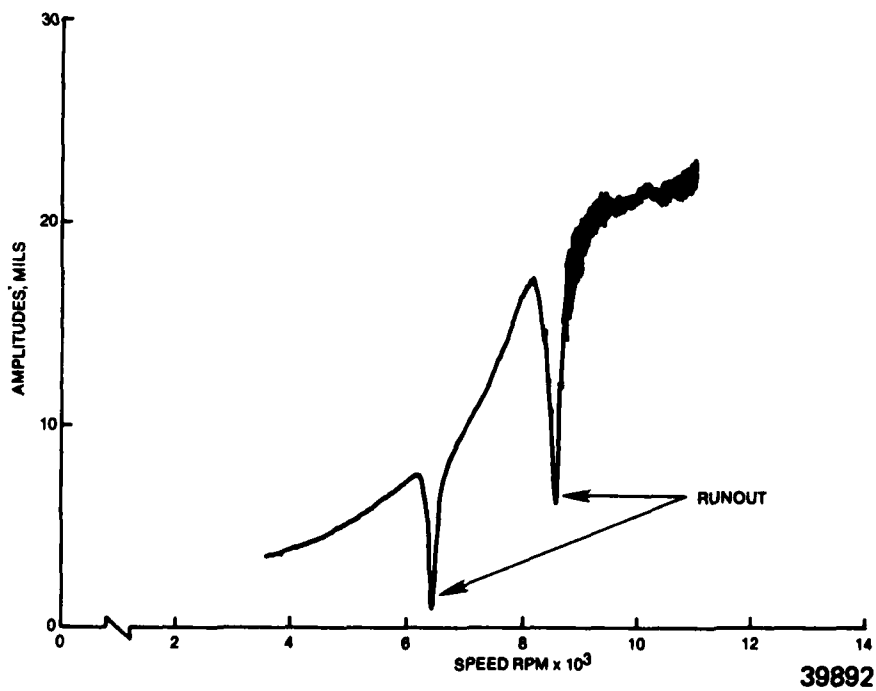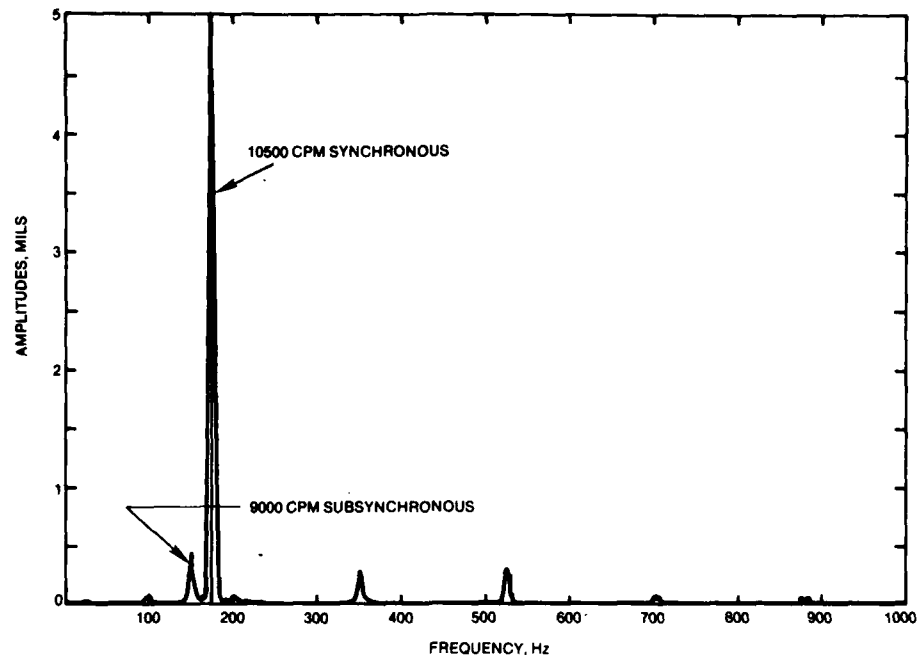Figure 26.   Initial Configuration Mid Span Amplitudes.

Figure 27.   Initial Configuration Mid Span Amplitudes.

40

39880

Figure 28.   Initial Configuration Onset of Instability.
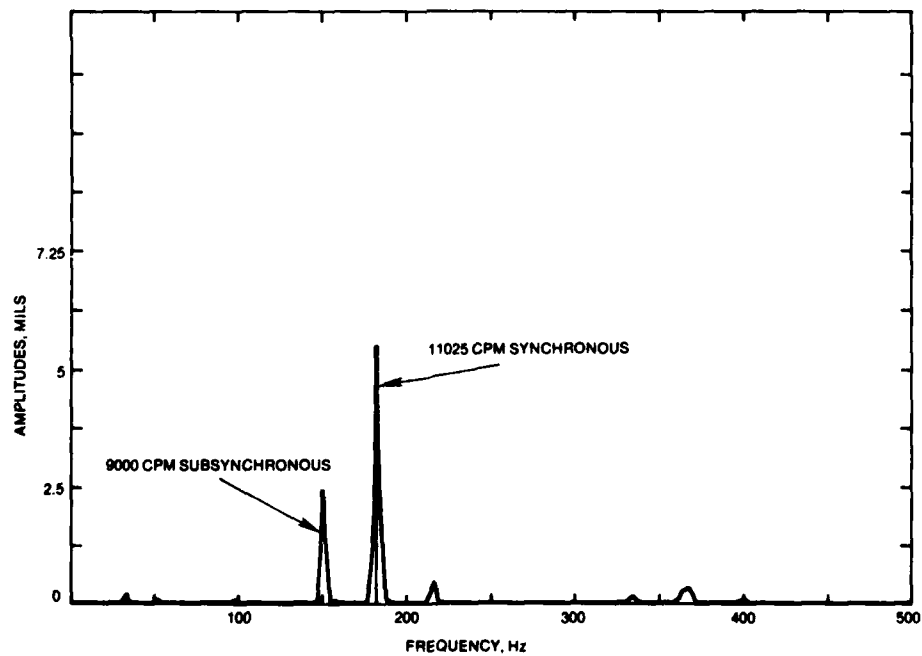
39881

Figure 29.   Initial Configuration Growth of Instability.

41

(b)   Positive Oil Flow to Damper Surface

A repeat of the best balance from the previous configuration was performed with the positive oil flow to the damper. This resulted in a much cleaner speed amplitude curve with a well defined peak at approximately 9200 rpm (Figure 30). The 9000 rpm instability was still present, this time at 12,500 rpm running speed. The observed second mode did not correlate closely with the analytically predicted second critical speed of 8000 rpm and the discrepancy is probably related to the description of the analytical model. Closer agreement could have been achieved by fine tuning the model; however, the important consideration is that the calculated and running mode shapes agreed. Figure 31 shows the instantaneous vibration spectrum for both 9000 rpm running speed (approximate location of mode) and 12,500 rpm (onset of instability). It appeared that the instability was caused by excitations of the mode at 9000 rpm. The harmonic components of the synchronous running speeds in Figure 31 are geometry related and probably due to misalignment. They were stable during the runs, and therefore of no concern. In contrast, the sub-harmonics were unstable and practically "exploded" in amplitude during running. The harmonics could have been a problem had they occurred at higher critical speeds.

In an attempt to refine the balance, a two-plane two-speed balance was performed using the nose cone and the shaft center. Although this attempt successfully reduced rotor amplitudes, the rotor instability was unaffected. To determine if the instability was damper related, the outer damper housing was removed, thereby eliminating the damper.

(c)   Damper Removed

With damper removed, the first critical speed (approximately 5,900 RPM) was no longer critically damped. Maximum speed reached with previous correction weights was 5,100 RPM. A single plane balance at the nose cone sufficiently reduced amplitudes to pass through the 5,900 RPM mode and acquire data at 8,600 RPM. Using the nose cone and shaft center, a two-plane two-speed balance permitted operation through both modes to 14,000 RPM with no signs of instability. Due to concern about losing the lead correction weight at the shaft center at higher speeds, it was decided to make a permanent correction by grinding the center balancing land on the shaft. Figure 32 presents the results of the center shaft rotor amplitudes after grinding the permanent correction.

A trim balance was performed at the center shaft since the amount of material actually removed by grinding was difficult to evaluate. With the trim weight installed, the rotor was operated to 18,000 RPM.

Figures 33 through 35 show vibration amplitudes at the nose cone, shaft center and turbine. A failure of the front bearing halted further testing. It should be noted
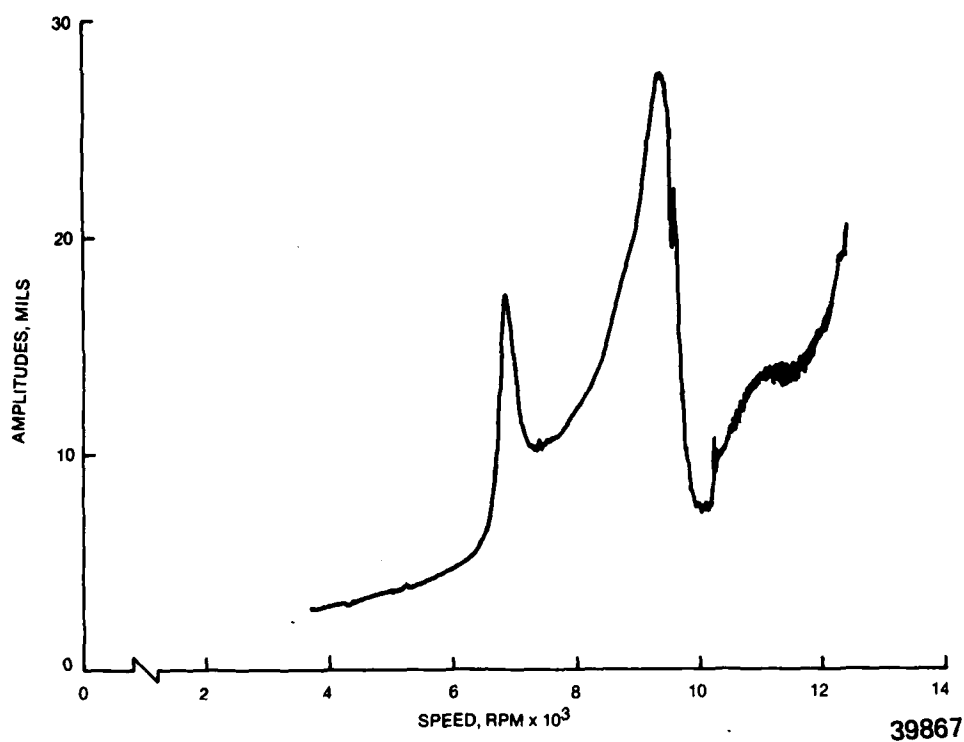
Figure 30.   Positive Oil Flow to Damper Mid Span Amplitudes.
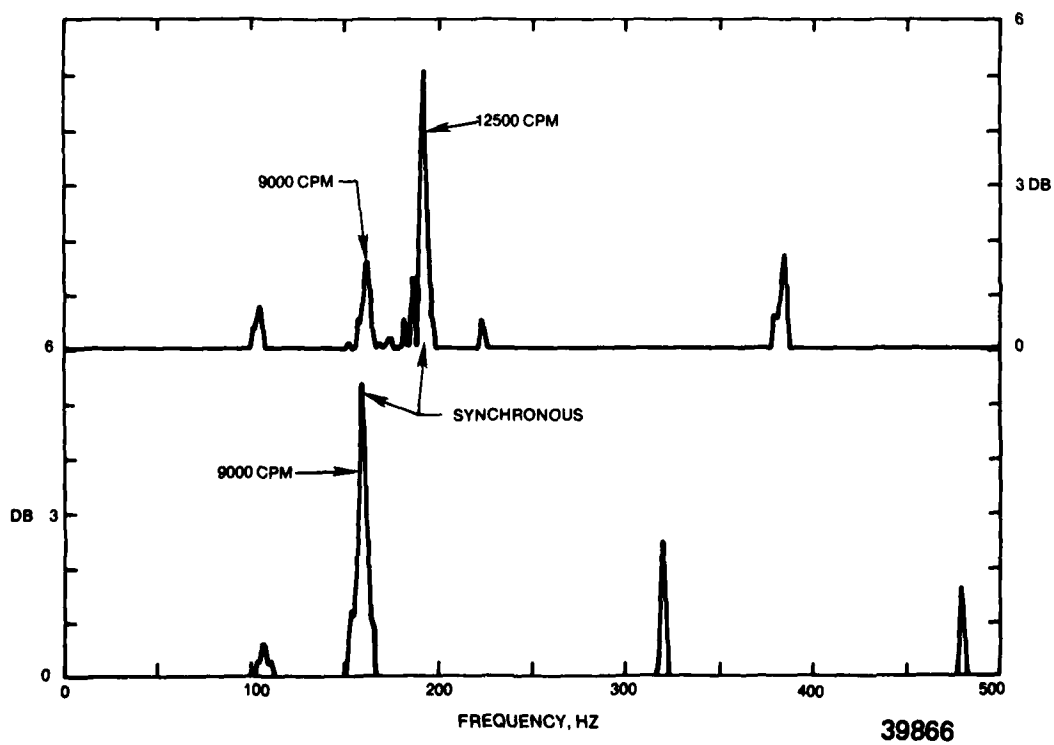
Figure   31.   Positive Oil Flow to Damper.   Frequency Spectrum
at 1st Mode and at 12,500 rpm.

43
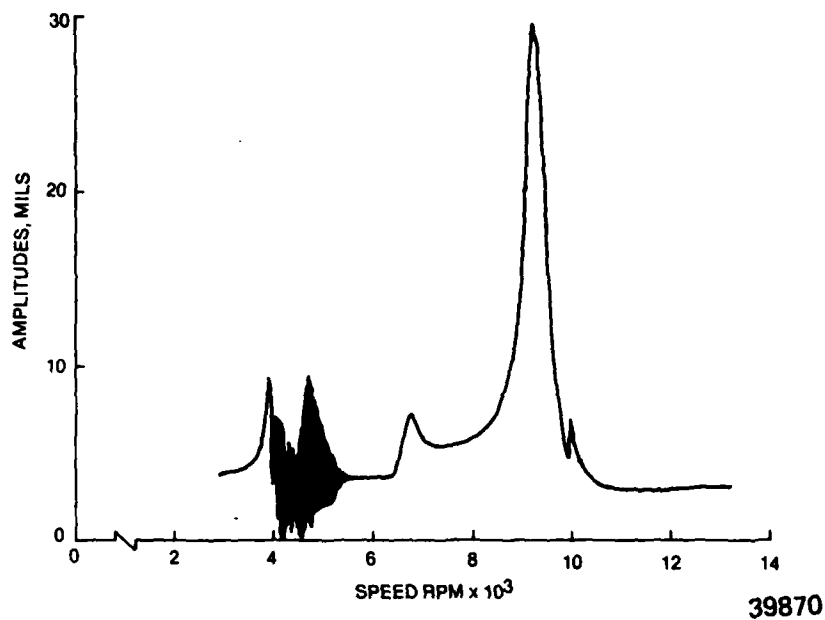
Figure 32.   Damper Removed Mid Span Amplitudes.
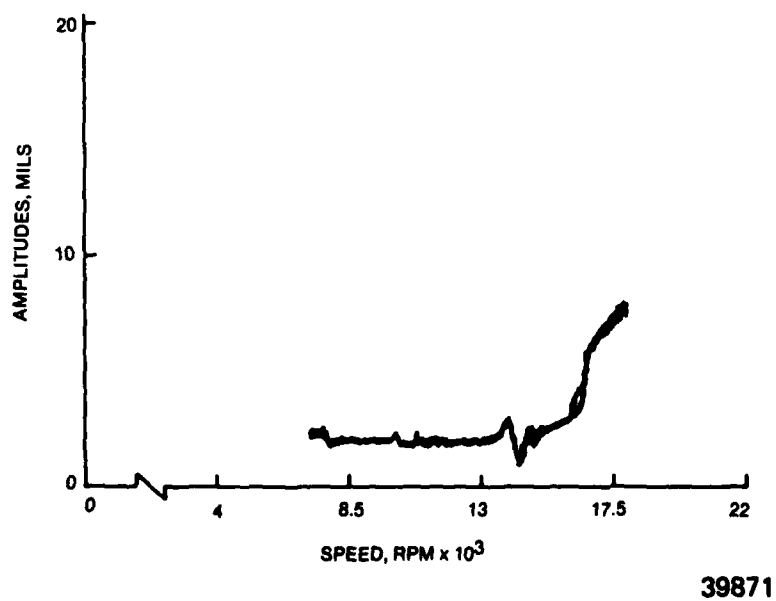
Figure 33.   Damper Removed Nose Cone Amplitudes.

44
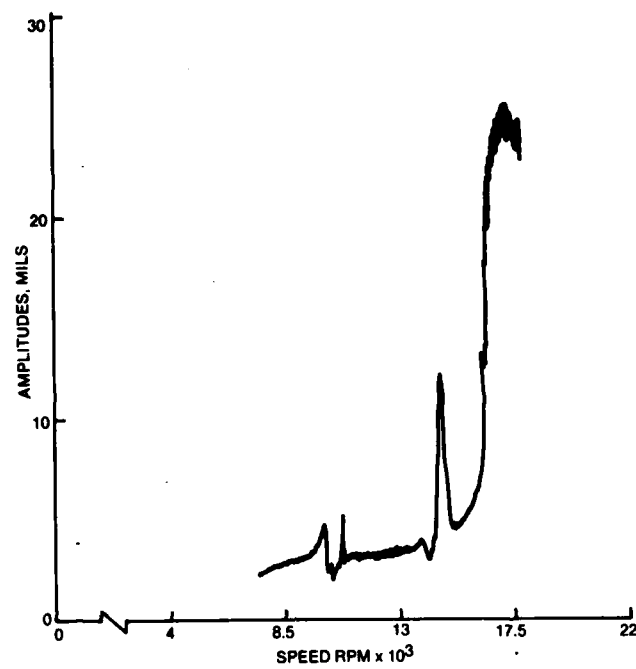
39889

Figure 34. Damper Removed Mid Span Amplitude.
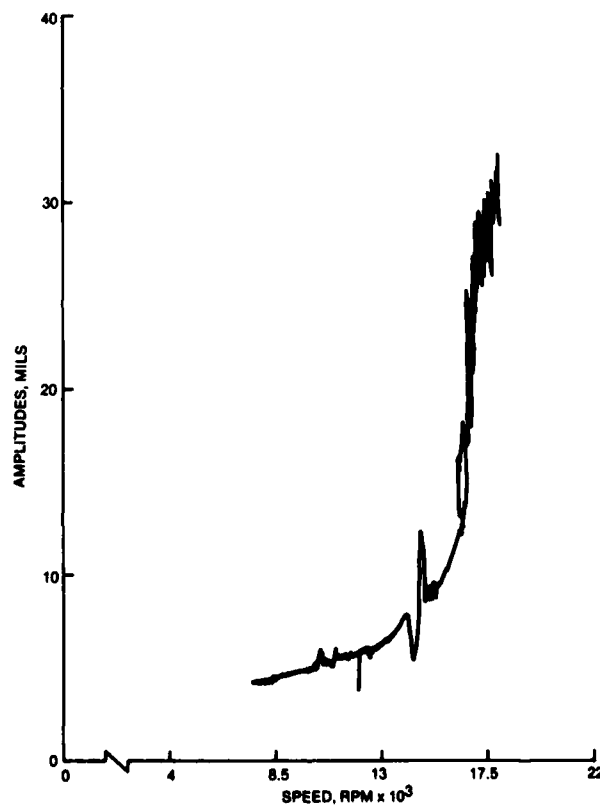
39890

Figure 35. Damper Removed Turbine Amplitudes.

45

that the aft bearing amplitudes were significantly higher than the forward bearing at the top speed (as predicted by the response analysis in the vicinity of the third mode). Disassembly of the front bearing also revealed fractured front flexures in the forward bearing support.

Possible causes of bearing failure:

o   Foreign material from grinding permanent correction.

o   Excessive loading from previous runs.

o   Insufficient oil to dissipate heat build-up in bearing.

Possible causes of flexure failure:

o   Excessive displacement while traversing first mode without damper.

o   Heat from bearing failure.

o   Instability related-oscillating amplitudes.

A new front bearing and bearing support were installed, and the rig was reassembled. The damper housing was reinstalled without "O" rings or damper oil supply. The function of the damper housing in this new configuration was only to act as a "bumper" by limiting deflection of the front flexures.

(d)   Damper Housing Reinstalled as a Bumper

With the previous correction weights still installed, a three-plane three-speed balance using the nose cone, shaft center and the second stage turbine was performed at 5,200, 8,600 and 16,500 RPM. The resulting correction weights enabled speeds up to 21,000 RPM with low amplitudes at this speed. Additional permanent correction was made at the shaft center. Figures 36 through 39 represent rotor amplitudes for nose cone, first balance land, shaft center and turbine for test runs to 25,000 RPM. The limiting factor was front bearing temperature which reached 330°F at 25,000 rpm. In order to reach higher speeds, the lubrication at this bearing was changed from oil mist to an oil jet.

39857
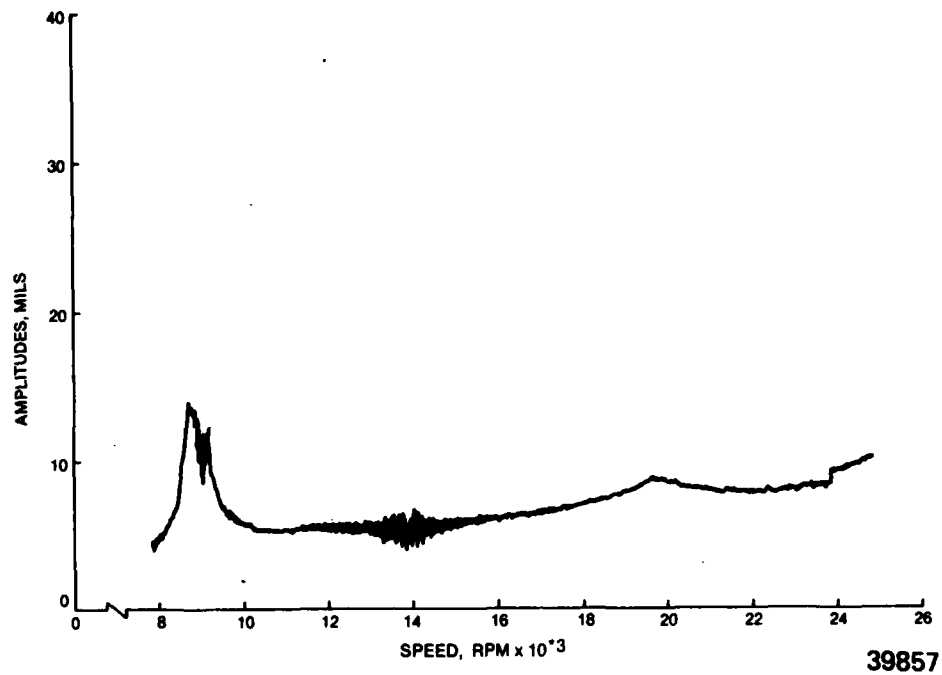
Figure 36. Damping Housing as Bumper - Nose Cone Amplitude.

39858
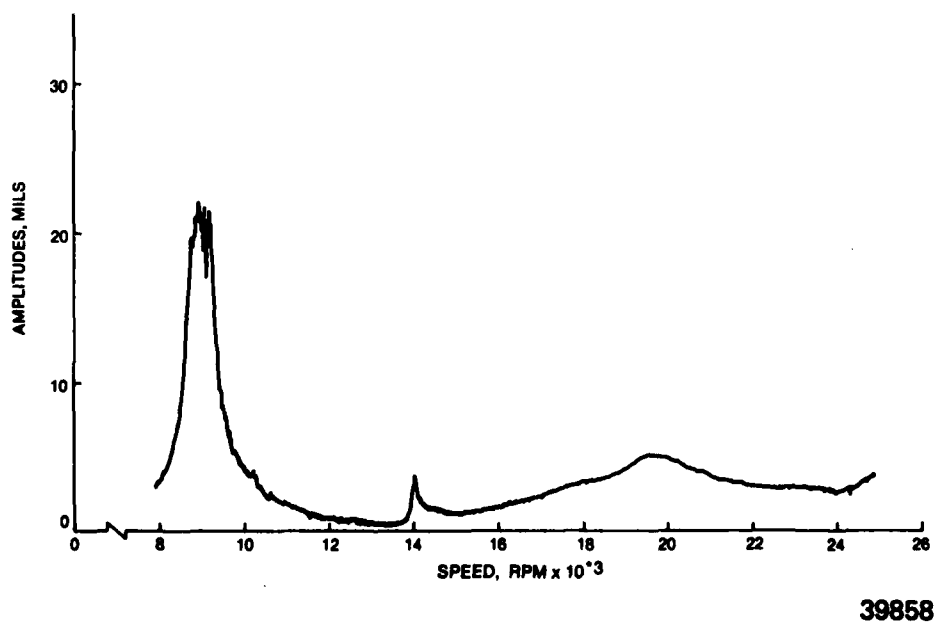
Figure 37. Damper Housing as Bumper - First Balancing Land
Amplitude.

47

39864
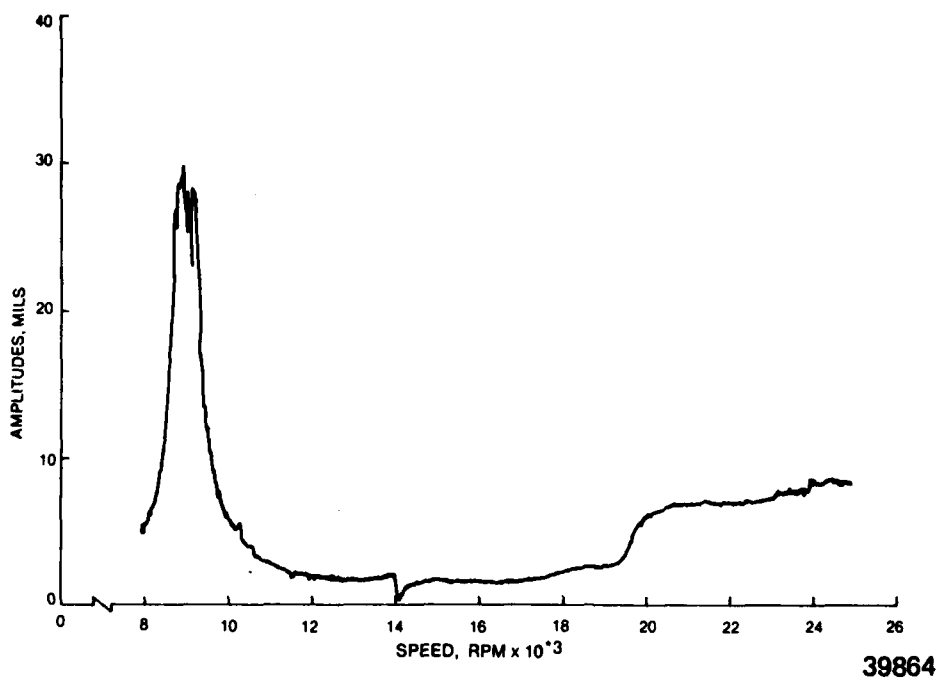
Figure 38.   Damper Housing as Bumper - Mid Span Amplitude.

39865
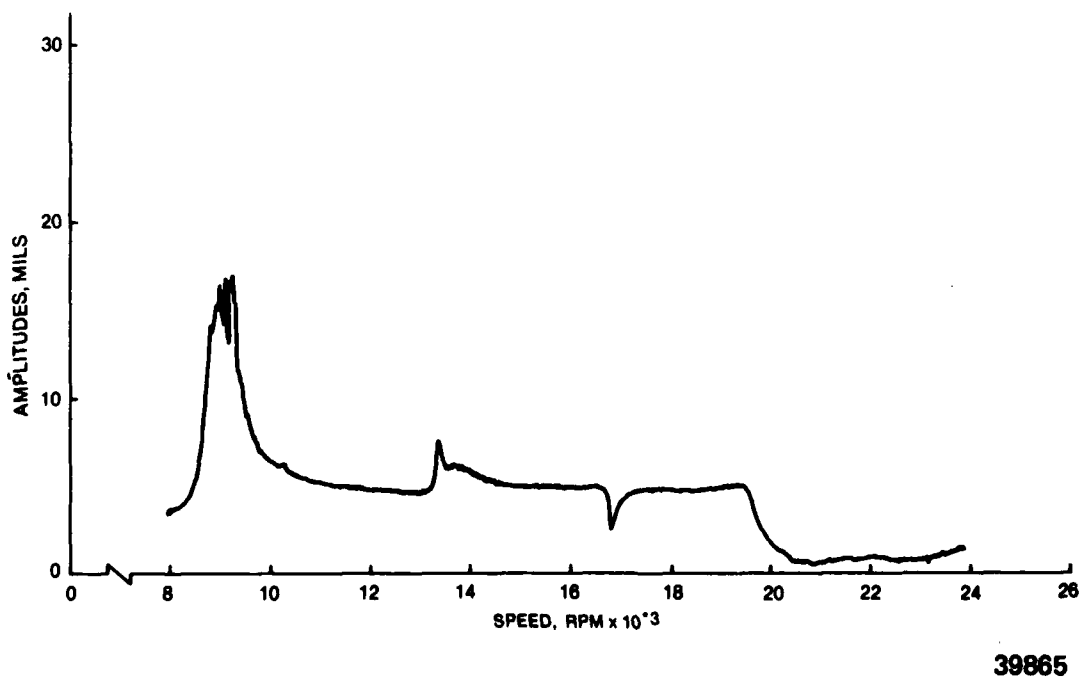
Figure 39.   Damper Housing as Bumper - Turbine Amplitude.

(e)   Oil Jet to Front Bearing

A test run was made to 28,000 RPM. Figures 40 through 43 represent rotor amplitudes for nose cone, first balance land, shaft center and turbine for this run. A marginal instability occurred at 23,000 RPM. On subsequent runs, an instability consistently prevented passing 23,200 RPM. The subsynchronous frequency was 11,700 CPM. This frequency is probably a gyroscopically stiffened second mode. Figure 44 shows a stability map which plots critical frequency versus rotor speed. It can be seen from this figure that the critical frequency of the second mode increases approximately 3,000 CPM with increasing rotor speed, supporting the possibility of the 9,000 CPM instability recurring at 11,700 CPM. Several runs were made to determine if oil supplied to the damper at pressures varying from 10 to 90 psi would effect the instability. No significant change was observed.

The test results indicated that the instability was related to the presence of an active damper on the rotor. It was decided to machine the damper housing to increase the clearance between the damper surfaces, thus minimizing the tendency for the damper to function with small amounts of throw off oil present around the front bearing.

(f)   Modification to Damper Housing

The inner diameter of the damper surface was bored out between "O" rings with a thin land left to act as a bumper. A variety of problems on subsequent runs appeared to be oil related. Some runs encountered the instability after traversing the first mode while other runs resulted in a beating between the second mode and the running speed. The front seal was installed to prevent oil entrapment in fan stage. However, even with the seal installed, large amplitudes of 9,600 CPM subsynchronous vibration at 13,500 RPM prevented operation at higher speeds.

6.   TI-BORSIC SHAFT ANALYSIS AND DESIGN

a.   Shaft Design

The Ti-Borsic LP shaft was designed to satisfy the structural, dynamic and environmental requirements of the Model 471-11DX Turbofan Engine. The primary design criteria for this LP shaft were adequate torsional shear strength to transmit the fan torque requirements and sufficient structural rigidity to avoid deleterious vibrational modes. In addition the shaft must have adequate tensile strength to accommodate the gyroscopic bending moments imposed by the fan and turbine rotors under all anticipated maneuver conditions, and transmit the net axial thrust force between the turbine and fan sections due to pressure and aero dynamic gas loads.

39862
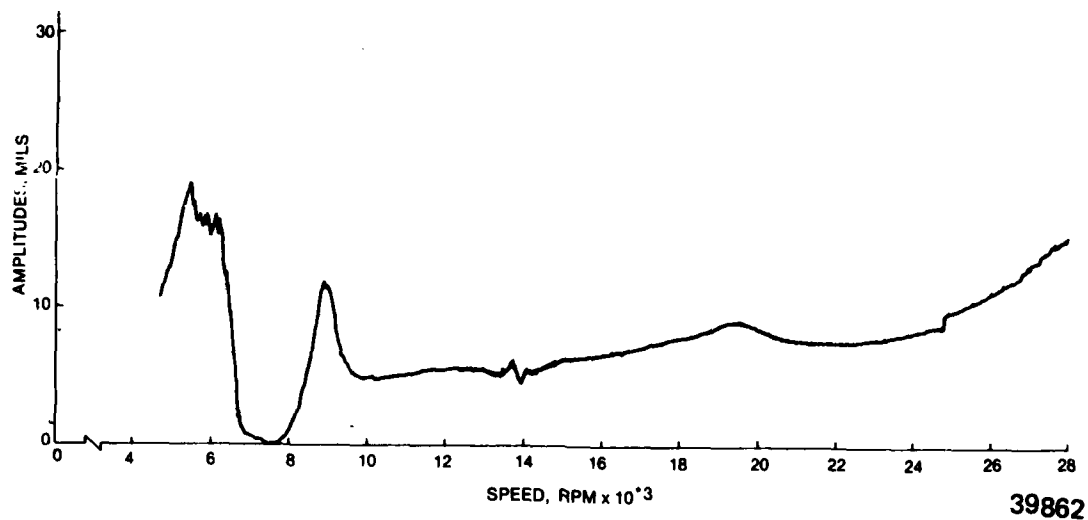
Figure 40.   Damper Housing as Bumper - Oil Jet to Forward
Bearing Nose Cone Amplitudes.

39863
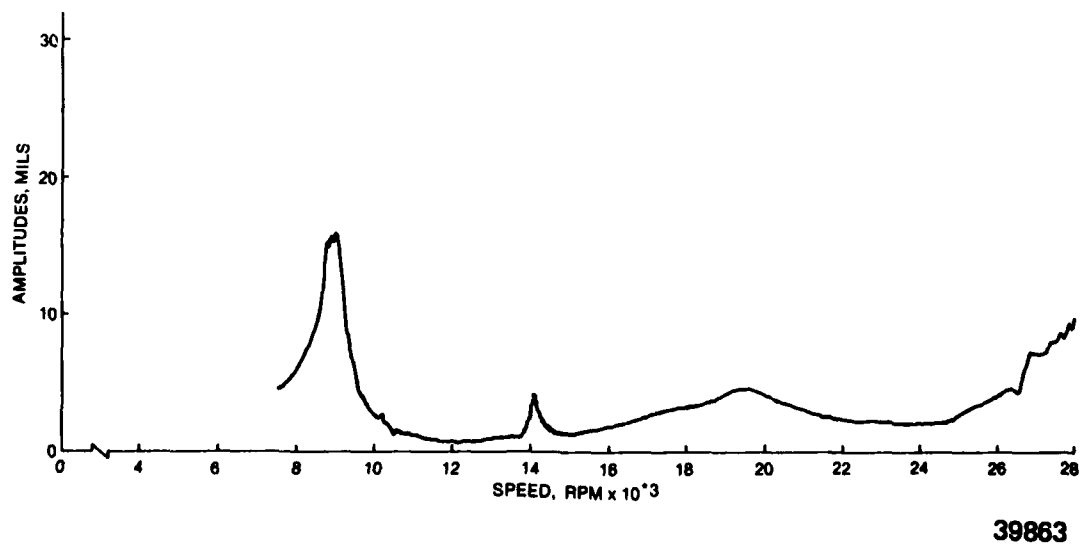
Figure 41.   Damper Housing as Bumper - Oil Jet to Forward
Bearing First Balance Land Amplitudes.

50
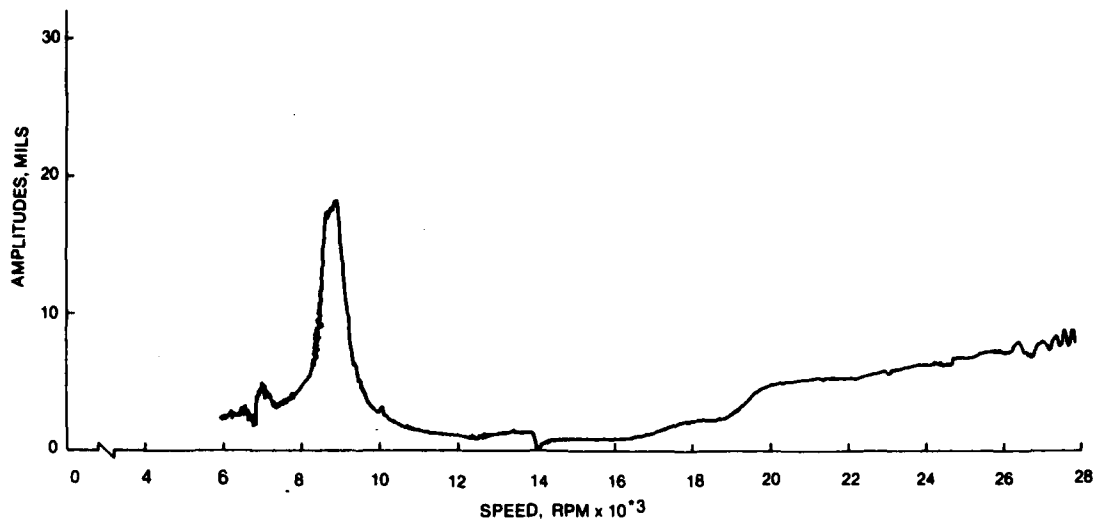
39868

Figure 42. Damper Housing as Bumper - Oil Jet to Forward
            Bearing Midspan Amplitudes.
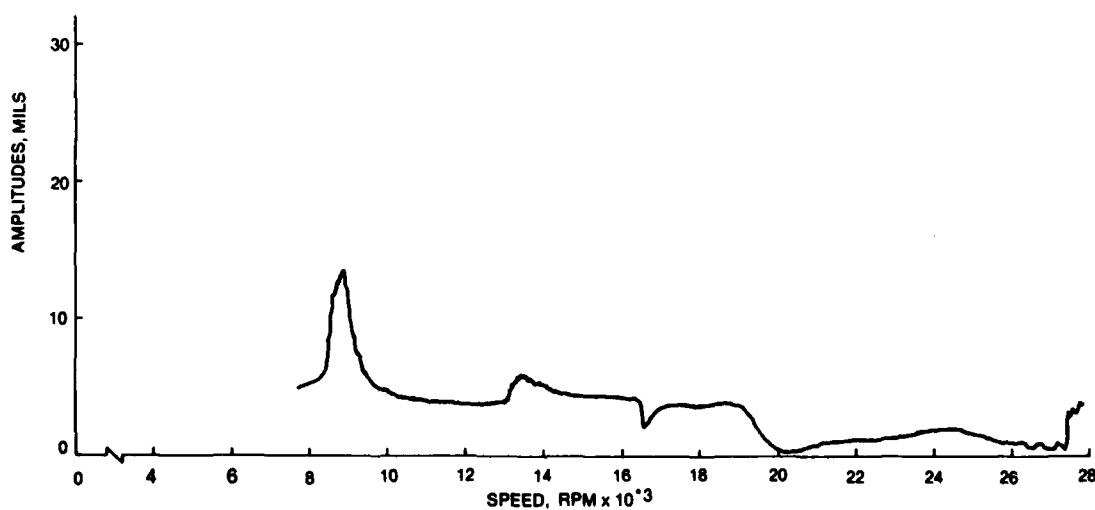
39869

Figure 43. Damper Housing as Bumper - Oil Jet to Forward
            Bearing Turbine Amplitudes.

51
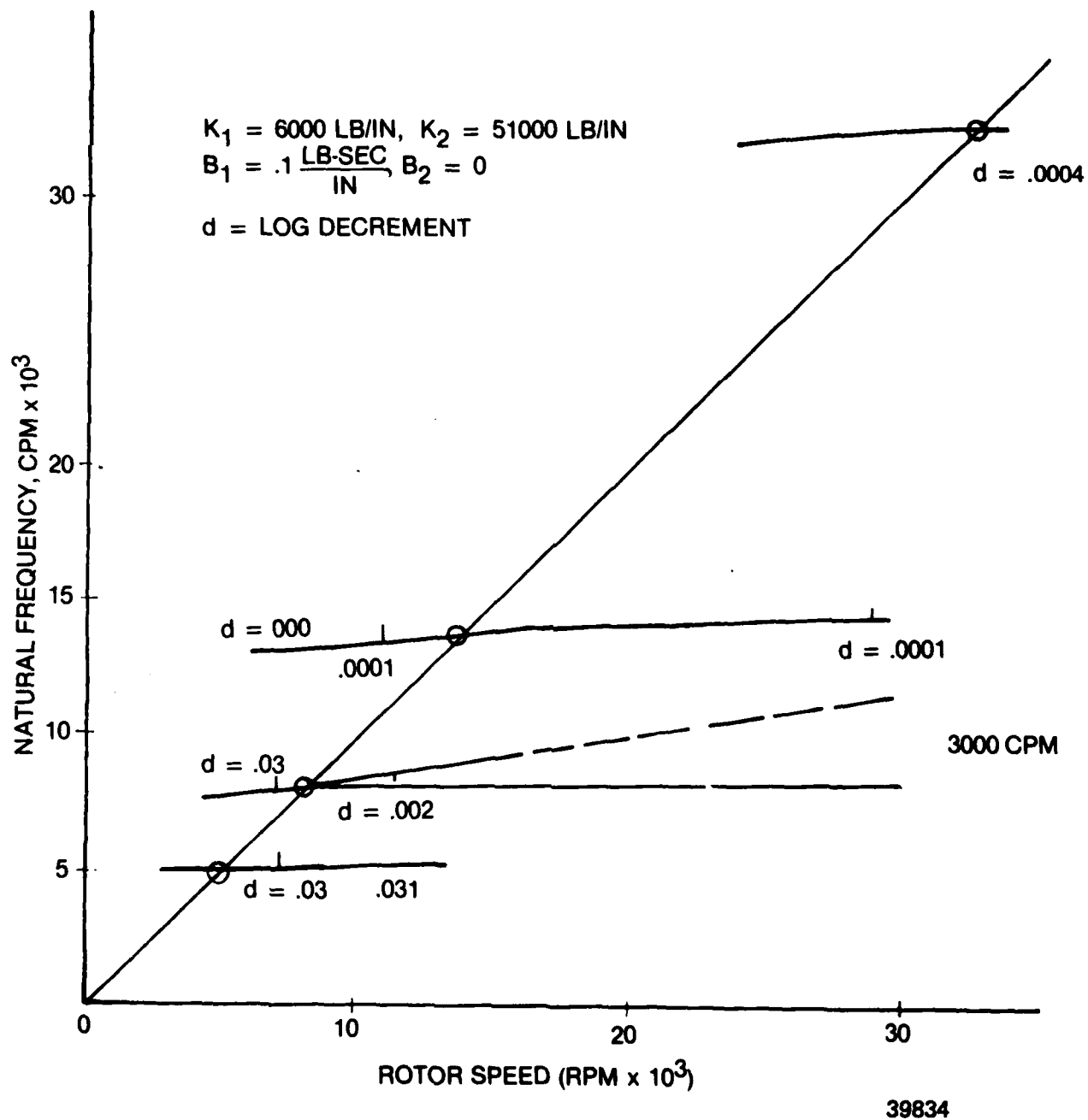
Figure 44. Damped Natural Frequencies of Modes With Low
Assumed Damping Values.

The design criteria were based on the thermal environment imposed by the engine on the shaft and on the attachment of the Ti-Borsic shaft to the turbine and fan rotor sections.

b.   Shaft Adaptation

(1)   Structural Analysis

Structural analyses indicated that the 60/40 TI-Borsic shaft and diffusion bond joint of the composite shaft and end pieces had adequate strength margins for the thermal environment and all imposed loading conditions on the LP shaft. Table 3 and Figure 45 summarize the results.

(2)   Thermal Analysis

The thermal analysis of the Ti-Borsic LP shaft was performed under the following conditions and resulted in the highest shaft operating temperature: 471-11DX cycle at S.L., M = .7, hot day. The shaft is immersed in the oil sump containing oil liquid, oil vapor and air at 500°F and 14.7 psia. The shaft center contains dead air. The tube surrounding the shaft prevents conduction and allows radiant heat exchange only. As a result of the above assumption, the heat flow is radial only and the shaft runs at nearly constant temperature. The shaft temperature is 549°F. Figure 46 depicts the radial temperature distribution at a typical point along the shaft. Figure 47 is a sample calculation at this typical point.

(3)   Undamped Critical Speed Analysis

The undamped critical speed analysis was an iterative process considering various mixture volume percentages for the Ti-Borsic material composition. The shaft geometry was finalized through an iterative process, involving front and rear bearing support stiffness parameters as well as shaft structural properties. The results of the critical speed analysis of the optimized shaft resulted in a third critical speed of 47,397 RPM providing a margin of 24% beyond the maximum LP shaft speed of 38,000 RPM. The composite shaft final design is a Ti-Borsic mixture composition of: 60/40 percent fiber volume, with 1.10 inch O.D., .94 inch I.D. and using front and rear bearing support spring rates of 150,000 and 300,000 pounds per inch respectively.

The critical speed analysis was a matrix solution for a multiple shaft system, see Figure 48, which considers both bending and shear effects, flexible bearing supports, and gyroscopic effects from the attached disks. In the analysis the actual rotor was transformed into an idealized equivalent system consisting of a series of disks connected by sections of elastic but massless shaft. The masses of the disks and their spacing were chosen to approximate the distribution of mass in the actual rotor. The bending flexibility of the connecting

53

4998E

TABLE 3

STRUCTURAL ANALYSIS 471-11DX 60/40 TI-BORSIC L. P. SHAFT

LOADING	AFFECTED AREA	SHAFT STRENGTH PSI/TYPE	TEMP MAX °F	STRENGTH REQ. PSI/TYPE	FACTOR OF SAFETY	MIN DESIGN FACTOR OF SAFETY
TURBINE TORQUE (M$_n$ .85, S.L., COLD DAY)	SHAFT	31,000/SHEAR (1)	550	17,110/SHEAR	1.8	1.5
	DIFFUSION BOND JOINT	70,000/SHEAR (2)	550	3,420/SHEAR	20.0	2.0
GAS LOADS	SHAFT	145,000/TENSILE (3)	550	10,430/TENSILE	14.0	1.5
	DIFFUSION BOND JOINT	70,000/SHEAR (2)	550	2,060/SHEAR	34.0	2.0
UNBALANCE MOMENT LOAD EXTERNALLY APPLIED LOADS	DIFFUSION BOND JOINT	70,000/SHEAR (2)	550	5,410/SHEAR	13.0	2.0
DURING LAUNCH	SHAFT	145,000/TENSILE (3)	550	15,250/TENSILE	2.0	1.5
	DIFFUSION BOND JOINT	70,000/SHEAR (2)	550	1,520/SHEAR	46.0	2.0
DURING FLIGHT	SHAFT	31,000/SHEAR (1)	550	3,060/SHEAR	10.0	1.5
	DIFFUSION BOND JOINT	70,000/SHEAR (2)	550	310/SHEAR	226.0	2.0

Footnotes:

(1) AFML-TR-72-205, Pg. 451: Titanium 6AL-4V Borsic(TM) 50% fiber volume at 600°F (measured value); interlaminar shear strength in fiber direction. This is a conservative rating compared to the 60% fiber volume specified because matrix constraint and triaxial stress state tend to improve shear strength with increased fiber volume percent. NASA Report NAS 3-20390 shows trend of increasing shear strength with increasing filament volume proportion for Fe Cr alloy.

(2) Bulletin #1, Titanium Metals Corporation of America: The strength of each end attachment joint is approximately equal to the shear strength of the titanium 6AL-4V matrix strength of 70,000 psi at 600°F.

(3) AFML-TR-72-205: Titanium 6AL-4V Borsic(TM) 50% fiber volume at 600°F (measured value). This is a conservative rating for the 60% fiber volume specified because longitudinal tensile properties of the composite are primarily dependent on the high modulus, high strength coated boron fibers.

54

FAN INDUCED TORQUE
$T = 2087$ IN-LB

$\leftarrow.44\rightarrow$

$R_0 = .55$

$r_i = .47$
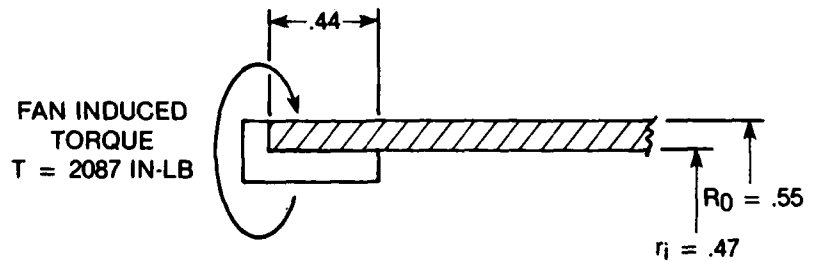
SHEAR STRESS (S_S) Ti-BORSIC SECTION

$$S_S = \frac{16T}{\pi\left[\frac{1}{2}\cdot\left(\frac{ID}{OD}\right)^4\right](OD)^3} = \frac{\cdot(16)\quad(2087)}{\pi\left[1\cdot\left(\frac{.94}{1.1}\right)^4\right](1.1)^3}$$

$S_S = 17{,}110$ PSI

SHEAR STRESS AT DIFFUSION BOND JOINT
DUE TO FAN INDUCED TORQUE OF 2087 IN-LB

$$F = \frac{T}{r_1} = \frac{2087}{.47} = 4440.3\ \text{LBS}$$

$$S_S = \frac{F}{A} = \frac{4440.3}{2\pi(4.7)\,(.44)} = 3417\ \text{PSI}$$

39888

Figure 45.   Structural Analysis 60/40 Ti-Borsic LP Shaft.

55

DIFFUSION BONDED

39859

CONDITIONS: S.L., Mn. 7, HOT DAY

DEAD AIR SPACE
TUBE 800°F
AIR/OIL VAPOR/OIL 500°F AND 14.7 PSIA
SHAFT 549°F
TRAPPED AIR 549°F AND 280 PSIA
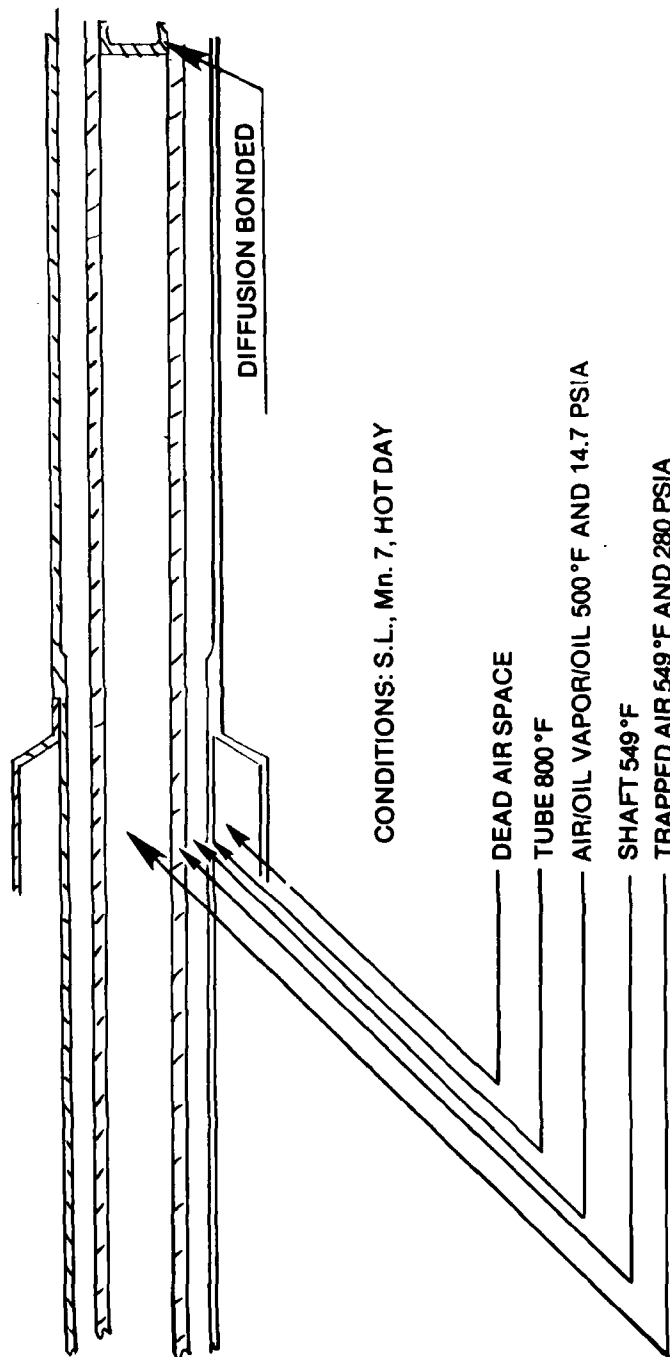
Figure 46. Radial Temperature Distribution 60/40 Ti-Borsic LP Shaft.

1. Heat Balance on Tube: (T = Tube, S = Shaft)

$$T^4_T + 14.818\ T_T - (20.209 + T^4_S/2) = 0$$

2. Heat Balance on Shaft

$$T^4_S + 29.635\ T_S - (T^4_T + 28.45) = 0$$

	Q_S (EQ.2)			Q_T (EQ.1)	
T_T	B	T_S		B	T_T
1000	−29.4	963		−20.639	1268
1200	−30.5	995		−20.700	1271
1270	−30.6	1012		−20.734	1259
1260	−30.96	1009		−20.729	1259

$$T_S = 1009^{\circ}R = 549^{\circ}F$$

$$T_T = 1259^{\circ}R = 799^{\circ}F$$

Figure 47. Sample Calculation.
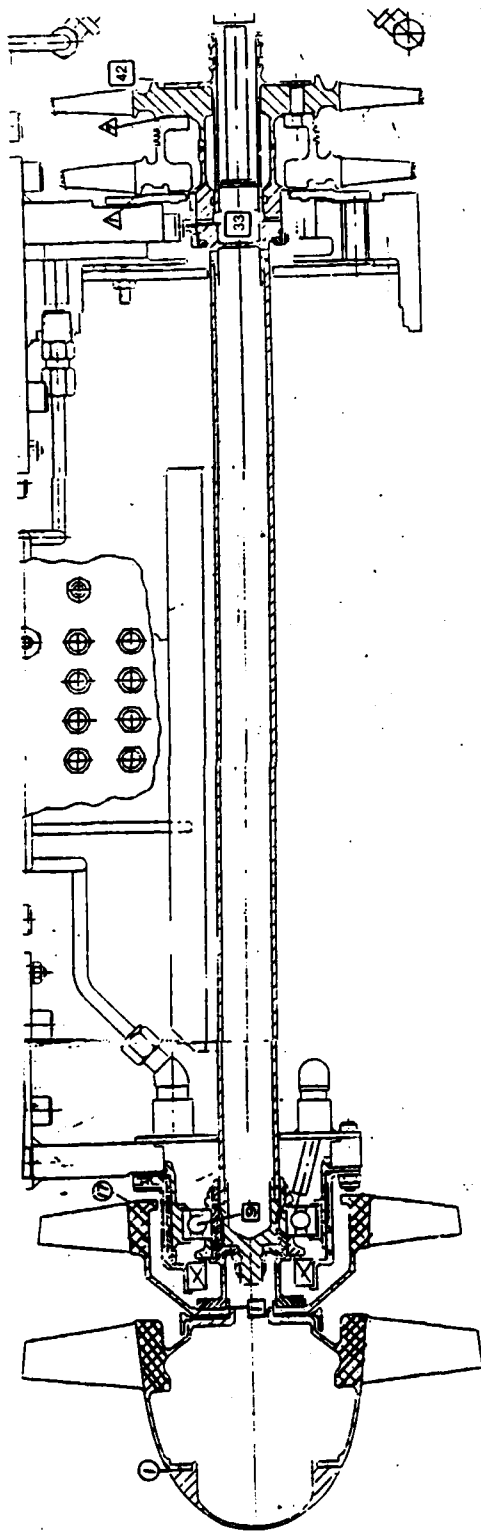
LEGEND:

① . . ⑰ SHAFT NO. 1, STATIONS 1 - 17

[1] . . [42] SHAFT NO. 2, STATIONS 1 - 42

△ . . △ SHAFT NO. 3, STATIONS 1 - 7

[9] FRONT BEARING SUPPORT SPRING RATE = 150,000 LB/IN.

[33] REAR BEARING SUPPORT SPRING RATE = 300,000 LB/IN.

Figure 48. 60/40 Ti-Borsic 471-11DX LP Shaft.

58

sections of the shaft was taken to correspond to the actual flexibility of the rotor. The matrix solution used in this program is essentially an iterative method. At a selected frequency it is used to compute progressively the deflection, slope, moment and shear from one station to the next in a manner similar to the Holzer method. The results of the undamped critical speed analysis are summarized in Table 4 and the relative Ti-Borsic shaft deflections (mode shapes) are depicted in Figures 49 through 51.

(4) Unbalance Response Sensitivity

The unbalance response sensitivity analysis used the same input data as the undamped critical speed analysis with the addition of the calculated value of the viscous damping coefficient for the front bearing support, 3.78 lb-sec/in. The unbalance response sensitivities were computed for an unbalance of 1 gram at appropriate radii separately at the first stage fan, at three random locations along the Ti-Borsic shaft and at the second stage turbine rotor.

For each location of unbalance the response analysis was conducted at each of the previously determined undamped critical speed, 16,015, 23,105 and 47,397 RPM. The unbalance response in terms of deflection and phase are summarized in Tables 5 through 8 and the bearing reaction loads in Tables 9 through 11.

The flexural strain energy (U) has been calculated for the final design configuration of the Ti-Borsic rotor system and was based on the vector totals (in y and z axes) of the bending moments, shear loads and bearing deflections from the unbalance response analysis at the first critical speed (16,015 RPM) which resulted in the largest total bending moment due to 1 gram (.003366 in-lb) unbalance imposed at the balancing ring of the first stage fan.

The total strain energy (U_T) of the rotor system is the sum of the total strain energy due to bending (U_B), shear strain energy (v_V) and strain energy in the bearing due to bearing deflections ($U_{d1} + U_{d2}$). Total strain energy (U_T) $= \Sigma U_B + v_V + U_{d1} + U_{d2}$, where U_B $= \Sigma M^2 \Delta x/2EI$, $v_V = V^2 \Delta x_Y$, $U_{d1} = K_1(\delta_1)^2/2$, and $U_{d2} = K_2(\delta_2^2)/2$. The total strain energy in the Ti-Borsic rotor system due to 1 gram (.003366 in-lb) unbalance at the first stage fan at the first mode (16,015 rpm) is 105.451 in-lbs (100%); the Ti-Borsic section contains 67.5% of the total strain energy; the front and rear bearings contain 16.1 and 2.5 percent of the total strain energy respectively. Since the mode shape of the Ti-Borsic shaft at the first critical speed (16,015 rpm) contains more than 50% of the total system strain energy, it is considered a bending mode but occurs below the idle speed and should be traversed quickly during the start cycles of the engine. The above strain energies were adjusted by the ratio $\frac{.000689}{.003366}$ to reflect the strain energies due to an unbalance of

59

.000689 in-lb resulting from the weight of the Ti-Borsic section of the shaft at the total maximum allowable eccentricity of the shaft relative to the front and rear bearing journals. The adjusted total strain energy is 21.596 in-lb (100%); the Ti-Borsic section of the shaft contains 14.586 in-lb strain energy and the front and rear bearings contain 3.481 and .547 in-lb respectively. The strain energies are summarized in Table 12.

The flexural strength and elastic modulii of 6AL-4V 60% fiber volume Ti-Borsic at 600°F is U_{TS} = 192,000 PSI and E = 42.14 x 10^6 PSI and the ultimate flexural strain energy density $U_{UF} = \frac{1}{2} \left(\frac{FLEX\ \sigma}{\Sigma} \right)$ (dAdx), where dAdx = volume of the Ti-Borsic shaft. U_{UF} = 2043 IN/LB the Ti-Borsic shaft therefore has a shear energy factor of safety of

$$\frac{2043\ in\text{-}lbs}{14.586\ in\text{-}lbs} = N = 140$$

(5) Ti-Borsic Material Properties Variation

The final design configuration of the Ti-Borsic shaft resulted in the third critical speed margin of 24%. Additional critical speed analyses were conducted to show the effect of degrading the values of the elastic modulus (42.14 x 10^6 PSI) and the shear modulus (9.9 x 10^6 PSI) by 10, 20 and 30%. The resultant critical speeds and third critical speed margins are summarized in Table 13.

TABLE 4

CRITICAL SPEED SUMMARY
60/40 TI-BORSIC LP SHAFT

BEARING SUPPORT SPRING RATES (LB/IN)		CRITICAL SPEED			% MARGIN 3RD N_{CR} ABOVE 38,000 RPM
FRONT	REAR	1ST (RPM)	2ND (RPM)	3RD (RPM)	
150,000	300,000	16,016	23,105	47,397	24
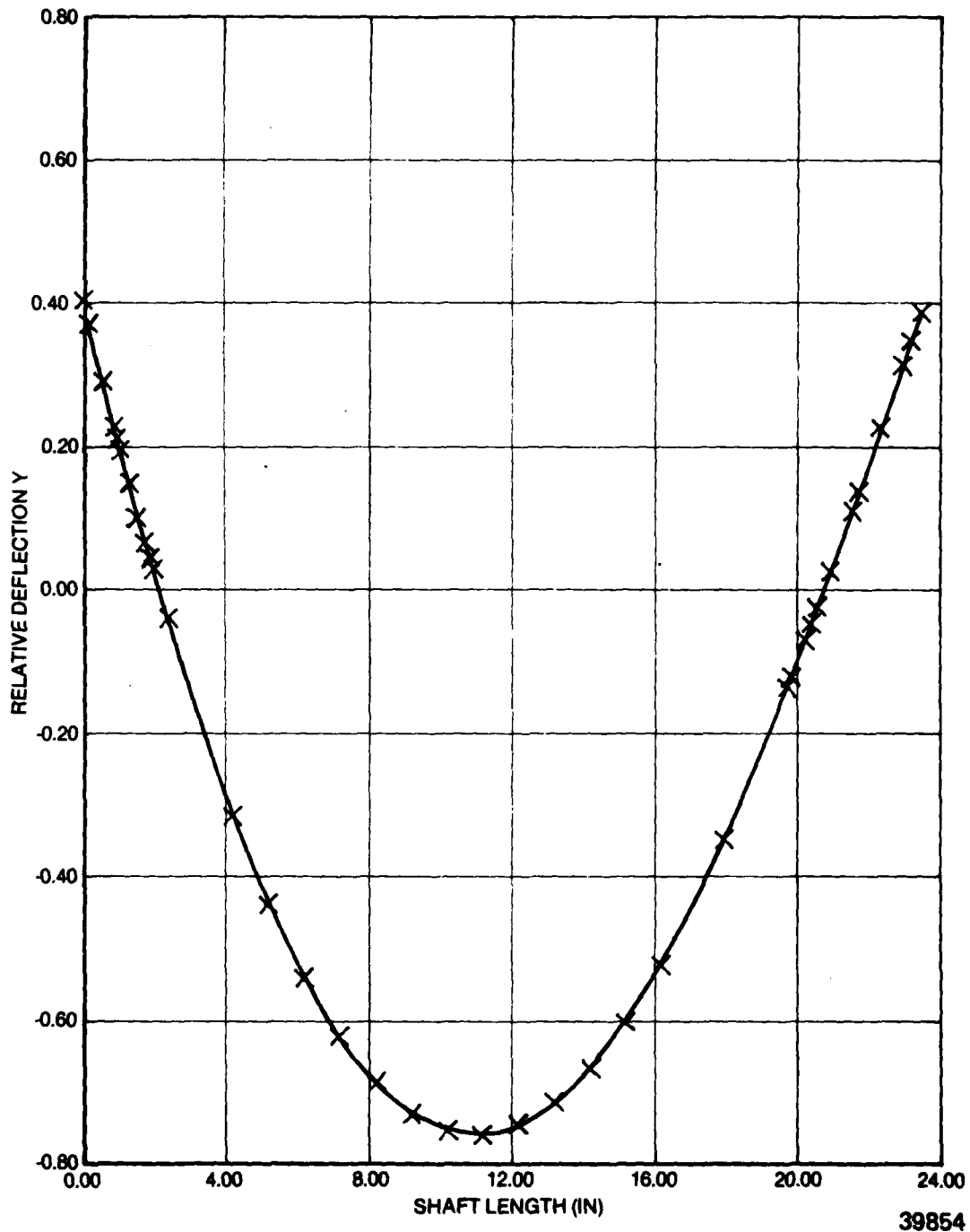
Figure 49.   Ti-Borsic Shaft Relative Deflection - 16,015 rpm.

62
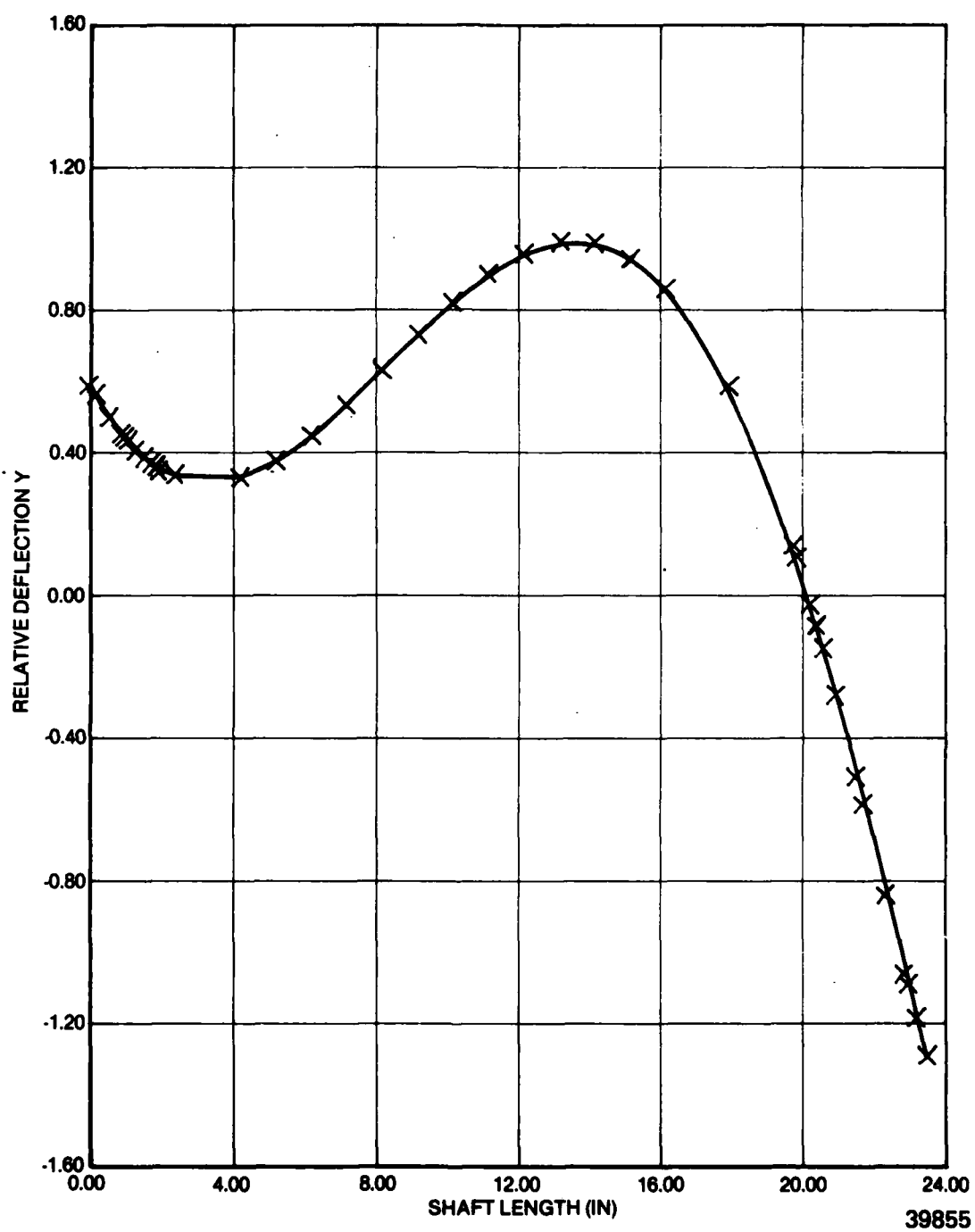
Figure 50.   Ti-Borsic Shaft Relative Deflection - 23,105 rpm.
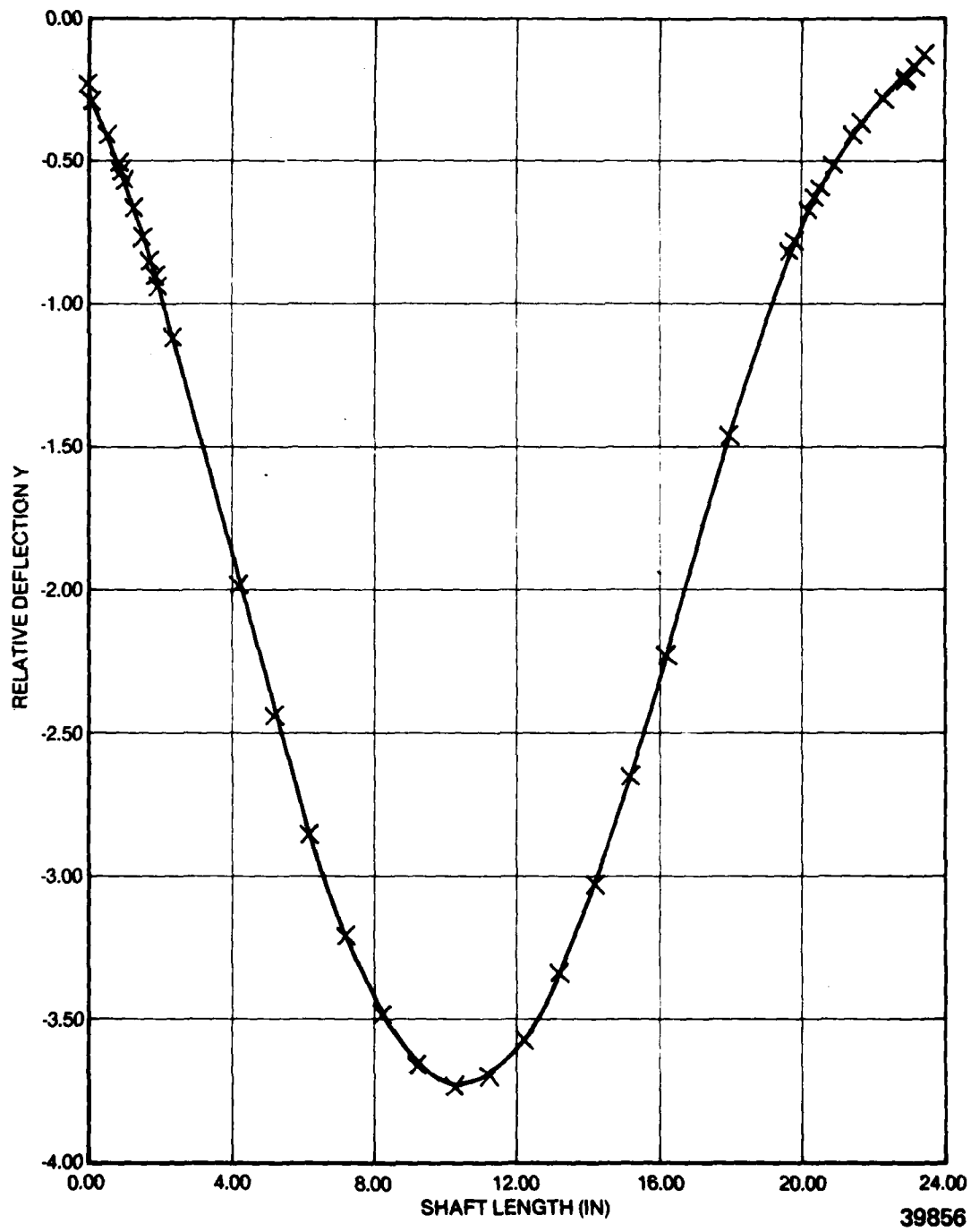
Figure 51.   Ti-Borsic Shaft Relative Deflection - 47,396 rpm.

64

TABLE 5

UNBALANCE RESPONSE (AMPLITUDE/PHASE)

471-11DX 60/40 TI-BORSIC L. P. SHAFT

FRONT BEARING K_9 = 150,000 LB/IN B_9 = 3.781 $\frac{LB\text{-}SEC}{IN}$

REAR BEARING K_{33} = 300,000 LB/IN B_{33} = 0

UNBALANCE OF 1 GRAM SEPARATELY APPLIED AT 5 PLANES
SPEED 16,015 RPM (1ST MODE)

			UNBALANCE LOCATION		
RESPONSE INCHES/DEGREES	PLANE NO.	1 (FAN AT 2" RAD)	2 (SHAFT AT .55" RAD)	3 (SHAFT AT .55" RAD)	4 (SHAFT AT .55" RAD)	5 (TURBINE AT 1.6" RAD)
	1	.095/357	.026/355	.044/356	.020/356	.062/356
	2	.066/355	.017/352	.029/353	.014/353	.042/353
	3	.113/356	.029/353	.051/353	.023/353	.071/354
	4	.052/356	.014/353	.023/353	.011/352	.033/353
	5	.059/356	.015/353	.026/354	.012/353	.037/353

PLANE 1 - FAN, STATION 6
PLANE 2 - TI-BORSIC SHAFT STATION 15
PLANE 3 - TI-BORSIC SHAFT STATION 20
PLANE 4 - TI-BORISC SHAFT STATION 27
PLANE 5 - 2ND TURBINE STATION 41

65

TABLE 6

UNBALANCE RESPONSE (AMPLITUDE/PHASE)
471-11DX 60/40 TI-BORSIC LP SHAFT

FRONT BEARING K_9 = 150,000 LB/IN B_9 = 3.781 $\frac{LB\text{-}SEC}{IN}$

REAR BEARING K_{33} = 300,000 LB/IN B_{33} = 0

UNBALANCE OF 1 GRAM SEPARATELY APPLIED AT 5 PLANES

SPEED 23,105 RPM (2ND MODE)

		UNBALANCE LOCATION			
PLANE NO.	1 (FAN AT 2" RAD)	2 (SHAFT AT .55" RAD)	3 (SHAFT AT .55" RAD)	4 (SHAFT AT .55" RAD)	5 (TURBINE AT 1.6"RAD)
1	.012/1.1	.002/354	.005/351	.004/351	.002/353
2	.006/354	.001/3	.003/9	.002/10	.011/12
3	.013/351	.003/9	.005/6	.004/5	.023/6
4	.009/351	.002/10	.004/5.	.003/359	.017/2
5	.021/353	.004/12	.009/6	.006/2	.036/360

RESPONSE INCHES/DEGREES

PLANE 1 - FAN, STATION 6
PLANE 2 - TI-BORSIC SHAFT STATION 15
PLANE 3 - TI-BORSIC SHAFT STATION 20
PLANE 4 - TI-BORSIC SHAFT STATION 27
PLANE 5 - 2ND TURBINE STATION 41

TABLE 7

UNBALANCE RESPONSE (AMPLITUDE/PHASE)
471-11DX 60/40 TI-BORSIC LP SHAFT

FRONT BEARING K_9 = 150,000 LB/IN B_9 = 3.781 $\frac{\text{LB-SEC}}{\text{IN}}$

REAR BEARING K_{33} = 300,000 LB/IN B_{33} = 0

UNBALANCE OF 1 GRAM SEPARATELY APPLIED AT 5 PLANES

SPEED 47,397 RPM (3RD MODE)

PLANE NO.	UNBALANCE LOCATION				
	1 (FAN AT 2" RAD)	2 (SHAFT AT .55" RAD)	3 (SHAFT AT .55" RAD)	4 (SHAFT AT .55" RAD)	5 (TURBINE AT 1.6"RAD)
1	.001/70	.003/17	.004/20	.002/21	.0004/15
2	.007/17	.032/359	.049/359	.019/360	.005/355
3	.010/20	.049/359	.076/358	.030/357	.007/353
4	.004/21	.019/360	.030/357	.011/353	.003/357
5	.003/15	.001/355	.003/353	.001/357	.001/8

RESPONSE INCHES/DEGREES

PLANE 1 - FAN, STATION 6
PLANE 2 - TI-BORSIC SHAFT STATION 15
PLANE 3 - TI-BORSIC SHAFT STATION 20
PLANE 4 - TI-BORSIC SHAFT STATION 27
PLANE 5 - 2ND TURBINE STATION 41

67

TABLE 8

UNBALANCE RESPONSE (BEARING DISPLACEMENT)

471-11DX 60/40 TI-BORSIC L.P. SHAFT

FRONT BEARING K_9 = 150,000 LB/IN B_9 = 3.781 $\dfrac{LB-SEC}{IN}$

REAR BEARING K_{33} = 300,000 LB/IN B_{33} = 0

UNBALANCE OF 1 GRAM SEPARATELY APPLIED AT 5 PLANES

BEARING RESPONSE

UNBALANCE @ PLANE	16,015 RPM (MODE 1)		23,105 RPM (MODE 2)		47,397 RPM (MODE 3)	
	FRONT BRG. IN./DEG.	REAR BRG. IN./DEG.	FRONT BRG. IN./DEG.	REAR BRG. IN./DEG.	FRONT BRG. IN./DEG.	REAR BRG. IN./DEG.
1	.015/360	.004/357	.006/1.0	.004/354	.002/357	.001/21.0
2	.004/360	.001/355	.001/356	.00086/13	.010/360	.007/360
3	.007/360	.002/360	.003/358	.002/8.0	.015/360	.010/357
4	.003/360	.0009/356	.002/358	.001/5.0	.006/360	.004/353
5	.009/360	.003/351	.011/360	.008/359	.0014/356	.001/31.0

PLANE 1 - FAN, STATION 6
PLANE 2 - TI-BORSIC SHAFT STATION 15
PLANE 3 - TI-BORSIC SHAFT STATION 20
PLANE 4 - TI-BORSIC SHAFT STATION 27
PLANE 5 - 2ND TURBINE STATION 41

TABLE 9

BEARING FORCES DUE TO UNBALANCE

471-11DX 60/40 TI-BORSIC L. P. SHAFT

FRONT BEARING K_9 = 150,000 LB/IN B_9 = 3.781 $\frac{LB\text{-}SEC}{IN}$

REAR BEARING K_{33} = 300,000 LB/IN B_{33} = 0

UNBALANCE OF 1 GRAM SEPARATELY APPLIED AT 5 PLANES

SPEED 16,015 RPM (1ST MODE)

RESPONSE (LBS.)	BEARING	UNBALANCE LOCATION				
		1 (FAN AT 2" RAD)	2 (SHAFT AT .55" RAD)	3 (SHAFT AT .55" RAD)	4 (SHAFT AT .55" RAD)	5 (TURBINE AT 1.6"RAD)
	FRONT	2,258	584	1,007	463	1,418
	REAR	1,226	329	566	260	806

PLANE 1 - FAN, STATION 6
PLANE 2 - TI-BORSIC SHAFT STATION 15
PLANE 3 - TI-BORSIC SHAFT STATION 20
PLANE 4 - TI-BORSIC SHAFT STATION 27
PLANE 5 - 2ND TURBINE STATION 41

69

TABLE 10

BEARING FORCES DUE TO UNBALANCE

471-11DX 60/40 TI-BORSIC L. P. SHAFT

FRONT BEARING K_9 = 150,000 LB/IN B_9 = 3.781 $\dfrac{\text{LB-SEC}}{\text{IN}}$

REAR BEARING K_{33} = 300,000 LB/IN B_{33} = 0

UNBALANCE OF 1 GRAM SEPARATELY APPLIED AT 5 PLANES

SPEED 23,105 RPM (2ND MODE)

RESPONSE (LBS.) BEARING	UNBALANCE LOCATION				
	1 (FAN AT 2" RAD)	2 (SHAFT AT .55" RAD)	3 (SHAFT AT .55" RAD)	4 (SHAFT AT .55" RAD)	5 (TURBINE AT 1.6" RAD)
FRONT	916	176	382	372	1,631
REAR	1,336	259	556	394	2,362

PLANE 1 - FAN, STATION 6.
PLANE 2 - TI-BORSIC SHAFT STATION 15
PLANE 3 - TI-BORSIC SHAFT STATION 20
PLANE 4 - TI-BORSIC SHAFT STATION 27
PLANE 5 - 2ND TURBINE STATION 41

TABLE 11

BEARING FORCES DUE TO UNBALANCE

471-11DX 60/40 TI-BORSIC L. P. SHAFT

FRONT BEARING K_9 = 150,000 LB/IN B_9 = 3.781 $\frac{LB\text{-}SEC}{IN}$

REAR BEARING K_{33} = 300,000 LB/IN B_{33} = 0

UNBALANCE OF 1 GRAM SEPARATELY APPLIED AT 5 PLANES

SPEED 47,397 RPM (3RD MODE)

RESPONSE (LBS.)	BEARING	UNBALANCE LOCATION				
		1 (FAN AT 2" RAD)	2 (SHAFT AT .55" RAD)	3 (SHAFT AT .55" RAD)	4 (SHAFT AT .55" RAD)	5 (TURBINE AT 1.6" RAD)
	FRONT	293	1,514	2,319	908	213
	REAR	417	2,027	3,109	1,226	329

PLANE 1 – FAN, STATION 6
PLANE 2 – TI-BORSIC SHAFT STATION 15
PLANE 3 – TI-BORSIC SHAFT STATION 20
PLANE 4 – TI-BORSIC SHAFT STATION 27
PLANE 5 – 2ND TURBINE STATION 41

71

TABLE 12

STRAIN ENERGY TI-BORSIC LP SHAFT
AT 1ST CRITICAL SPEED 16,015 RPM

| STRAIN ENERGY | STRAIN ENERGY DUE TO UNBALANCE | | PERCENT STRAIN ENERGY |
	(.003366 IN.-LB.) (IN.-LB.)	(.000689 IN.-LB.) (IN.-LB.)	%
U_{Total}	105.451	21.596	100.0
$U_{Ti-Borsic\ Shaft}$	71.219	14.586	67.5
$U_{Front\ Bearing}$	16.999	3.481	16.1
$U_{Rear\ Bearing}$	2.699	0.547	2.5
U_{Fans}	0.864	0.177	0.8
$U_{First\ Turbine}$	0.021	0.004	0.02
$U_{Second\ Turbine}$	13.678	2.801	13.0

TABLE 13

SUMMARY: EFFECT OF MATERIAL PROPERTY DEGRADATION
ON CRITICAL SPEEDS

MATERIAL PROPERTY VALUE DEGRADATION (%)	E PSIx10^6	G PSIx10^6	CRITICAL SPEEDS (RPM)			% MARGIN 3RD N_CR ABOVE 38,000 RPM
			1ST	2ND	3RD	
0	42.14	9.9	16,015	23,043	46,993	23.7
10	37.93	8.91	15,399	22,606	46,054	21.2
20	33.71	7.92	14,717	22,101	45,028	18.5
30	29.5	6.93	13,957	21,510	43,890	15.5

SECTION IV

CONCLUSIONS AND RECOMMENDATIONS

1. CONCLUSIONS

    a. Multi-Plane High Speed Balancing Demonstration

        When operating above the second critical speed with
the squeeze film damper, non synchronous vibration corresponding
to the second mode prevented running to full speed. With the
squeeze film effect eliminated, the rotor was successfully run
through three critical speeds (more sensitive without the
damper, but controllable) before increasing bearing temperature
prevented higher speed operation. The high bearing temperature
was caused by insufficient lubrication which resulted from the
minimum flows necessary to prevent captured excess oil from
activating the damper through capillary action. Since higher
speeds have been attained with the damper made inactive it is
inferred that the problems are associated with the damper. The
existing damper was designed for the original engine hollow
shaft configuration which included two inter-shaft bearings, and
perhaps has some inherent destabalizing characteristics when
supporting the modified flexible rotor.

    b. Ti-Borsic Shaft

        The Ti-Borsic shaft will fulfill all structural and
operating engine requirements.

2. RECOMMENDATIONS

    a. Multi-Plane High Speed Balancing Demonstration

        In view of the demonstrated success in running through
three critical speeds (two bending modes) by means of the high
speed multi plane balancing techniques, it is recommended that
further work be undertaken to attempt to predict the
sub-synchronous instabilities that occurred. The analytical
tools generated in a current AFWAL-MTI damper program would form
the basis for such a program, and should be used to design a
damper which would allow full speed operation with no
sub-synchronous vibration encountered (increasing stability
range). The damper support system design would be coordinated
with the rotor system to provide an integrated, vibration free,
LP shaft system. Rig verification including multi-plane high
speed balancing would be demonstrated leading to a full scale
TCAE funded engine test program.

    b. Ti-Borsic Shaft

        It is recommended that funding be provided to
fabricate full scale Ti-Borsic shafts for rig testing and engine
verification.

Appendix A

**MTI UNDAMPED CRITICAL SPEED
MATHEMATICAL MODEL**

MATHEMATICAL MODEL OF THE ROTOR

CASE 2   TELEDYNE 3-15-79

STATIONS	BRGS	STIFF	COUPL	PFD.FLEX	HORF=0	NYM	MDST	NGRPH	LPLOT	H365C	NHAT	NLANFL	NGYRO	JOPT	NCNTRL	JUNITS
56	2	1	0	0	1	0	0	-1	0	.1	5	0	1	1	0	0

NO PLOT TAPE HAS BEEN CREATED

MAT NO.	YOUNGS MOD. (LB/IN**2)	DENSITY (LB/IN**3)	SHEAR MOD. (LB/IN**2)
1	.2400E+07	.9000E-01	.9000E+06
2	.1650E+08	.1600E+00	.6100E+07
3	.2994E+08	.2060E+00	.1160E+08
4	.2990E+08	.2960E+00	.1160E+08
5	.2900E+08	.2970E+00	.1100E+08

ROTOR DATA

Mathematical Model of TCAE Cruise Missile Rotor

77

```
47  0.  .269E-01         .450  1.400  1.400  1.200  .290E+00 .290E+00  .110E-08 .110E-08
48  0.  .020E-01         .600  1.900  3.900   .900  .240E+00 .294E+00  .110E-08 .110E-08
49  0.                   .100  1.200  2.400   .400  .290E+00 .297E+00  .110E-08 .110E-08
50  0.  .117E-00         .150   .900   .700   .600  .290E+00 .297E+00  .110E-08 .110E-08
51  0.                   .150  1.000  1.400   .600  .740E+00 .297E+00  .110E-08 .110E-08
52  0.                   .150   .900   .900   .600  .290E+00 .297E+00  .110E-08 .110E-08
53  0.                   .250  1.000  1.000   .600  .290E+00 .297E+00  .110E-08 .110E-08
54  0.                   .150   .900   .900   .600  .290E+00 .297E+00  .110E-08 .110E-08
55  0.                   .100  1.000  1.000   .600  .290E+00 .297E+00  .110E-08 .110E-08
56  0.                  0.000  0.000  0.000  0.000  .290E+00 .297E+00  .110E-08 .110E-08
```

BEARING STATIONS
B 4 3

ROTOR WT.	ROTOR IP	ROTOR IT	BRG.1 -CG	LOAD,BRG.1	LOAD,BRG.2	DISTANCE	ROTOR LENGTH
(LBS)	(LB-IN**2)	(LB-IN**2)	(IN)	(LBS)	(LBS)	BRG.1- BRG.2 (IN)	(IN)
.1310E+02	.105972E+02	.127623E+06	11.001	.541E+01	.769E+01	16.7500	23.6000

78

47	0.	.269E-01	0.	.1097E-02	0.	.1040E-02	.150	1.400	1.400	.2900E-08	.110E-08
48	0.	.028E-01	0.				.600	1.900	3.900	.2900E-08	.110E-08
49	0.		0.				.104	1.200	7.600	.2900E-08	.110E-08
50	0.	.117E-08	0.				.150	.900	.900	.2900E-08	.110E-08
51	0.		0.				.150	1.000	1.600	.2900E-08	.110E-08
52	0.		0.				.150	.900	.200	.2900E-08	.110E-08
53	0.		0.				.250	1.000	1.000	.2900E-08	.110E-08
54	0.		0.				.150	.900	.600	.2900E-08	.110E-08
55	0.		0.				.100	1.000	.600	.2900E-08	.110E-08
56	0.		0.				0.000	0.000	0.000	.2900E-08	.110E-08

BEARING STATIONS
A 4)

ROTOR WT. (LBS)	ROTOR IP (LB-IN**2)	ROTOR IT (LB-IN**2)	BRG.1 -CG (IN)	LOAD,BRG.1 (LBS)	LOAD,BRG.2 (LBS)	DISTANCE BRG.1- BRG.2 (IN)	ROTOR LENGTH (IN)
.1310E-02	.305972E-02	.127423E-04	11.001	.541E-01	.749E-01	10.7500	23.6000

Appendix B

MTI UNBALANCE RESPONSE SUMMARY

AMPLITUDE AND PHASE ANGLE

RESPONSE TO UNBALANCE

$K_1 = 6000$ LB/IN $B_1 = .1 \frac{\text{LB-SEC}}{\text{IN}}$

$K_2 = 51000$ LB/IN $B_2 = 0$

UNBALANCE OF 1 GRAM WAS PLACED ON .76" SHAFT DIAMETER SEQUENTIALLY.

SPEED = 5917 RPM

		UNBALANCE LOCATION	
PLANE NO.	1	2	3
1	.012/270	.011/270	.005/270
2	.011/270	.009/270	.004/270
3	.005/270	.004/270	.002/270

RESPONSE IN/DEG

Figure B-1. Amplitude and Phase at First Critical Speed With Assumed Teledyne CAE Damping Value.

AMPLITUDE AND PHASE ANGLE
RESPONSE TO UNBALANCE

$K_1 = 6000$ LB/IN $\qquad B_1 = .1 \dfrac{\text{LB-SEC}}{\text{IN}}$

$K_2 = 51000$ LB/IN $\qquad B_2 = 0$

UNBALANCE OF 1 GRAM WAS PLACED ON .76" SHAFT DIAMETER SEQUENTIALLY.

SPEED = 7909 RPM

UNBALANCE LOCATION

PLANE NO.	1	2	3
1	.043/265	.094/265	.059/265
2	.092/265	.202/265	.129/265
3	.059/265	.129/265	.082/265

RESPONSE IN/DEG

Figure B-2. Amplitude and Phase at Second Critical Speed With Assumed Teledyne CAE Damping Value.

AMPLITUDE AND PHASE ANGLE

RESPONSE TO UNBALANCE

$K_1 = 6000$ LB/IN $B_1 = .1 \dfrac{\text{LB-SEC}}{\text{IN}}$

$K_2 = 51000$ LB/IN $B_2 = 0$

UNBALANCE OF 1 GRAM WAS PLACED ON .76" SHAFT DIAMETER SEQUENTIALLY.

SPEED = 13,823 RPM

		UNBALANCE LOCATION	
PLANE NO.	1	2	3
1	17.1/306	26.5/298	16.6/261
2	24.3/306	37.8/298	23.7/261
3	13.6/306	21.1/298	13.2/261

RESPONSE IN/DEG

Figure B-3. Amplitude and Phase at Third Critical Speed With Assumed Teledyne CAE Damping Value.

81

AMPLITUDE AND PHASE ANGLE

RESPONSE TO UNBALANCE

K_1 = 6000 LB/IN B_1 = .1 $\frac{\text{LB-SEC}}{\text{IN}}$

K_2 = 5000 LB/IN B_2 = 0

UNBALANCE OF 1 GRAM WAS PLACED ON .76" SHAFT DIAMETER SEQUENTIALLY.

SPEED = 33,278 RPM

UNBALANCE LOCATION

PLANE NO.	1	2	3
1	2.66/252	.468/284	2.90/72
2	.46/252	.08/284	.50/72
3	2.91/72	.51/104	3.17/252

RESPONSE IN/DEG

Figure B-4. Amplitude and Phase at Fourth Critical Speed With Assumed Teledyne CAE Damping Value.

AMPLITUDE AND PHASE ANGLE

RESPONSE TO UNBALANCE

$K_1 = 6000$ LB/IN $B_1 = .1 \dfrac{\text{LB-SEC}}{\text{IN}}$

$K_2 = 5000$ LB/IN $B_2 = 0$

UNBALANCE OF 1 GRAM WAS PLACED ON .76" SHAFT DIAMETER SEQUENTIALLY.

SPEED = 69,800 RPM

UNBALANCE LOCATION

	PLANE NO.	1	2	3
RESPONSE IN/DEG	1	1.35/272	1.47/92	1.32/270
	2	1.47/92	1.59/272	1.43/90
	3	1.32/272	1.43/92	1.29/270

Figure B-5. Amplitude and Phase at Fifth Critical Speed With Assumed Teledyne CAE Damping Value.

83

1.0

1.1

1.25   1.4   1.6

4.5
5.0
5.5
6.3

2.8   2.5
3.2   2.2
3.6
4.0   2.0

1.8
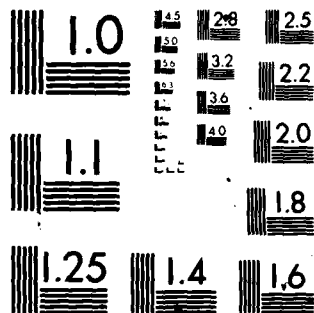
MICROCOPY RESOLUTION TEST CHART
NATIONAL BUREAU OF STANDARDS-1963-A

BEARING FORCES

RESPONSE TO UNBALANCE

$K_1 = 6000$ LB/IN $B_1 = .1 \frac{LB-SEC}{IN}$

$K_2 = 51000$ LB/IN $B_2 = 0$

UNBALANCE OF 1 GRAM WAS PLACED ON .75" SHAFT DIAMETER SEQUENTIALLY.

SPEED = 5917 RPM

UNBALANCE LOCATION

BEARING NO.	RESPONSE LR/NFG	PLANE NO. 1	2	3
1		77.4/89	67.7/89	30.9/88
2		13.2/-91	11.5/-91	5.28/-96

Figure B-6. Bearing Forces at First Critical Speed With Assumed Teledyne CAE Damping Value.

BEARING FORCES

RESPONSE TO UNBALANCE

$$B_1 = .1 \ \frac{LB\text{-}SEC}{IN}$$

$$B_2 = 0$$

$$K_1 = 6000 \ LB/IN$$

$$K_2 = 5000 \ LB/IN$$

UNBALANCE OF 1 GRAM WAS PLACED ON .76" SHAFT DIAMETER SEQUENTIALLY.

SPEED = 7900 RPM

UNBALANCE LOCATION

BEARING NO.	PLANE NO.		
	1	2	3
1	166.1/-93	361.5/-92	229.1/-92
2	370.7/-96	806.3/-94	510.9/-94

RESPONSE LB/DEG

Figure B-7. Bearing Forces at Second Critical Speed With Assumed Teledyne CAE Damping Value.

BEARING FORCES

RESPONSE TO UNBALANCE

$K_1 = 6000$ LB/IN $B_1 = .1 \frac{\text{LB-SEC}}{\text{IN}}$

$K_2 = 5000$ LB/IN $B_2 = 0$

UNBALANCE OF 1 GRAM WAS PLACED ON .76" SHAFT DIAMETER SEQUENTIALLY.

SPEED = 13,823 RPM

UNBALANCE LOCATION

	PLANE NO.		
BEARING NO.	1	2	3
1	3946.6/128	6134.8/120	3848.5/83
2	652592.5/126	1014359.3/118	636323.0/81

RESPONSE LB/DEG

Figure B-8. Bearing Forces at Third Critical Speed With Assumed Teledyne CAE Damping Value.

86

BEARING FORCES

RESPONSE TO UNBALANCE

$K_1 = 6000$ LB/IN $\qquad B_1 = .1 \dfrac{\text{LB-SEC}}{\text{IN}}$

$K_2 = 5100$ LB/IN $\qquad B_2 = 0$

UNBALANCE OF 1 GRAM WAS PLACED ON .76" SHAFT DIAMETER SEQUENTIALLY.

SPEED = 33,278 RPM

UNBALANCE LOCATION

BEARING NO.		PLANE NO.	
	1	2	3
1	2625.39 /75	462.2 /107	2861.77 /-106
2	5316/4.88 /-108	11124.99 /-76.2	6885.63 /71

RESPONSE
LB/DEG

Figure B-9. Bearing Forces at Fourth Critical Speed With
Assumed Teledyne CAE Damping Value.

87

BEARING FORCES

RESPONSE TO UNBALANCE

$B_1 = .1 \frac{LB\text{-}SEC}{IN}$

$K_1 = 6000 \, LB/IN$

$B_2 = 0$

$K_2 = 51000 \, LB/IN$

UNBALANCE OF 1 GRAM WAS PLACED ON .76" SHAFT DIAMETER SEQUENTIALLY.

SPEED = 69,800 RPM

UNBALANCE LOCATION

BEARING NO.	PLANE NO. 1	PLANE NO. 2	PLANE NO. 3
1	2799.66 /99	3036.37 /-81	2732.76 /97
2	13210.32 /92	16862.33 /-83	42177.08 /90

RESPONSE LB/DEG

Figure B-10. Bearing Forces at Fifth Critical Speed With Assumed Teledyne CAE Damping Value.

AMPLITUDE AND PHASE ANGLE

RESPONSE TO UNBALANCE

$K_1 = 6000$ LB/IN $B_1 = 6.7$ $\frac{LB\text{-}SEC}{IN}$

$K_2 = 51700$ LB/IN $B_2 = 0$

UNBALANCE OF 1 GRAM WAS PLACED ON .76" SHAFT DIAMETER SEQUENTIALLY.

SPEED = 5917 RPM

UNBALANCE LOCATION

PLANE NO.	1	2	3
1	CRITICALLY DAMPED		
2	CRITICALLY DAMPED		
3	CRITICALLY DAMPED		

RESPONSE
IN/DEG

Figure B-11. Amplitude and Phase at First Critical Speed With
MTI Damping Value.

89

AMPLITUDE AND PHASE ANGLE

RESPONSE TO UNBALANCE

$K_1 = 6000$ LB/IN $B_1 = 6.7 \frac{\text{LB-SEC}}{\text{IN}}$

$K_2 = 51900$ LB/IN $B_2 = 0$

UNBALANCE OF 1 GRAM WAS PLACED ON .76" SHAFT DIAMETER SEQUENTIALLY.

SPEED = 7771 RPM

PLANE NO.	UNBALANCE LOCATION		
	1	2	3
1	.0029/250	.005/250	.0031/250
2	.005/250	.009/250	.006/250
3	.0031/250	.005/250	.0034/250

RESPONSE IN/DEG

Figure B-12. Amplitude and Phase at Second Critical Speed With MTI Damping Value.

AMPLITUDE AND PHASE ANGLE
RESPONSE TO UNBALANCE

$K_1 = 6000$ LB/IN $B_1 = 6.7 \dfrac{LB\text{-}SEC}{IN}$

$K_2 = 51000$ LB/IN $B_2 = 0$

UNBALANCE OF 1 GRAM WAS PLACED ON .76" SHAFT DIAMETER SEQUENTIALLY.

SPEED = 13,823 RPM

UNBALANCE LOCATION

PLANE NO.	1	2	3
1	.36/269	.51/269	.29/269
2	.51/269	.73/269	.41/269
3	.29/269	.41/269	.23/269

RESPONSE IN/DEG

Figure B-13. Amplitude and Phase at Critical Speed With MTI Damping Value.

AMPLITUDE AND PHASE ANGLE

RESPONSE TO UNBALANCE

$K_1 = 6000$ LB/IN $B_1 = 6.7 \frac{\text{LB-SEC}}{\text{IN}}$

$K_2 = 51000$ LB/IN $B_2 = 0$

UNBALANCE OF 1 GRAM WAS PLACED ON .76" SHAFT DIAMETER SEQUENTIALLY.

SPEED = 33,262 RPM

UNBALANCE LOCATION

PLANE NO.	1	2	3
1	.04/271	.007/270	.05/90
2	.007/271	.001/270	.008/97
3	.05/91	.007/100	.05/270

RESPONSE IN/DEG

Figure B-14. Amplitude and Phase at Fourth Critical Speed With MTI Damping Value.

AMPLITUDE AND PHASE ANGLE

RESPONSE TO UNBALANCE

K_1 = 6000 LB/IN B_1 = 6.7 $\frac{LB\text{-}SEC}{IN}$

K_2 = 5000 LB/IN B_2 = 0

UNBALANCE OF 1 GRAM WAS PLACED ON .76" SHAFT DIAMETER SEQUENTIALLY.

SPEED = 69,399 RPM

UNBALANCE LOCATION

	PLANE NO.	1	2	3
RESPONSE IN/DEG	1	.02/270	.02/93	.02/270
	2	.02/90	.02/270	.02/90
	3	.02/270	.02/270	.02/270

Figure B-15. Amplitude and Phase at Fifth Critical Speed With MTI Damping Value.

93

BEARING FORCES

RESPONSE TO UNBALANCE

$K_1 = 6000$ LB/IN $B_1 = 6.7 \dfrac{\text{LB-SEC}}{\text{IN}}$

$K_2 = 5000$ LB/IN $B_2 = 0$

UNBALANCE OF 1 GRAM WAS PLACED ON .76" SHAFT DIAMETER SEQUENTIALLY.

SPEED = 5917 RPM

UNBALANCE LOCATION

BEARING NO.	RESPONSE LB/DEG	PLANE NO. 1	PLANE NO. 2	PLANE NO. 3
1			CRITICALLY DAMPED	
2			CRITICALLY DAMPED	

Figure B-16. Bearing Forces at First Critical Speed With MTI Damping Value.

BEARING FORCES

RESPONSE TO UNBALANCE

$K_1 = 6900$ LB/IN $B_1 = 6.7 \dfrac{\text{LB-SEC}}{\text{IN}}$

$K_2 = 51000$ LB/IN $B_2 = 0$

UNBALANCE OF 1 GRAM WAS PLACED ON .76" SHAFT DIAMETER SEQUENTIALLY.

SPEED = 7771 RPM

UNBALANCE LOCATION

BEARING NO.	RESPONSE LB/DEG	PLANE NO. 1	PLANE NO. 2	PLANE NO. 3
1		6.82/5	12.5/5	7.64/5
2		18.51/-103	33.07/-99	20.24/-100

Figure B-17. Bearing Forces at Second Critical Speed With MTI Damping Value.

BEARING FORCES

RESPONSE TO UNBALANCE

$K_1 = 6900$ LB/IN $B_1 = 6.7 \frac{\text{LB-SEC}}{\text{IN}}$

$K_2 = 5100$ LB/IN $B_2 = 0$

UNBALANCE OF 1 GRAM WAS PLACED ON .76" SHAFT DIAMETER SEQUENTIALLY.

SPEED = 13,823 RPM

UNBALANCE LOCATION

| | | PLANE NO. | |
		1	2	3
BEARING NO.	1	147.74/168	210.57/168	117.70/168
RESPONSE LB/DEG	2	13712.73/90	19544.37/90	10023.95/90

Figure B-18. Bearing Forces at Third Critical Speed With MTI Damping Value.

BEARING FORCES

RESPONSE TO UNBALANCE

$K_1 = 6000$ LB/IN $B_1 = 6.7 \frac{\text{LB-SEC}}{\text{IN}}$

$K_2 = 5000$ LB/IN $B_2 = 0$

UNBALANCE OF 1 GRAM WAS PLACED ON .76" SHAFT DIAMETER SEQUENTIALLY.

SPEED = 33,262 RPM

UNBALANCE LOCATION

BEARING NO.	PLANE NO.		
	1	2	3
1	166.14/171	28.22/174	181.83/-8.9
2	1002./-80	172.81/-80	1106.45/99

RESPONSE LB/DEG

Figure B-19.   Bearing Forces at Fourth Critical Speed With MTI
Damping Value.

97

BEARING FORCES

RESPONSE TO UNBALANCE

$B_1 = 6.7 \frac{LB\text{-}SEC}{IN}$

$K_1 = 6000$ LB/IN

$K_2 = 5100$ LB/IN

$B_2 = 0$

UNBALANCE OF 1 GRAM WAS PLACED ON .76" SHAFT DIAMETER SEQUENTIALLY.

SPEED = 69,800

UNBALANCE LOCATION

BEARING NO.		PLANE NO. 1	PLANE NO. 2	PLANE NO. 3
	1	341.35/172	370.13/-5	332.94/175
RESPONSE LB/DEG	2	645.04/90	700.1/-90	630.07/88

Figure B-20. Bearing Forces at Fifth Critical Speed With MTI Damping Value.
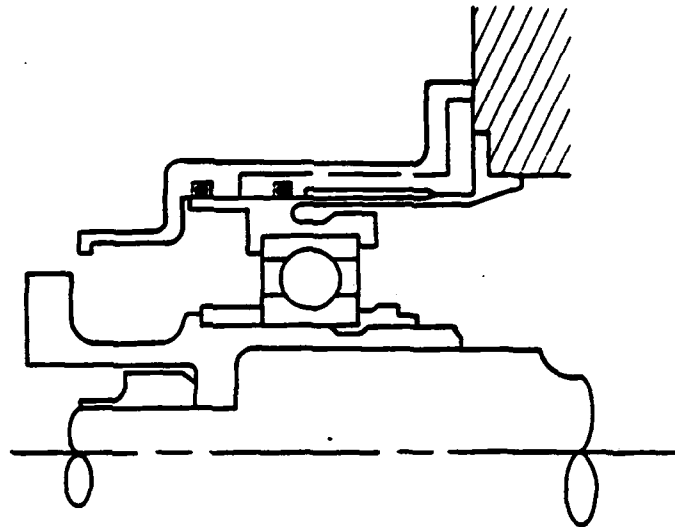
Appendix C

HIGH SPEED BALANCING
DEMONSTRATION OF RESULTS
AND ROTOR CONFIGURATIONS

A. INITIAL CONDITION:

- DAMPER IN PLACE
- O-RINGS INSTALLED
- OIL PRESSURE TO DAMPER
- NO SEAL
- OIL MIST LUBE

FINDINGS:

- FIRST MODE DAMPED
- INTERMITTENT REPEATABILITY PROBLEMS
- SECOND MODE NOT WELL DEFINED
- INSTABILITY AT 11,500 RPM. SUBSYNCHRONOUS AT 9000 RPM
- NO DAMPER OIL BLEED HOLE

ACTION:

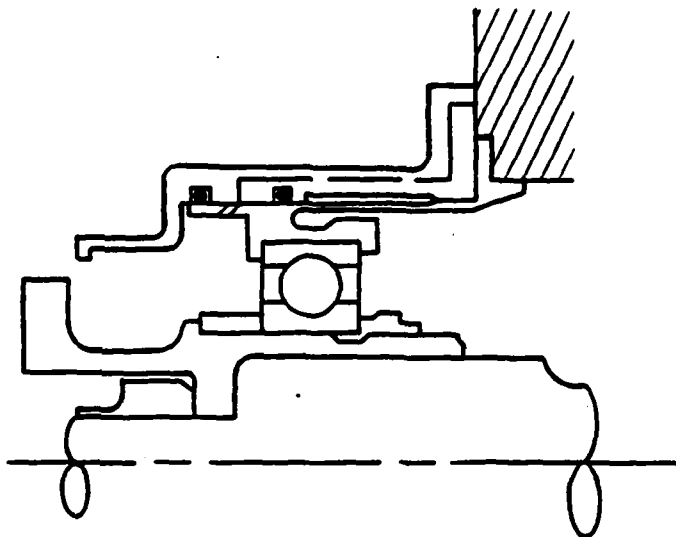- ADD BLEED HOLE FOR DAMPER OIL

99

B. DAMPER MODIFIED:

- ADDED DAMPER OIL-BLEED
  HOLE

FINDINGS:

- AMPLITUDES MORE CONSISTENT

- SECOND MODE WELL DEFINED AT
  9000 RPM

- STILL UNSTABLE AT 11,500-
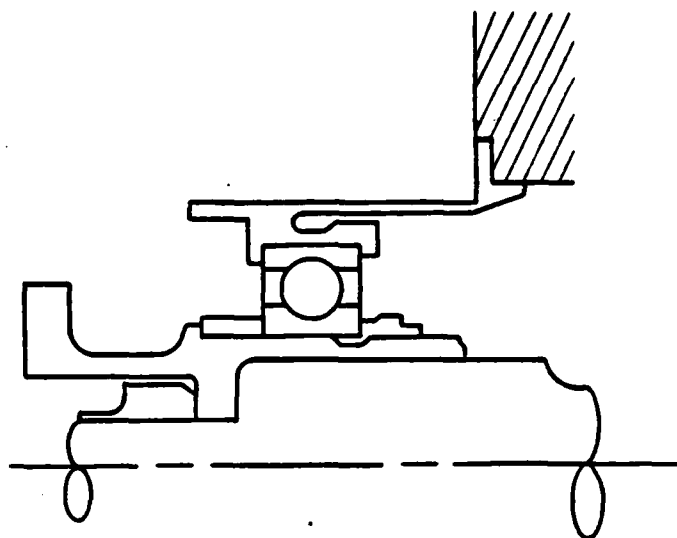 12,500 RPM

ACTION:

- ELIMINATE DAMPER

100

C. DAMPER ELIMINATED:

   • REMOVED DAMPER OUTER
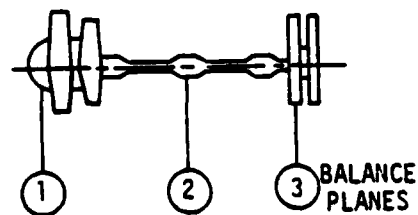   HOUSING

FINDINGS:

   • ROTOR EXTREMELY SENSITIVE
     TO UNBALANCE

   • FIRST MODE UNDAMPED (5900
     RPM)

   • TWO PLANE BALANCE THROUGH
     FIRST TWO MODES

   • PERMANENT WEIGHT CORRECTION
     AT CENTER OF SHAFT

   • RAN TO 18,000 RPM

   • FRONT BEARING FAILURE;
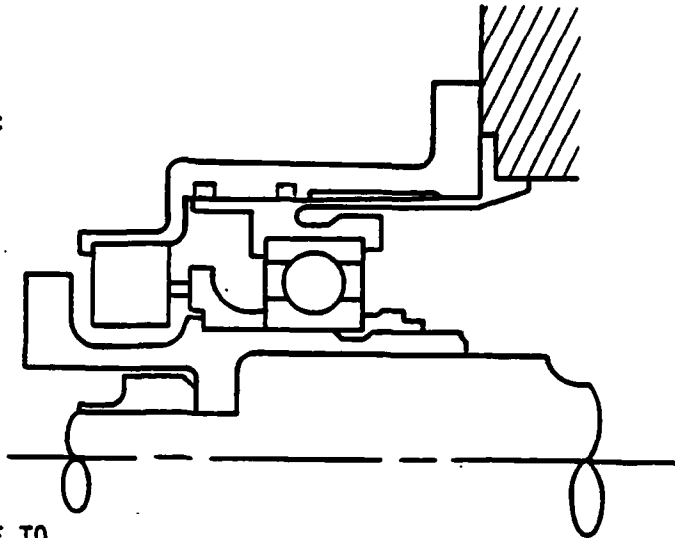   DISASSEMBLY REVEALED
     FRACTURED FLEXURES

ACTION:

   • "BUMPER" NEEDED TO LIMIT
     DEFLECTION AT FRONT BEARING

   • INCREASED OIL SUPPLY NEEDED
     TO LUBE/COOL FRONT BEARING

① ② ③ BALANCE PLANES

D. DAMPER HOUSING REINSTALLED:

- OUTER DAMPER HOUSING REINSTALLED
- NO O-RINGS
- NO OIL SUPPLY TO DAMPER
- FRONT BEARING REPLACED
- SEAL INSTALLED
- OIL MIST INCREASED

FINDINGS:

- ROTOR REMAINED SENSITIVE TO UNBALANCE BUT NOW HAD SMALL VIBRATION LIMIT (6-8 MILS, PP) AT FRONT END

- SEAL REMOVED BECAUSE OF EX- CESS DRAG & HEAT BUILDUP

- THREE PLANE BALANCE THROUGH THREE CRITICAL SPEEDS

- ADDITIONAL PERMANENT WEIGHT CORRECTION AT CENTER OF SHAFT

- RAN TO 28,000 RPM. HIGH FRONT BEARING TEMPERATURE

- CHANGED OIL LUBE TO FRONT BEARING TO JET. INSTABILITY AT 23,000 RPM

- VARIED BEARING PRELOAD. NO SIGNIFICANT EFFECT ON INSTABILITY

- VARIED DAMPER OIL SUPPLY PRES- SURE: 0-40, 90 PSIG NO SIGNIF- ICANT EFFECT ON INSTABILITY

ACTION:

- ENLARGE DAMPER CLEARANCES TO PREVENT INADVERTENT DAMPING ACTION FROM EXCESS BEARING LUBE OIL ENTERING DAMPER CAVITY